Effects of Inflammation and Soy Isoflavones on Irinotecan Pharmacokinetics and Toxicity

by
Pavan Kumar Chityala

A dissertation submitted to the Department of Pharmacological and Pharmaceutical Sciences,
College of Pharmacy
in partial fulfillment of the requirements for the degree of

DOCTOR OF PHILOSOPHY

in Pharmaceutics

Chair of Committee: Romi Ghose, Ph.D.

Committee Member: Diana S-L Chow, Ph.D.

Committee Member: Ming Hu, Ph.D.

Committee Member: Bhagavatula Moorthy, Ph.D.

Committee Member: Sundararajah Thevananther, Ph.D.

University of Houston
December 2019

ACKNOWLEDGMENTS

First, I would like to acknowledge my research adviser, Dr. Romi Ghose for accepting me into her research group, providing guidance and help with my research projects and for giving me ample opportunities to work collaboratively on multiple projects, which expanded my knowledge and improved my scientific thinking and skills. I would like to specially thank Dr. Diana Chow for sharing her knowledge in classroom lectures and her suggestions during my research discussions. I would also thank Dr. Chow for the collaboration on the Aim 1 project and for providing her expert advice on the project, which allowed me to successfully finish the project. I would like to thank Dr. Ming Hu for the valuable advice during the meetings and for suggesting key experiments for my project. I would also like to thank Dr. Hu's lab for providing a few important chemicals needed for my research. I would like to take this opportunity to also thank Dr. Sundararajah Thevananther for serving as my dissertation committee member and for his valuable suggestions and feedback during the committee meetings. My thanks also go to Dr. Bhagavatula Moorthy for his willingness to serve as my committee member and for his availability and feedback on my presentations.

I would like to thank Dr. Song Gao at TSU for his immense help with my research. Although not in my dissertation committee, Dr. Gao has always been a source of help and guidance for my research. In addition, I would like to thank Dr. Lei Wu in Dr. Chow's lab for the collaboration on the Aim 1 project and for her patience and willingness to answer my questions about the modeling. I would also like to thank Dr. Wu for her help with the modeling work and contribution to the manuscript writing.

I would also like to thank my seniors in the lab, Dr. Pankajini Mallick and Dr. Guncha Taneja, who spent a significant amount of their own time to teach me research techniques in the early years of my Ph.D. and for always be willing to answer my questions with patience. I would also like to thank Gabriel Tao, the current graduate student for his help with my experiments.

I would like to take this opportunity to also thank the previous PPS chair, Dr. Douglas Eikenburg, PPS staff, and Ms. Melissa Nieto for their timely help. Finally, I would like to thank all my friends in the PPS department and in Houston.

ABSTRACT

Colorectal cancer (CRC) is a form of cancer that starts in the colon or rectum. According to the GLOBOCON statistics, there are over 1.8 million new colorectal cancer cases and 881,000 deaths are estimated to occur in 2018. Colorectal cancer is also the 3rd most common type of cancer diagnosed in both men and women in the USA and worldwide. Metastatic colorectal cancer (mCRC) is an advanced stage where the cancer cells from the colon or rectal tumor detach and spread to other parts of the body, such as the liver or lungs through the bloodstream. Irinotecan is an intravenous (i.v.) infusion chemotherapy drug that was approved by FDA in 1996 and it is a topoisomerase I inhibitor indicated for first-line therapy in combination with 5-fluorouracil and leucovorin for patients with metastatic colorectal cancer and Patients with metastatic colorectal cancer whose disease has recurred or progressed after initial fluorouracil-based therapy. Irinotecan belongs to a class of topoisomerase I inhibitors and it is a prodrug to its cytotoxic metabolite SN-38 (7-ethyl-10-hydroxy-camptothecin), which is about 100-1000-fold more cytotoxic than irinotecan. Although irinotecan is a very potent chemotherapy drug, elevated blood concentrations of its active metabolite, SN-38 leads to increased gastrointestinal (GI) toxicity and diarrhea in patients. Irinotecan is metabolized by Cyp3a4, carboxylesterase and Ugt1a1 enzymes and these enzymes are known to be downregulated during inflammation. Therefore, there is a possibility of reduced metabolism and clearance of irinotecan during inflammation, which may lead to increased toxicity in patients. Along with diarrhea, irinotecan chemotherapy is also associated with hepatotoxicity in patients undergoing liver resection for colorectal liver metastasis. The irinotecan associated hepatotoxicity is in the form of steatosis or steatohepatitis. These toxicities result in life-threatening complications in patients and reduce the use of irinotecan as a chemotherapeutic agent. Therefore, there is an urgency to better understand the effects of inflammation on irinotecan

PK and to develop new interventions to prevent diarrhea and steatosis associated with irinotecan. To achieve these goals, we pursued the following 3 aims. **Aim 1:** To determine the effects of inflammation on irinotecan pharmacokinetics and the development of a best-fit PK model. In this aim, we investigated the effects of inflammation on the pharmacokinetics (PK) of irinotecan (CPT-11) and its active metabolite, SN-38. Mice were i.p.-injected with either saline or lipopolysaccharide (LPS) to induce inflammation. After 16 h, irinotecan was administered orally. Blood was collected from the tail vein of mice from 0-24 h after dosing. Concentrations of irinotecan, SN-38 and SN-38G were analyzed using LC-MS/MS. The AUC, C_{max}, and t_{max} were derived using WinNonlin® 5.2. A PK model was developed using Phoenix NLME® to describe the PK of irinotecan and SN-38 during inflammation. Results indicated a significant increase in the blood concentrations of irinotecan and SN-38 in mice during inflammation. The AUC of irinotecan and SN-38 in the LPS group were 2.6 and 2-folds, respectively, of those in control saline-treated mice. The C_{max} of irinotecan and SN-38 in LPS treated mice were 2.4 and 2.3-folds of those in saline-treated mice. The PK model was successfully developed and validated. The best-fit plots of individual PK analysis showed a good correlation between observed and predicted concentrations of irinotecan and SN-38. Together, this study reveals that SN-38 concentrations are elevated during inflammation, which may increase the GI toxicity and diarrhea in patients who receive irinotecan; and the developed PK model can quantitatively describe the PK of irinotecan and SN-38 during inflammation. **Aim 2:** To determine the role of TLR2 in irinotecan-induced diarrhea and steatosis. Evidence from the literature strongly suggests that toll-like receptors (TLRs), especially TLR2 is involved in the pathogenesis of gastrointestinal and hepatotoxicity. Therefore, in this aim, we investigated the role of TLR2 in irinotecan-induced diarrhea and steatosis. Specifically, we used TLR2 WT and KO mice and treated with either saline (control) or irinotecan (treatment group) for

8 days and sacrificed the mice on day 9. To measure the extent of GI toxicity in TLR2 WT and KO mice, we conducted body weight measurements, the incidence of diarrhea, blood concentration analysis, and histological analysis of intestinal damage. Similarly, to determine the role of TLR2 in irinotecan-induced hepatotoxicity, H&E and Oil-Red-O histological analysis of liver sections, gene expression of enzymes and pro-inflammatory cytokines, and enzyme activity assays were conducted. The results indicate that the TLR2 KO mice showed significantly lower damage both in terms of diarrhea and steatosis after irinotecan treatment. Together, the results indicate a key role of TLR2 in the pathogenesis of irinotecan-induced toxicity. In the future, pharmacological inhibition of TLR2 may help in healing irinotecan-induced GI and hepatotoxicity. **Aim 3:** To determine the effects of soy isoflavones on irinotecan-induced diarrhea and steatosis. Soy isoflavones have been shown to have beneficial effects on both gastrointestinal (GI) and hepatotoxicity caused by chemotherapy. Here, we studied the effects of NovaSoy, a soy-based isoflavone concentrate with a total isoflavone of 40% (20% genistein, ~18% daidzein, ~2% other isoflavones), on irinotecan-induced diarrhea and steatosis in mice. Results showed that the mice treated with Novasoy and irinotecan (NS/IRI) showed significantly less bodyweight loss and incidence of diarrhea compared to mice treated with saline and irinotecan (Sal/IRI). Histopathological analysis of liver and intestine sections revealed a less severe fat accumulation (<10% steatosis) and intestinal damage in NS/IRI group. Analysis of liver and intestine concentrations showed less accumulation of SN-38 concentrations in the NS/IRI group compared to the Sal/IRI group. Enzyme activity assays exhibited a significant increase in the activity of carboxylesterase, whereas ugt1a1 activity is reduced. Toxicokinetic (TK) studies showed no significant changes in blood concentrations of irinotecan and metabolites. Together, the results

suggested that soy isoflavone treatment could delay the incidence of diarrhea and steatosis caused by irinotecan and can be used as an intervention to reduce the toxicities associated with irinotecan.

TABLE OF CONTENTS

LIST OF TABLES

LIST OF FIGURES

ABBREVIATIONS

ACN	Acetonitrile
APC	7-ethyl-10-[4-N-(5-aminopentanoic acid)-1-piperidino] carbonyloxycamptothecin
AUC	Area Under Curve
BCA	Bicinchoninic Acid
BSA	Bovine serum albumin
CEs	Carboxylesterases
CLM	Colorectal Liver Metastasis
C_{max}	Maximum Plasma Concentration
CPT	Camptothecin
CYP450	Cytochrome P450
DEPC	Diethylpyrocarbonate
DMEs	Drug Metabolizing Enzymes
DTT	Dithioerythritol
FA	Formic Acid
FU	Fluorouracil
IL	Interleukin
IP	Intraperitoneal

IRI	Irinotecan
IS	Internal Standard
LPS	Lipopolysaccharide
MRP	Multidrug resistance-associated protein
MyD88	Myeloid differentiation factor 88
NAFLD	Non-alcoholic fatty liver disease
NASH	Non-alcoholic steatohepatitis
NPC	7-ethyl-10-[4-(1-piperidino)-1-amino] carbonyloxycamptothecin
NO	Nitric Oxide
NF-κB	Nuclear factor-kappa B
NS	Novasoy
PK	Pharmacokinetic
PXR	Pregnane X Receptor
ROS	Reactive Oxygen Species
SAL	Saline
SN-38	7-ethyl-10-hydroxycamptothecin
SN-38G	SN-38 Glucuronide
t ½	Half-life

TLRs	Toll-like receptors
T_{max}	Time at maximum plasma concentration
TNF	Tumor Necrosis Factor
UGT	Uridine glucuronosyl transferase

CHAPTER 1

INTRODUCTION

1.1 Colorectal Cancer and Metastatic Colorectal Cancer

Colorectal cancer (CRC) is a form of cancer that starts in the colon or rectum. According to the GLOBOCON statistics, there are over 1.8 million new colorectal cancer cases and 881,000 deaths are estimated to occur in 2018.[1] Colorectal cancer is also the 3rd most common type of cancer diagnosed in both men and women in the USA and worldwide (9.7%), after lung (13.0%) and breast cancer (11.9%) and 4th most cause of cancer-related deaths, after lung, liver, and stomach cancers.[2] The estimates given by the American Cancer Society (ACS) for the number of incidences of colorectal cancer in the USA for the year 2019 are 101,420 of colon cancer and 44,180 of rectal cancer. The overall lifetime risk of developing colorectal cancer in men is about 1 in 22 and about 1 in 24 in women.[3] Specifically, the mortality rates for rectal cancer are predicted to increase by 27.8% in the United States by year 2035.[4]

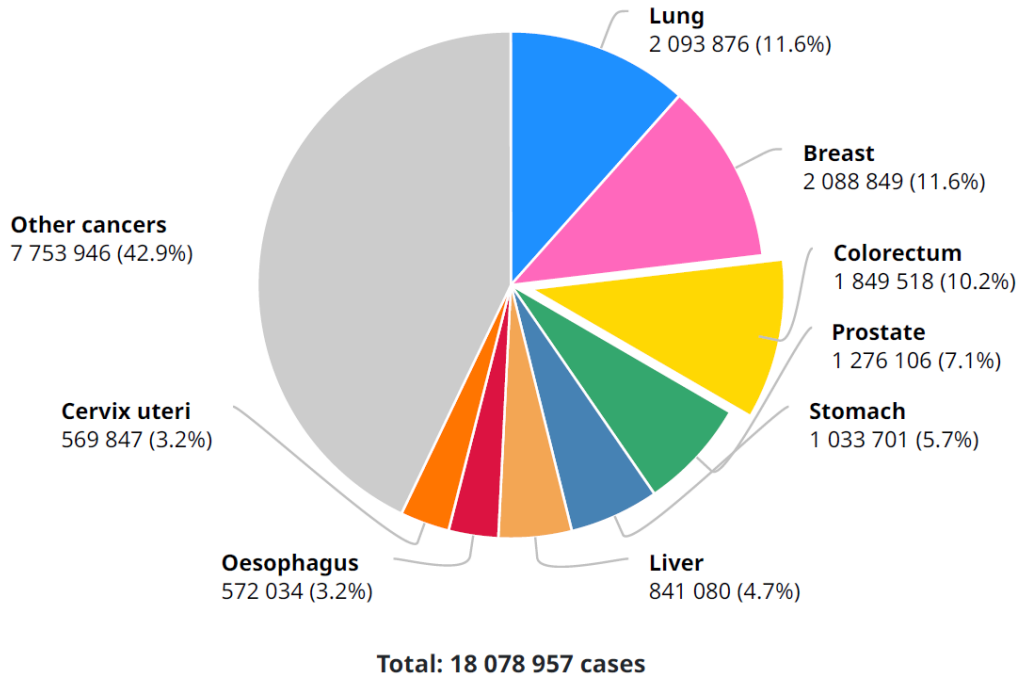

Figure 1.1. Number of new cases of Colorectal Cancer in 2018, including men and women and all ages, according to Globocan 2018 Statistics[5]

The risk factors for CRC is defined by both genetic predisposition as well as age, low-fiber diet, obesity, alcohol, cigarette smoking, and physical inactivity. Among these factors, approximately 5% of CRC cases are due to inherited genetic mutations and ~20% of cases are a result of dietary and environmental factors. Colorectal cancer results through a stepwise accumulation of genetic and epigenetic alterations, causing the transformation of normal mucosa into invasive cancer.[6]

Metastatic colorectal cancer (mCRC) is called when the cancer cells from the colon or rectal tumor detach and spread to other parts of the body, such as the liver or lungs through the bloodstream. When the cancer cells metastasize and settle on other organs, they can also form new tumors. The most common organ that is affected when colorectal cancer metastasizes is the liver. In some other cases, colorectal cancer cells may also spread to lungs, bones, spinal cord, or brain.[7] Advanced colorectal cancer is described as colorectal cancer that is either metastatic or so locally advanced and therefore a surgical resection will not likely be carried out to cure the disease. Most patients with advanced colorectal cancer undergo curative surgery and use adjuvant chemotherapy; however, approximately 50% of patients advanced colorectal cancer die eventually due to subsequent metastatic disease. Moreover, the 5-year survival rate for advanced colorectal cancer is less than 5%.[8]

Chemotherapy is the use of drugs to kill cancer cells and it is a common practice in the treatment of colorectal cancer. 2 types of chemotherapy are available: 1. Systemic chemotherapy, where drugs are given into blood through a vein or taken by mouth for systemic exposure. 2. Regional chemotherapy, in which drugs are given right into an artery that is connected to the specific part of the body with the tumor.[9] Some of the drugs that are commonly used for colorectal cancer treatment are Irinotecan (Camptosar), 5-Fluorouracil (5-FU), Capecitabine (Xeloda), and Oxaliplatin (Eloxatin). More commonly, a combination of 2 or more of these drugs is used for the

treatment to achieve a higher efficacy. Many patients with advanced colorectal cancer die without having received chemotherapy. Chemotherapy improves survival of patients by an average of 6 months and also improves the overall quality of life of patients.[8]

1.2 Irinotecan (CPT-11)

Irinotecan (CPT-11) is a semi-synthetic analog derived from a naturally occurring alkaloid called Camptothecin (CPT) and was approved by FDA in 1996.[10] Irinotecan is an intravenous (i.v.) infusion chemotherapy drug and is a topoisomerase inhibitor indicated for:

i. First-line therapy in combination with 5-fluorouracil and leucovorin for patients with metastatic colorectal cancer

ii. Patients with metastatic colorectal cancer whose disease has recurred or progressed after initial fluorouracil-based therapy.[11]

Irinotecan is given in combination with other chemotherapy drugs or as a single agent. The dosage and administration of irinotecan are:

- Regimen 1, combination therapy for colorectal cancer: CAMPTOSAR 125 mg/m2 intravenous infusion over 90 minutes on days 1, 8,15, 22 with LV 20 mg/m2 intravenous bolus infusion on days 1, 8, 15, 22 followed by 5-FU intravenous bolus infusion on days 1, 8, 15, 22 every 6 weeks.
- Regimen 2, combination therapy for colorectal cancer: CAMPTOSAR 180 mg/m2 intravenous infusion over 90 minutes on days 1, 15, 29 with LV 200 mg/m2 intravenous infusion over 2 hours on days 1, 2, 15, 16, 29, 30 followed by 5-FU 400 mg/m2 intravenous bolus infusion on days 1, 2, 15, 16, 29, 30 and 5-FU 600 mg/m2 intravenous infusion over 22 hours on days 1, 2, 15, 16, 29, 30.

- Regimen 1, Single agent for colorectal cancer: CAMPTOSAR 125 mg/m2 intravenous infusion over 90 minutes on days 1, 8, 15, 22 then 2-week rest.
- Regimen 2, single-agent for colorectal cancer: CAMPTOSAR 350 mg/m2 intravenous infusion over 90 minutes on day 1 every 3 weeks.[11]

1.3 Irinotecan: Mechanism of Action

Irinotecan belongs to a class of topoisomerase I inhibitors and it is a prodrug to its cytotoxic metabolite SN-38 (7-ethyl-10-hydroxy-camptothecin), which is about 100-1000-fold more cytotoxic than irinotecan.[12] Topoisomerase I is a 100-kD protein with enzymatic activity in the 67.7-kD region at the carboxyl-terminal end of the protein. The enzyme relaxes supercoiled double-stranded DNA, thereby facilitating normal DNA replication, recombination, and RNA transcription. Irinotecan shows its cytotoxic activity by binding noncovalently to the DNA-topoisomerase I-cleavable complex and interfering with the DNA relegation, which results in the stabilization of the cleavable complex and accumulation of protein-linked single-stranded breaks in the DNA. Although this degree of damage to DNA is not sufficient to cause cell death, the encounter of DNA replication fork creates cytotoxic double-stranded breaks in the DNA, which ultimately causes cell death.[13]

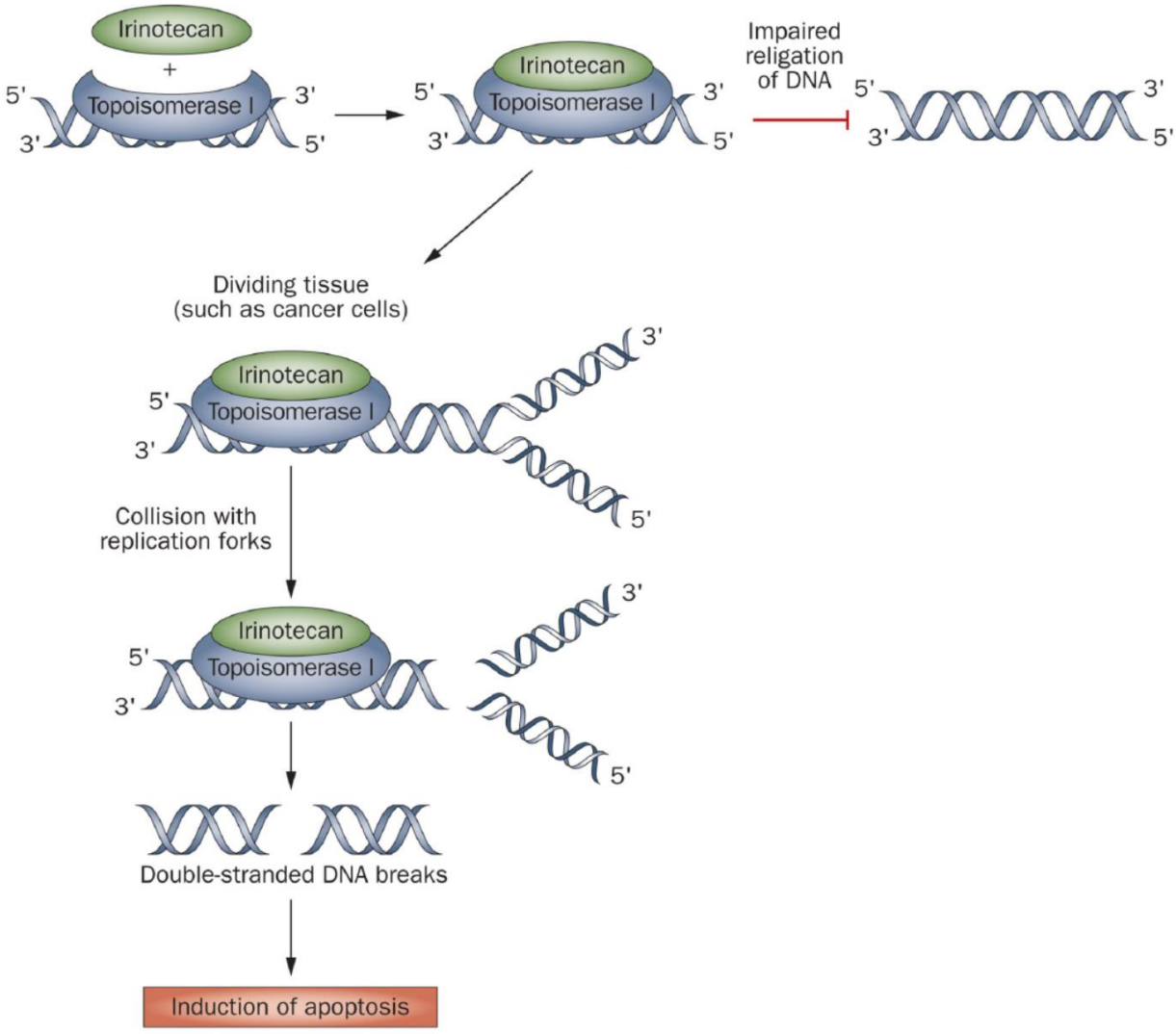

Figure 1.2. Mechanism of apoptosis induced by Irinotecan in cancer cells.[14]

1.4 Irinotecan Metabolism and Pharmacokinetics

Hepatic metabolism and biliary secretion are the major routes of irinotecan elimination in both rodents and humans. The enzymes involved irinotecan metabolism are carboxylesterases, UGTs, CYP3As, and β-glucuronidases.[12] Irinotecan is a prodrug and is converted to active metabolite SN-38 by carboxylesterase (CEs) enzyme. SN-38 is the primary metabolite and responsible for the efficacy and toxicity caused by irinotecan therapy. It is reported that the plasma of mice contains high levels of carboxylesterases and the conversion from irinotecan to SN-38 is much better than

in humans.[12] Moreover, irinotecan shows higher cytotoxic activity in cell lines having higher carboxylesterase levels. The SN-38 formed in the first step is subsequently metabolized by UGT1A1 in the liver, to form inactive SN-38 glucuronide (SN-38G). Irinotecan is also metabolized by CYP3A4/5 to form 2 inactive metabolites APC and NPC.[15] When SN-38G is excreted in bile and intestine, the intestinal bacterial β-glucuronidase enzyme converts the SN-38G to the active SN-38 metabolite.

Interindividual variability in the clearance of irinotecan is reported as ~30%, and SN-38 about 80%. Variability in SN-38 Pharmacokinetics (PK) is also one of the major reasons for irinotecan-associated toxicity.[15] Genetic polymorphism is reported with respect to UGT1A1*28 in humans, which contributes to the variability in SN-38 concentrations and cytotoxic activity.

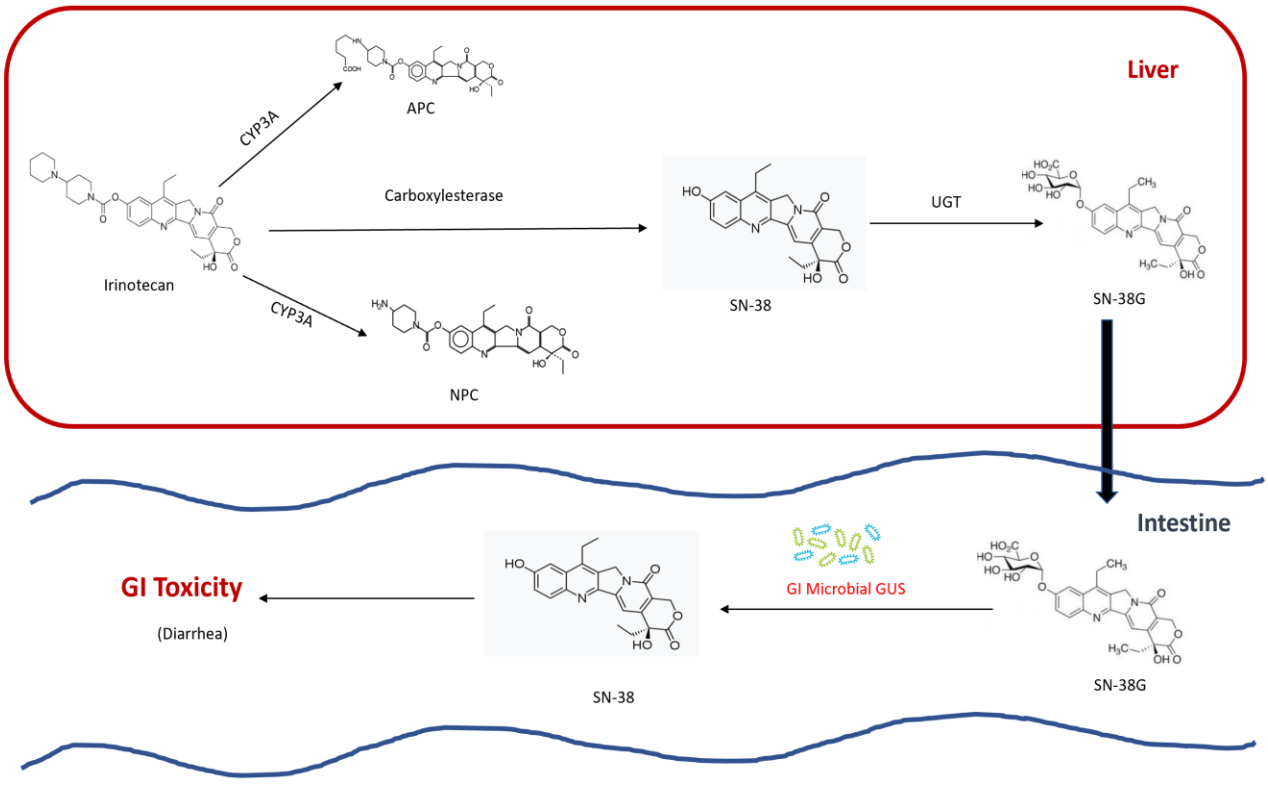

Figure 1.3 Irinotecan metabolic pathway and toxicity mechanism in humans.

In both humans and animals, studies have reported that irinotecan is excreted in bile, feces, and urine. Irinotecan, APC, and SN-38G are the major compounds eliminated in the urine within 24 h after irinotecan administration. SN-38G is more predominantly eliminated by kidneys, owing to the presence of the polar glucuronic acid group.[12] The biliary excretion of irinotecan, SN-38, and SN-38G ranges between 3-22, 0.1-0.9, and 0.6-1.1%, respectively.[16] NPC was also detected in bile at negligible concentrations. A mass balance study found that the major excretion of irinotecan is via fecal route, with 63.7% of administered drug recovered.[17] Similarly, a very high SN-38 and low SN-38G concentrations in the feces samples suggest that β-glucuronidase activity plays a major role in the excretion of SN-38 and SN-38G in human intestinal contents.[17] APC and NPC are also mainly excreted in feces.

The fact that irinotecan is a substrate of CYP3A also makes the drug prone to drug-drug interactions (DDIs). DDIs may arise as a result of altered pharmacokinetics or pharmacodynamics (PK/PD). In most cases, the DDIs from PK alterations result from the combination therapy where other drugs, such as 5-Fluorouracil are co-administered along with irinotecan.

1.5 Irinotecan Treatment in Metastatic Colorectal Cancer (mCRC)

As described earlier, colorectal cancer cells metastasize and spread to other organs. The liver is the most commonly affected organ, and this is due to the blood supply from the colon is connected to the liver. This stage is also called Advanced Colorectal Cancer. When colorectal cancer is diagnosed in early stages, it can be cured by performing a radical resection. Most often, the patients are diagnosed when colorectal cancer reaches the liver (Colorectal Liver Metastasis) and surgical resection of liver metastasis is typically employed as a treatment option. Surgeons can remove both colon and liver tumors. However, if the cancer is advanced, chemotherapy is typically used as neoadjuvant therapy to reduce the tumor size before surgery can be done. For this purpose,

irinotecan is commonly used as a chemotherapeutic agent. Irinotecan chemotherapy often is also combined with surgery or other therapies.[18]

Previously, the combination of fluorouracil and leucovorin was used as standard therapy for metastatic colorectal cancer.[19] However, studies have shown that a synergistic or additive effect exists between SN-38 (the active metabolite of irinotecan), oxaliplatin, 5-FU, which prolongs the survival in patients with colorectal liver metastasis that is refractory after fluorouracil and leucovorin treatment.[20] Currently, Irinotecan is used as a first-line therapy along with 5-fluorouracil and leucovorin for colorectal liver metastasis.[11] Owing to its broad-spectrum activity, irinotecan is also widely used in other forms of cancer, including non-small cell lung cancer (NSCLC), pancreatic, cervical, ovarian, leukemia, esophageal, and gastric cancers.[21]

1.6 Irinotecan-induced Toxicity

1.6.1 Gastrointestinal Toxicity: Diarrhea

Irinotecan is a potent inhibitor of topoisomerase I enzyme and widely used to treat various cancers. However, irinotecan treatment induces severe gastrointestinal (GI) toxicity, especially late-onset diarrhea. Diarrhea is a common adverse reaction and dose-limiting toxicity of irinotecan therapy and therefore limiting the clinical application of irinotecan.[22] Along with irinotecan, a variety of other chemotherapeutic agents for colorectal cancer treatment, including fluorouracil (FU) and capecitabine exhibit dose-limiting toxicities in the form of diarrhea. These drugs either in combination or alone cause diarrhea in ~50-80% of patients. Diarrhea caused by Chemotherapy is categorized by the National Cancer Institute into different grades (grade 1-5) based on the severity of toxicity in patients. Low-Grade diarrhea (grade 1-2) caused by chemotherapy can also significantly interfere with the treatment and can cause treatment delays in 28-71% of patients, dose reductions in 22-45% of patients, or even complete treatment discontinuation in 3-15% of

patients.[22] On the other hand, more severe diarrhea (grade 3-4) can cause remarkable dehydration, imbalance of electrolytes, nutritional deficiency and can ultimately affect patient survival rate in about 5% of patients.[22] Continuous and severe diarrhea with irinotecan treatment is often debilitating and also can be life-threatening. Although treatment options such as octreotide and loperamide are given to patients to reduce the severity of diarrhea with irinotecan treatment, they are non-specific and often give unsatisfactory outcomes.[22–24] Therefore, there is currently a great interest in inventing new herbal agents that can alleviate diarrhea induced by irinotecan.[22] Along with diarrhea, the other common adverse reactions that patients experience with irinotecan chemotherapy are neutropenia and myelosuppression.

	Grade				
	1	2	3	4	5
Diarrhea (version 3.0)	Increase of <4 stools per day over baseline; mild increase in ostomy output compared to baseline	Increase of 4–6 stools per day over baseline; iv fluids indicated <24 hrs; moderate increase in ostomy output compared to baseline; not interfering with ADL	Increase of ≥7 stools per day over baseline; incontinence; iv fluids ≥24 hrs; hospitalization; severe increase in ostomy output compared to baseline; inter-fering with ADL	Life-threatening consequences (eg hemodynamic collapse)	Death
Diarrhea (version 4.02)	Increase of <4 stools per day over baseline; mild increase in ostomy output compared to baseline	Increase of 4–6 stools per day over baseline; moderate increase in ostomy output compared to baseline	Increase of ≥7 stools per day over baseline; incontinence; hospitalization indicated; severe increase in ostomy output compared to baseline; limiting self care ADL	Life-threatening consequences; urgent intervention indicated	Death

ADL, activities of daily living; iv, intravenous.

Table 1.1 Common toxicity criteria for diarrhea induced by chemotherapy (National Cancer Institute)[25]

The intestinal toxicity of irinotecan is regulated by its active metabolite, SN-38.[26] Although the SN-38 induced toxicity has been explained by various mechanisms, the explanations are controversial and the underlying pathophysiology is still under investigation. SN-38 causes

delayed diarrhea by structurally and functionally destroying the intestinal epithelium. In the irinotecan metabolic pathway, SN-38 is detoxified to SN-38G by UGT1A1 enzyme in liver and irinotecan and its metabolites are excreted through bile and urine. In the intestine, the SN-38G is deconjugated back to SN-38 by intestinal bacterial β-glucuronidase, causing SN-38 to accumulate in the intestinal lumen. This buildup of SN-38 causes injury to the intestinal epithelial cells and therefore induces delayed-onset diarrhea.[26] Irinotecan-induced toxicity is also attributed to polymorphisms in UGT1A1*28. A meta-analysis study in Caucasians showed a 2-fold increase in the risk of diarrhea with the UGT1A1*28/*28 genotype.[27] The NF-κB and associated pro-inflammatory cytokine upregulation with irinotecan treatment are also suggested to play a role in the induction of mucositis.[28] Ribeiro et al. 2016 observed that IL-1β contributes to the apoptosis of enterocytes in mucositis caused by chemotherapy treatment.[29] It is also suggested that intestinal microbiota, the presence of the β-glucuronidase enzyme, and the enterohepatic recirculation of the active metabolite SN-38 is also suggested to contribute to irinotecan-induced diarrhea and mucositis. Moreover, the pathogenesis is also thought to be mediated by IL-1/Toll-like receptor family members, leading to epithelial cell apoptosis.[29] One study by Stringer et al. 2009 suggested that irinotecan treatment induces mucin secretion, which leads to altered mucin expression and therefore contributes to irinotecan-induced diarrhea.[30] The toxicity induced by irinotecan therapy in the intestinal mucosa can be distinguished by symptoms such as abdominal pain, bloody diarrhea, reduced body weight, cytokine upregulation, that causes inflammation and ulceration in the intestine.[26]

1.6.2 Hepatotoxicity: Steatosis and Steatohepatitis

1.6.2.1 Irinotecan Chemotherapy in Patients with Liver Resections

The liver is the most common organ for colorectal cancer metastasis due to the mesenteric venous outflow via the portal vein, which carries the tumor cells to the liver. Approximately 15-20% of patients with colorectal cancer show liver metastasis at presentation and about 50% of patients will eventually develop liver metastasis at a certain point. Apart from colorectal cancer, liver metastasis is also seen in cases of lung, breast, pancreatic, and gastric cancer types as well.[31] When colorectal cancer metastasizes and reaches the liver, often the metastases are surgically removable. In those patients where surgical resection is possible, the overall survival rate is in the range of 25-58%. Often, surgical resection is only limited to patients with good preoperative health, anatomic location. Upon initial presentation, patients are typically categorized into either as having surgically resectable, potentially convertible, or unresectable disease. In recent times, more importance is given to surgical management of liver metastasis due to improved surgical techniques and postoperative care. However, approximately only 20% of patients can be offered a curative surgical resection at the time of presentation (80% of patients have unresectable liver).[31] If no further treatment is possible, the median survival rate for patients who developed colorectal liver metastasis is very poor (30% 1-year survival rate and 0-5% 5-year survival rate). In patients with surgically resectable livers and who do not undergo surgery, the survival rates are slightly better (1-year survival rates from 20-80%).[32]

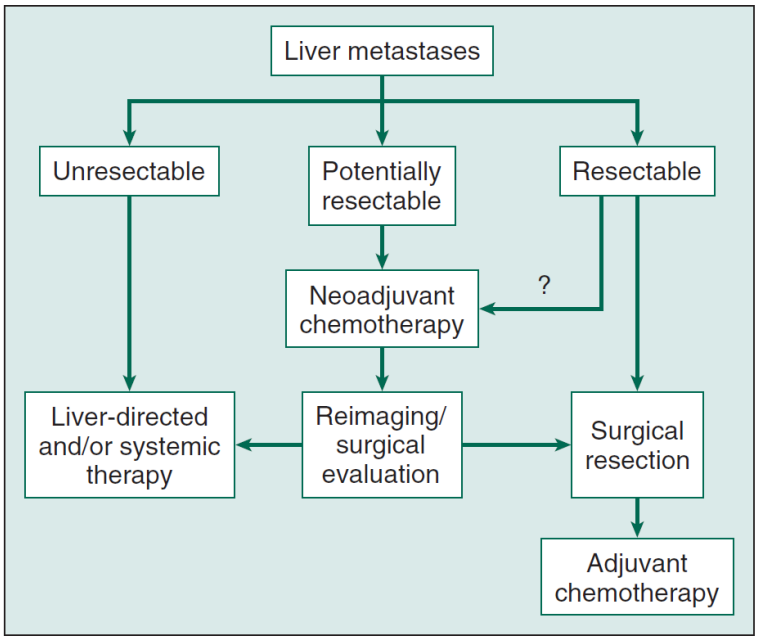

Figure 1.4. The general approach to management in patients with colorectal liver metastasis[32]

Patients who have borderline resectable liver disease are typically given irinotecan as neoadjuvant chemotherapy for tumor regression. Although traditionally chemotherapy is used postoperatively, it has been increasingly used in preoperative therapy before liver resection due to advantages such as a potential downsizing of the tumor prior to resection and to increase curative resection rates.[33] Irinotecan is used along with leucovorin and 5-FU to treat metastatic colorectala cancer. Irinotecan is given in 2 regimens. Regimen 1, combination therapy for colorectal cancer: CAMPTOSAR 125 mg/m^2 intravenous infusion over 90 minutes on days 1, 8,15, 22 with LV 20 mg/m^2 intravenous bolus infusion on days 1, 8, 15, 22 followed by 5-FU intravenous bolus infusion on days 1, 8, 15, 22 every 6 weeks. Regimen 2, combination therapy for colorectal cancer: CAMPTOSAR 180 mg/m2 intravenous infusion over 90 minutes on days 1, 15, 29 with LV 200 mg/m^2 intravenous infusion over 2 hours on days 1, 2, 15, 16, 29, 30 followed by 5-FU 400 mg/m^2 intravenous bolus infusion on days 1, 2, 15, 16, 29, 30 and 5-FU 600 mg/m^2 intravenous infusion over 22 hours on days 1, 2, 15, 16, 29, 30. Chemotherapy-induced steatosis has been shown to delay or prevent liver

regeneration. Moreover, chemotherapy before resection of colorectal liver metastasis may cause hepatic injury and affect the postoperative outcome. In a study conducted by Vauthey et al. 2006, 400 patients who underwent resection of colorectal liver metastasis were studied for the effects of chemotherapy on the perioperative outcome and found that irinotecan therapy was associated with steatohepatitis in 20.2% of patients compared 4.4% with no chemotherapy.[32] In addition, patients with steatohepatitis showed a much higher 90-day mortality rate compared with patients who did not have steatohepatitis (14.7% vs 1.6%, respectively).[32] In general, irinotecan chemotherapy is linked with steatosis or steatohepatitis in 12-25% of patients. In a systematic review by Zorzi et al. 2007, it was reported that non-alcoholic steatohepatitis, a serious form of non-alcoholic fatty liver disease (NAFLD) can result with irinotecan treatment, especially in obese patients.[34] The steatohepatitis occurred with pre-operative irinotecan therapy includes inflammation and hepatocyte injury and can increase morbidity and mortality rate after liver resection.

1.6.2.2 Mechanisms of Irinotecan-induced Steatosis and Steatohepatitis: Clinical and Preclinical Evidence

In general, non-alcoholic steatosis or steatohepatitis is believed to be the hepatic manifestation of metabolic syndrome and insulin resistance. This can further develop to cirrhosis and hepatocellular carcinoma. The occurrence of steatohepatitis is much more severe than simple steatosis when conducting a liver resection. Studies have shown that patients with steatohepatitis experience an increase in perioperative mortality, especially death from liver failure.[32,35] The presence of steatohepatitis in irinotecan treated patients results in a significant increase in the 90-day perioperative mortality.

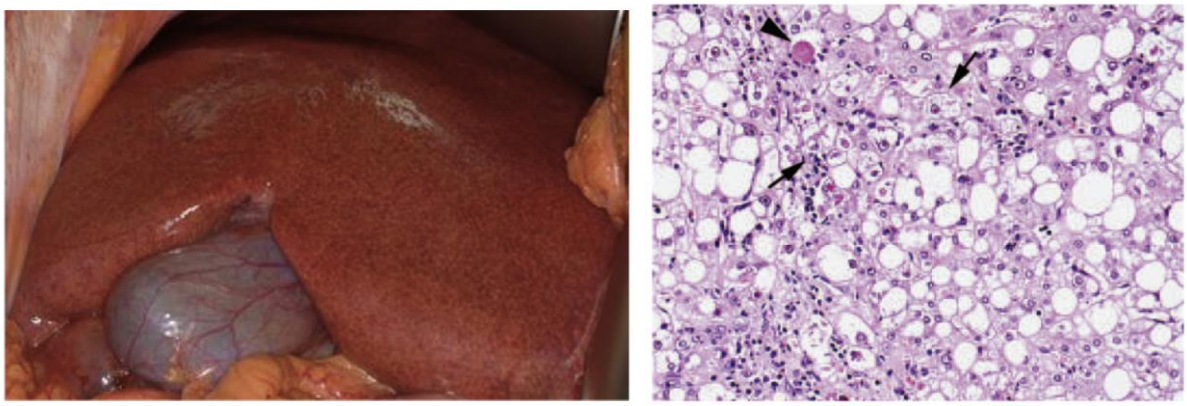

(A) (B)

Figure 1.5. (A) Image of the liver with steatohepatitis induced by Irinotecan in humans. (B) Histology image of a liver section showing chemotherapy-induced steatohepatitis in humans.[35]

Although the precise mechanisms of irinotecan-induced steatosis or steatohepatitis remain unknown, several mechanisms have been widely believed. For example, hepatotoxicity thought to involve a 2-hit process. Firstly, there is an accumulation of fat droplets in the liver cells caused by oxidative stress due to irinotecan chemotherapy. As a next step, the development of hepatotoxicity occurs. It is also believed that mitochondrial dysfunction plays a role in the development of steatohepatitis. The mitochondrial DNA (mtDNA) that is located in the mitochondrial matrix is responsible for encoding the expression of various polypeptides and mitochondrial function and the respiratory chain are dependent on the expression of these polypeptides. Adequate levels of mtDNA are required for the proper function of mitochondria and if the mtDNA levels become lower than 20-40% basal levels, there can be a dysfunction of mitochondria. This can result in the elevated formation of reactive oxygen species (ROS) via the dysfunctional respiratory chain, increased lipid peroxidation, and damage of beta-oxidation, which can further release the pro-apoptotic (TNF-α), pro-fibrotic (TGF-β) cytokines by Kupffer cells. This will ultimately lead to inflammation, cell death, and fibrosis. Therefore, these pathways can be targets for novel therapy

to prevent chemotherapy-induced hepatotoxicity. Moreover, irinotecan is a topoisomerase I inhibitor and therefore impairs the mitochondrial topoisomerases and inhibits the mtDNA replication, which can also be a possible mechanism by which irinotecan-induced steatosis or steatohepatitis occurs.[35] In support of this phenomenon, several studies have shown that mtDNA also contains topoisomerase I[36] and mtDNA is sensitive to camptothecin, from where irinotecan is derived.[37,38] Overall, the mtDNA levels are depleted with irinotecan treatment, which can lead to mitochondrial dysfunction and steatohepatitis.

1.7 Inflammation and Drug Metabolism

1.7.1 Effects of Inflammation on Drug Metabolism and Pharmacokinetics

Inflammatory responses in humans are complex and can occur in response to a variety of pathological disorders, including infection, tumors, autoimmune disease and damage to tissue. Typically, toll-like receptors are activated when there is inflammation, which triggers the release of pro-inflammatory cytokines, mediators, acute phase proteins, and hormones. When these agents are released, an acute phase response occurs and as a result, a number of proteins are formed.[39] Lipopolysaccharide (LPS) is an active component derived from the outer membrane of gram-negative bacteria and when LPS is injected in rodents, it causes the secretion of various inflammatory cytokine such as tumor necrosis factor-α (TNF-α), IL-1β, and IL-6 and also interferons.[40]

The drug metabolism and pharmacokinetics could be altered when there is an infection or inflammation due to the changes in the regulation of DMEs and transporters. This change in the drug pharmacokinetics because of the inflammatory disease state could be due to multiple mechanisms. The major organs responsible for drug clearance are liver and kidney and any change in the blood flow to these organs could also change the drug clearance rates. The liver is the major

site of drug clearance and changes in the liver enzyme expression and activity could modify the hepatic clearance of the drugs, whose clearance is not dependent on blood flow.[41] Similarly, changes in the expression of DMEs and transporters in the liver as well as in the epithelial cells of small intestine triggered by inflammation could also affect the bioavailability of drugs. For example, the absorption of the drugs through the GI tract can be changed. Importantly, changes in the CYP expression could trigger the changes in the pharmacokinetics of drugs.

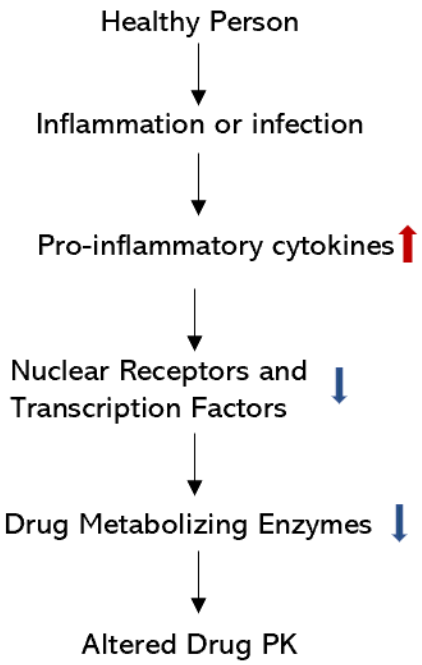

Figure 1.6. Effects of of inflammation on drug metabolizing enzymes and pharmacokinetics of drugs.

Cancer also has been associated with inflammation at every stage of the disease: risk of development, initiation, invasion, metastasis, and mortality.[42] For example, Rivory et al. 2002 showed that cancer patients with an acute phase response had reduced metabolism compared to controls, which may reduce the safety of chemotherapy in cancer patients.[43] Moreover, circulating

inflammatory markers such as C-reactive protein and IL-6 have been shown to correlate with drug toxicity due to reduced CYP3A4 dependent metabolism.[44]

1.7.2 Regulation of Drug Metabolizing Enzymes and Transporters During Inflammation

A vast number of papers in the literature have reported that during inflammation, the expression of drug-metabolizing enzymes (DMEs) is downregulated for the most part; however, in some cases, an upregulation of few enzymes is also reported. Witkamp et al. studied the effects of LPS induced acute phase response on the hepatic CYP450-mediated drug metabolism and found induction of TNF-α and IL-6 serum levels within 1-2 h of IV administration of LPS. Furthermore, this study also found that the total CYP450 content and microsomal CYP450-dependent activities were significantly decreased after 24 h of LPS injection.[45] Watson et al. investigated the effects of endotoxin injection (8 mg/kg) on the activities of GST and UGT in rats and reported a significant decrease in their activities after 24 h and remained lower until 72 h.[46] IL-6 is the main regulator of the hepatic phase response and Jover et al. discovered that injection of IL-6 downregulates human CYP3A4 via translational induction of C/EBPβ-LIP.[47] The effects of LPS, IL-6, TNF-α, and interferon γ were also studied on the expression of CYP enzymes in human hepatocytes by Aitken et al. 2007. This study found that the expression of CY3A4 and CYP2C8 were downregulated with all cytokine treatments. However, CYP2C18 in the liver was not affected, whereas other CYP2C enzymes showed cytokine-specific changes.[48]

The drug-metabolizing enzymes and transporters involved in irinotecan metabolism are also affected by inflammation and disease states. Specifically, cyp3a11 RNA levels are reduced in mouse liver by lipopolysaccharide (LPS), or lipoteichoic acid (LTA), which are components of gram-negative and gram-positive bacteria, respectively[49,50]. Treatment with LPS was shown to decrease the expression and hydrolytic activity of human carboxylesterase 1 and 2 (hCE 1 and

hCE 2) *in vitro* and *in vivo*[51]. Hepatic expression of the phase-II enzyme, ugt1a1 was also reduced by LPS treatment for 16 h in mice[52]. LPS also reduced the mRNA and protein expression of Mdr1 (P-glycoprotein), Bcrp (breast cancer resistance protein), and Mrp4 (multi-drug resistance associated protein 4) in mice microglia.[53,54] Vee et al. determined the effects of IL-1β 24 h treatment on expression of organic onion transporters in primary human hepatocytes and found that the expression of MRP2, MRP3, MRP4, and BCRP were downregulated at the mRNA levels.[55] Therefore, it is likely that irinotecan metabolism and PK will be altered during infection or inflammation due to the reduced expression and activity of several key enzymes.

Enzyme	mRNA Expression	Protein Expression	Enzyme Activity	Reference
CYP3A4	↓	↓	↓	Ghose et al. 2009 & Gandhi et al. 2011
Carboxyl Esterase 1&2	↓	↓	↓	Mao et al., 2011
UGT1A1	↓	↓	↓	Richardson, 2006; Alkharfy 2008

(A)

Enzyme	mRNA Expression	Protein Expression	Enzyme Activity	Reference
CYP3A4	↓	↓	↓	Kalitsky-Szirtes et al., DMD 32:20–27, 2004
Carboxylesterase 1&2	↓	↓	↓	Yang, L. et al. 2010
UGT1A1	↓	↓	↓	Panaro et al. 2010
β-Glucuronidase	Unknown	Unknown	↑	Shimoi et al. 2005

(B)

Figure 1.7. Regulation of enzymes involved in the irinotecan metabolic pathway during inflammation in liver (A) and intestine (B).

1.7.3 Mechanisms of DME Regulation During Inflammation

The downregulation of CYP450 during inflammation involves a variety of mechanisms that are common to host defense mechanisms including the formation of a series of mediators. The release of these mediators generally results in the loss of the enzyme at the gene expression or enzyme stability level.[56] Interferons have been shown to reduce different forms of enzymes in rodents. Specifically, humans treated with IFN-2b showed a decrease in the CYP1A2 by more than 60%. Cytokines such as IL-1, IL-1α, IL-1β, IL-6, TNF-α have also been proven to show downregulatory effects on CYP450 similar to inflammation. Moreover, when there is an inflammatory stimulus, Nitric Oxide (NO) is formed in response, which could also alter CYP450 by reducing CYP450 mRNA levels, and altering the enzyme protein.[56] It is also suggested that oxidative stress is involved in enzyme loss during inflammation. It is widely accepted that when there is inflammation or after administration of cytokines, for most of the enzyme forms, there is a loss in the specific mRNA expression and subsequent protein synthesis. Typically, the loss in mRNA precedes the loss in enzyme activity.[56]

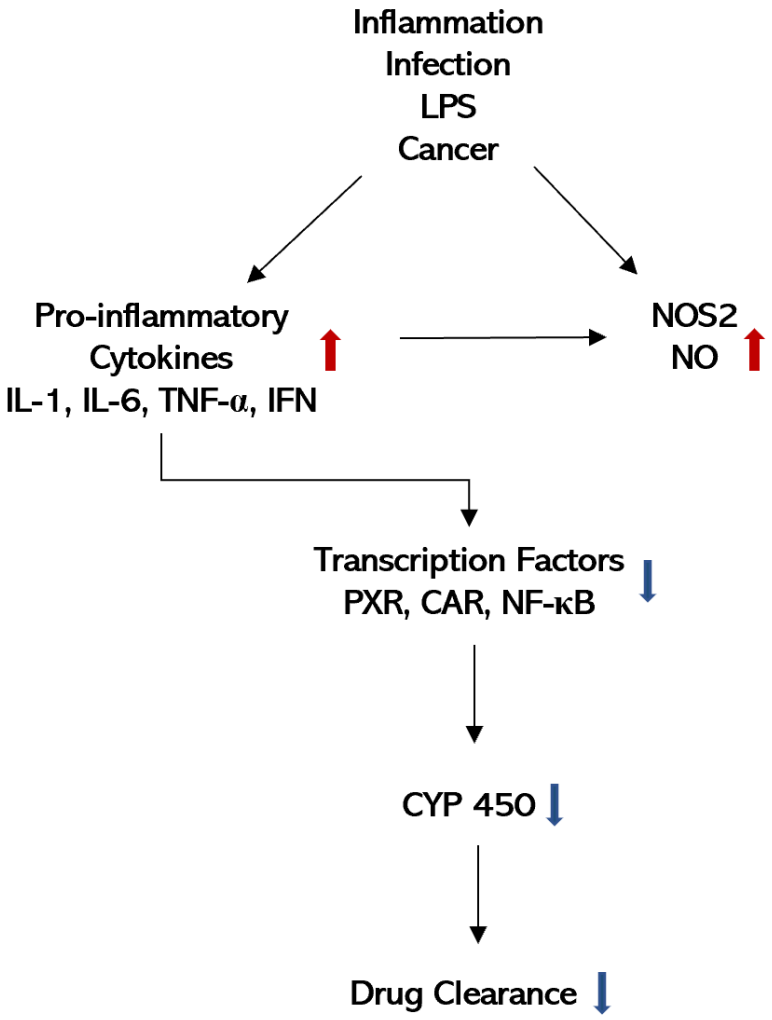

Figure 1.8. The potential mechanism for the downregulation of CYP450 enzyme during inflammation. Mechanism adapted from Reference[56].

1.8 Toll-like Receptors (TLRs)

Toll-like receptors (TLRs) play an important role in the activation of innate immunity by recognizing specific patterns of microbial components, by which TLRs sense the invasion of pathogenic microorganisms. In addition, stimulation of various TLRs triggers different patterns of gene expression. This, in turn, activates the innate immunity and also causes the development of antigen-specific acquired immunity.[57] TLRs are the type I integral membrane glycoproteins.

Lipopolysaccharide (LPS) is a bacterial endotoxin that activates the TLR4 receptor, whereas C3H/HeJ mice do not respond to LPS treatment because of a mutation in the TLR4 gene, which abrogates LPS signaling. Different TLRs can recognize various structurally unrelated compounds. TLR1, TLR2, and TLR4 are membrane receptors and are located on the cell surface and are recruited phagosomes after activation by their ligands, whereas TLR3, TLR7, and TLR 9 are not present on the cell surface and recognize the nucleic acid-like structures.[57]

After binding with the ligand, TLRs/IL-1Rs dimerize and experience a conformational change, which then recruits downstream signaling molecules. The downstream molecules include the adaptor molecule myeloid differentiation primary response protein 88 (MyD88), IRAKs, and TAK-1.[57] The MyD88 was first characterized as a critical component for the activation of innate immunity by all toll-like receptors. MyD88 was originally identified as a gene and subsequently cloned as an adaptor molecule that recruits IRAK to the IL-1R complex after stimulation with IL-1. MyD88 serves as an adaptor linking TLRs and IL-1Rs with downstream molecules.[57] Mice lacking MyD88 do not generate TNF-α or IL-6 when exposed to IL-1 or other microbial components that activate TLR2, TLR4, TLR5, TLR7 or TLR9. Hence, MyD88 is an essential adaptor molecule for responses to a wide variety of microbial components. More in-depth studies have identified the presence of 2 pathways: MyD88-dependent and MyD88-independent. However, both of these signaling pathways mediate the LPS signaling. As an example, a TLR2 ligand, mycoplasmal lipopeptide based activation of NF-κB is totally abolished in macrophages that are MyD88 deficient; however, the activation of NF-κB is present in TLR4 activation by LPS. The discovery of the MyD88-independent pathway led to the characterization of the TLR signaling pathways. There are several adaptors and these adaptors are used by different TLRs and the activation of these TLRs causes various patterns of gene expression.[57]

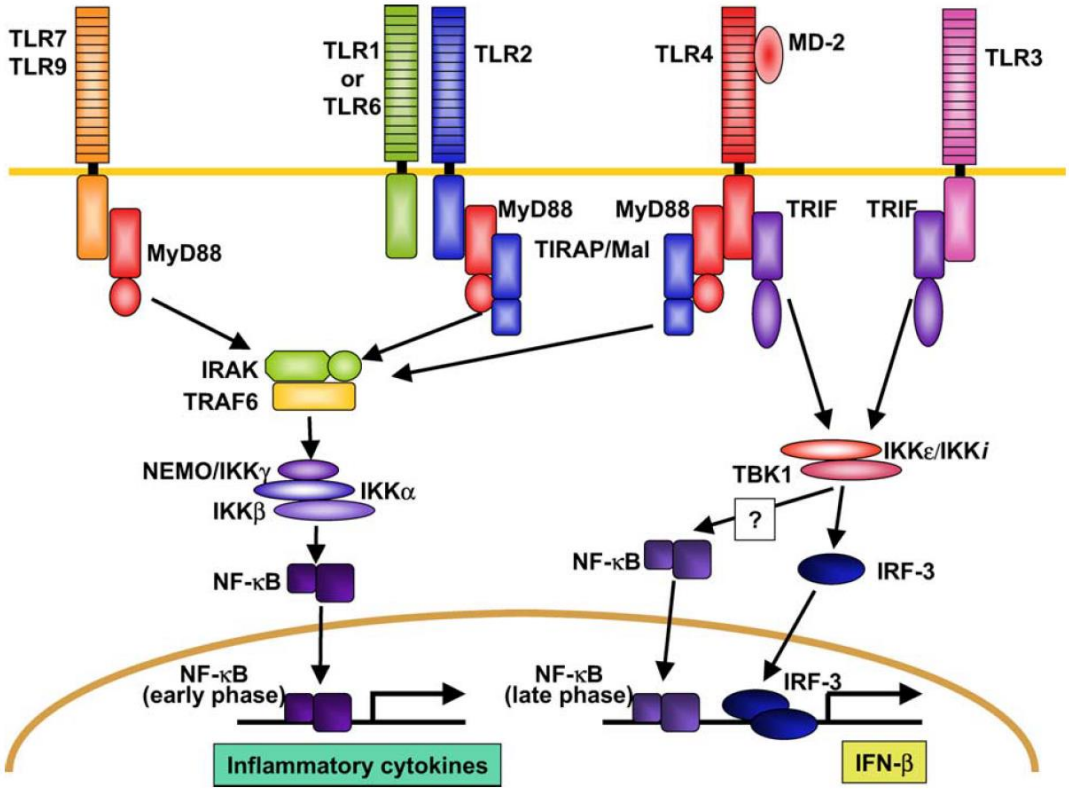

Figure 1.9. TLR signaling and TIR domain-containing adaptors.[58]

1.8.1 Role of TLRs in the Development of Steatosis and Steatohepatitis

Toll-like receptors have also been suggested to play a role in the development of steatosis. For example, metabolic syndrome is well known to induce fat accumulation in hepatocytes and one study by Himes et al. reported that mice lacking TLR2 are protected from hepatic steatosis and these mice also showed diminished inflammatory cytokine expression.[59] Gut-derived bacterial endotoxins also may play a role in the development of non-alcoholic fatty liver disease (NAFLD). A study measured the expression of TLRs 1-9 in mice liver with fructose-induced hepatic steatosis and found that the expression of TLR 1-4 and 6-8 were significantly induced.[60] Owing to the amount of evidence in the literature suggesting a key role of toll-like receptors, especially TLR2 in the pathogenesis hepatotoxicity, it is important to evaluate the role of TLR2 in the pathogenesis

of irinotecan-induced liver toxicity. The evidence also suggests that pharmacological inhibition of these TLRs may reduce toxicity following chemotherapy.[29]

1.8.2 Role of TLRs in the Development of Gastrointestinal Toxicity

Gastrointestinal mucositis is a major side effect caused by the cytotoxic effects of chemotherapy. Toll-like receptor 2 (TLR2) plays a key role in the initiation and maintenance of innate immune responses and previous research has shown that TLRs expression may be altered after chemotherapy treatment and correlate well with gastrointestinal mucositis.[61] Several studies have found increased mRNA expression and protein levels of TLR2 along with TLR4 in samples of patients with gastrointestinal inflammatory diseases such as coeliac disease, inflammatory bowel disease and ulcerative colitis .[62–64] These studies suggest a potential mechanism that TLRs mediate gastrointestinal dysfunction and pain. Specifically, a study by Wardill et al. identified that TLR4 mediates the irinotecan-induced gut toxicity and pain and suggest that TLR4 can be a target for improved toxicity outcomes.[65] In this study, the authors aimed to investigate if TLR4 deletion improves irinotecan-induced gut toxicity and pain. Therefore, 42 female wild-type mice and 42 TLR4 null (-/-) BALB/c mice were given i.p. dose of irinotecan and the gut toxicity was assessed by measuring clinical and histopathological markers, permeability assays, and inflammatory markers. The authors found that the mice with TLR4 deletion showed attenuation in gut toxicity with improved weight loss and diarrhea. Moreover, the intestinal permeability and LPS translocation were higher in wild-type mice than mice with TLR4 deletion.[65] Another study by Frolova et al. investigated the expression of TLR2 and TLR4 in Biopsy samples of patients with inflammatory bowel diseases.[64] Specifically, small intestine and colon samples were obtained from patients with Crohn's disease and Ulcerative colitis and performed a immunohistochemical analysis of cryostat sections using polyclonal and monoclonal antibodies specific for TLR2 and

TLR4 and found that the TLR2 expression in the terminal ileum of the collected patient's samples was significantly upregulated compared to controls.[64] A more recent study by Fakiha et al., 2019 showed that Amitriptyline, which is known to inhibit TLR2 and TLR4 activity in in vitro models, also inhibited diarrhea and colonic apoptosis caused by irinotecan treatment in rats.[66] TLR mediated inflammatory pathways have also been linked with chemotherapy-induced gut toxicity and pain.[67] The alimentary mucositis caused by chemotherapy is also heavily linked with the human gut microbiome and bacteria and these bacteria is tightly regulated by the TLR family, because TLRs play a vital role in the gut homeostasis and bacterial regulation.[68] A review by Ribeiro et al. suggests that TLR2 is a potential therapeutic target to modulate or minimize the toxicity associated with chemotherapy, and also to optimize cancer treatment dosing and clinical outcomes. Another review by Stringer reports that TLR2 along with TLR4, TLR5, and TLR9 are involved in intestinal mucositis.[69] TLR-2/GSK-3β signaling pathway also has been suggested to play a key role in the development of intestinal mucositis caused by doxorubicin.[70] More importantly, a study investigated the involvement of TLRs and MyD88 in the pathogenesis of intestinal mucositis caused by anticancer regimens using MyD88- and TLR2-knock out mice. This study found that genetic deletion of TLR2 and MyD88 effectively controlled the signs of intestinal injury when compared with wild-type control mice.[71]

1.9 Soy Isoflavones

Scientific evidence both in the forms of experimental and epidemiological studies proves that isoflavones show beneficial effects on chronic diseases such as cancer, diabetes, and various other forms of disease.[72] Isoflavones are widely found in soybeans and they exhibit similar structure to the estrogen hormone and therefore are suggested to share some of the physiological properties of estrogen. In addition to showing antiestrogen activity, their properties may also impact many

biological and physiological processes. More studies in the literature suggest that people with low intake of soy isoflavones, such as daidzein and genistein exhibit a higher incidence of certain types of cancer and also cardiovascular diseases. According to FDA, it is suggested that 40-60 mg/day of isoflavone would exert beneficial effects.[72] Because of the cholesterol-lowering effect of soy protein, it has been widely studied for mechanisms and soy protein was approved by FDA in 1999. Soy is now considered a functional food with the prevention and treatment of multiple diseases. Different types of isoflavones concentrates are available as dietary supplements in the powder form. Novasoy 400 is a soy-based isoflavone concentrate extracted from soybeans and contain one of the highest ratio of isoflavones and also maintain both aglycone and glycoside isoforms, similar to soybeans or unfermented soy foods. Specifically, Novasoy contains 40% of total isoflavones.[73] Genistein is the most active and abundant isoflavone in soy.

1.9.1 Protective Effects of Soy Isoflavones on hepatotoxicity

Isoflavones have shown protective effects against fatty liver disease by various novel mechanisms.[74] These include modulation of fatty acid β-oxidation, oxidative stress, and lipid synthesis. The aldose reductase/polyol pathway is involved in the development of the fatty liver disease by altering the hepatic fructose production, PPAR-α activity, intestinal bacterial endotoxin triggered cytokine release, and also CYP450-2E1 expression. Soy isoflavones showed potent aldose reductase/polyol pathway inhibitory activity. More specifically, isoflavones are suggested to block the Aldose reductase (AR)/polyol pathway and as a result, reduce the fructose production and fat accumulation in the liver. Moreover, the inhibition of AR/polyol pathway in rodents by isoflavones may also improve PPAR-α mediated fatty acid oxidation, decrease steatosis, and inhibit oxidative stress and cytokine over-secretion in the gut to prevent the progression of fatty liver disease.[74] Dietary isoflavones have been shown to be protective against endotoxin-induced

inflammatory reactions in both the liver and the intestine. In a study by Paradkar et al., the anti-inflammatory activity of dietary isoflavones was examined.[75] Mice were i.p. injected with LPS and Novasoy, a dietary soy isoflavone extract was given to mice and the protective effects of both liver and intestinal damage were measured. Specifically, the LPS-induced decrease in the liver antioxidant glutathione levels was alleviated in mice fed with Novasoy.

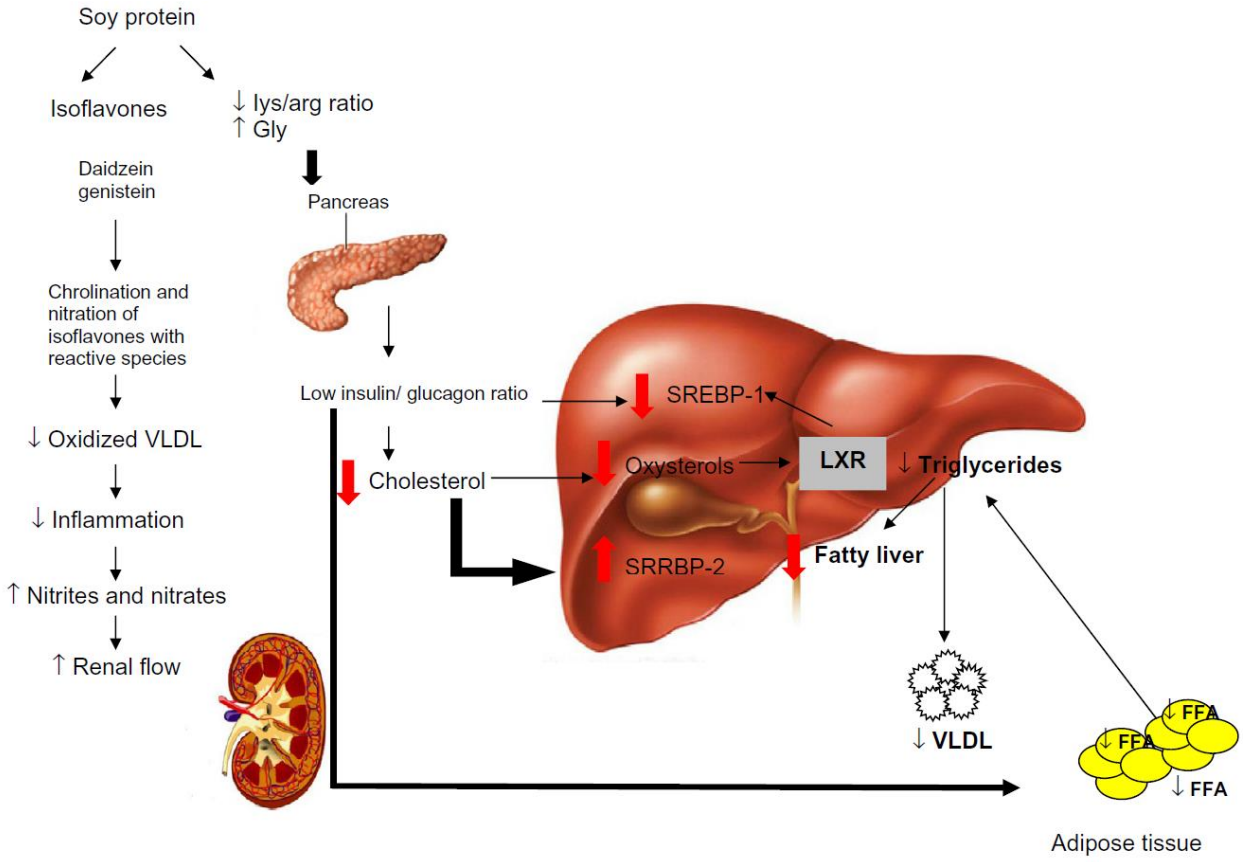

Figure 1.10. Mechanisms of Soy isoflavone protective effects on Non-alcoholic fatty liver disease and fat accumulation.[72]

Non-alcoholic fatty liver disease (NAFLD) is generally associated with obesity and metabolic syndrome. NAFLD is considered as the hepatic manifestation of Metabolic Syndrome (MS). The the first incidence in the development of NAFLD is the accumulation of triglycerides (TG) in the

cytoplasm of hepatocytes. Soy protein intake reduces the triglyceride deposition in the hepatocytes, decreasing the incidence of hepatic steatosis. Soy isoflavones reduce the fatty acid and TG biosynthesis in the liver and activate the PPAR-α transcription factor, whereby increase the fatty acid oxidation.[72] PPAR-α controls fatty acid oxidative metabolism via the induction of CPT-1 (Carnitine palmitoyl transferase-1) and few other enzymes for β-oxidation. Soy isoflavones act by upregulating PPAR-α gene expression in the liver and therefore induces CPT-1 mRNA.[72] In addition, soy isoflavones also can alter some gene expression in the liver, leading to a reduction in the fat accumulation in liver (steatosis), inhibiting insulin resistance, inflammatory state and oxidative stress.[72] Several other experimental studies also provide evidence in support of beneficial effects of isoflavones on hepatic steatosis and inflammation.[76–82]

1.9.2 Protective Effects of Soy Isoflavones on Gastrointestinal Toxicity

In recent times, there is an increased interest in studying herbal medicines and dietary supplements to treat chemotherapy-induced gastrointestinal and hepatotoxicity. Several studies have reported the protective effects of these herbal medicines.[83] A study by Lam et al. showed that the chemical constituents present in PHY906, a 4-herb Chinese medicine formula inhibited NF-kB, COX-2, and inducible nitric oxide synthase and concluded that PHY906 herbal medicine can alleviate the toxicity of irinotecan via various mechanisms.[84] This study proves that genistein downregulates the inflammatory response in inflamed caco-2 cells by regulatory mechanisms that are post-transcriptional. Another study with soy isoflavone treatment showed that Novasoy prevented the inflammation-associated induction of metallothionein in the mouse intestine. It was found that the Novasoy diet to mice diminishes the intestinal response to inflammation by altering the action of IL-6, a pro-inflammatory cytokine. Specifically, Genistein reduced the IL-6 secretion and STAT3 nuclear translocation in response to IL-6.[75] Another study by Meng et al., investigated the effect

of Daidzein on Cisplatin-induced nephrotoxicity in mice.[85] Sergent et al. showed that incubation of genistein in caco-2 cells reduced the IL-6 and IL-8 over-secretion in inflamed cells, by 50- and 60%, respectively.[86] Kao et al. investigated the effect of soy isoflavone powder and discovered that all of the isoflavone powders and also genistein showed efficient inhibition of LPS-induced inflammation by reducing the leukocyte number in mice blood and also decreased the production of IL-6, IL-1β, and Nitric oxide.[87] Daidzein also has been shown to downregulate the pro-inflammatory gene expression in LPS-stimulated microglia.[88] Genistein suppressed the MRP2-mediated biliary and intestinal secretion of irinotecan and metabolites and thereby reducing their intestinal concentrations and increasing plasma concentrations.[89] A recent review by Sahin et al. also highlighted the inhibition of NF-κB, antioxidant and anti-inflammatory effects of Genistein.[90] Genistein and daidzein are also reported to show moderate inhibitory effects against human carboxylesterase 2 (hCE2), with the IC50 values of 20.52 μM, and 57.48 μM, respectively, suggesting that these isoflavones could be used to alleviate the toxicity induced by drugs that are hCE2 drugs.[91] In addition, the effects of isoflavones on PXR-signaling and CYP3A expression and activity is also reported previously.[92] Ronis et al. 2016 reported a significant inhibition of activity of CYP3A4 in humans with daidzein at a concentration range of 1-30 μM. However, this study reported no change in the activity of CYP3A4 with genistein.[92] The effects of genistein and daidzein on the Phase II enzymes, including UGT were studied previously by Froyen et al. 2009.[93] They reported a slight decrese in the UGT activity in the small intestine in male mice; however, no significant difference was observed in the intestinal activity of female mice. No significant difference in the UGT activity was found in the liver and kidney of male mice treated with genistein and daidzein.[93] In few other studies, a significant increase in the UGT activity with genistein was reported.[94–96] Isoflavones also have been shown to alter the intestinal microbiota,[97]

which could alter the intestinal metabolism of chemotherapy drugs. Several other studies also showed that soy isoflavones exhibit anti-inflammatory effect that can protect from intestinal injury.[98,99]

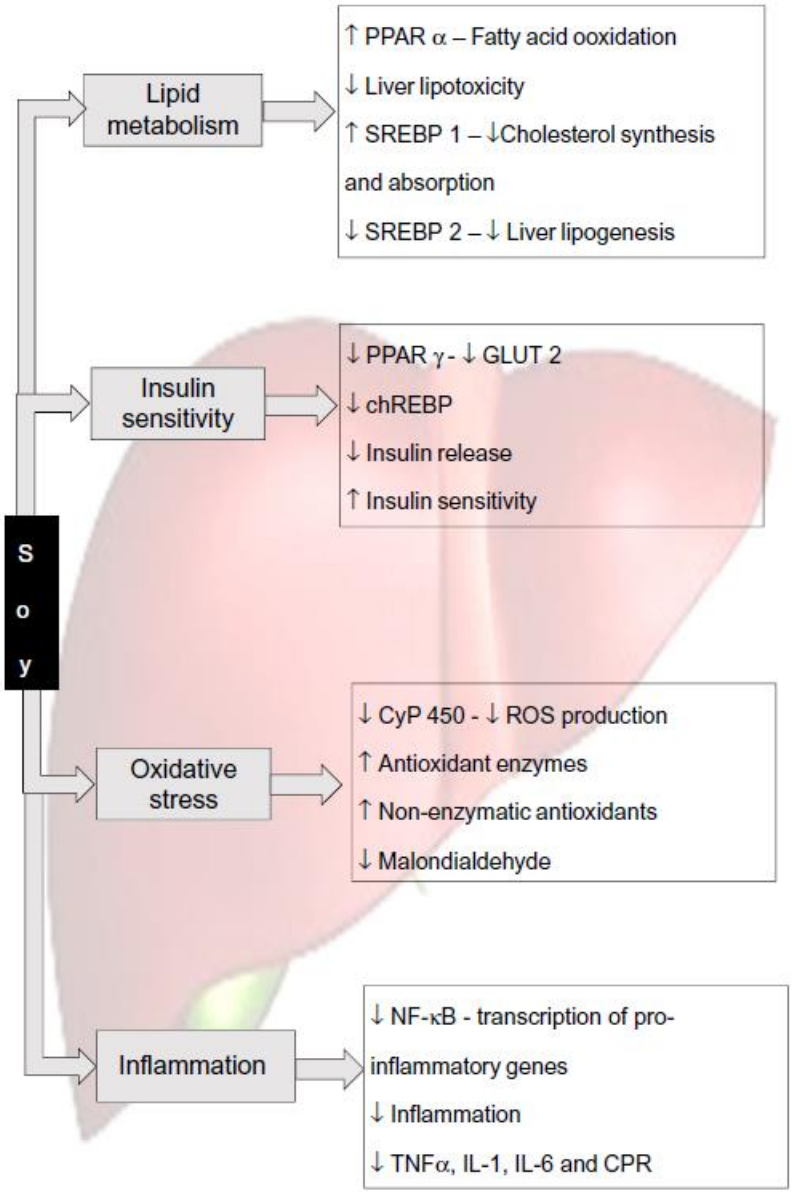

Figure 1.11. Actions of Soy isoflavones on hepatic inflammation, lipid metabolism, and oxidative stress.[72]

CHAPTER 2

HYPOTHESIS AND SPECIFIC AIMS

Specific Aims

Central Hypothesis: Inflammation alters irinotecan pharmacokinetics due to changes in the regulation of drug-metabolizing enzymes and soy isoflavons and TLR2 play a role in irinotecan-induced liver toxicity in mice.

Specific Aim 1: To determine the effects of inflammation on irinotecan pharmacokinetics and Development of a best-fit PK model

Specific Aim 2: To determine the role of TLR2 in irinotecan-induced steatosis and diarrhea

Specific Aim 3: To determine the effects of soy isoflavones on irinotecan-induced diarrhea and steatosis

2.1 Specific Aim 1: To determine the effects of inflammation on irinotecan pharmacokinetics and development of a best-fit PK model

SN-38, the active metabolite of irinotecan, is a potent inhibitor of topoisomerase-I and elevated concentrations of SN-38 induces GI toxicity in the form of diarrhea, which is a dose-limiting toxicity of irinotecan chemotherapy. It has been widely reported that during inflammation, the enzyme and transporter expression and activity in the liver and intestine are downregulated, which may alter the clearance and increase the AUC of drugs. Specifically, inflammation downregulates the enzymes involved in irinotecan metabolism, namely, cyp3a11, carboxylesterase, and ugt1a1. These enzymes are involved in the conversion of irinotecan to SN-38 and inactivation of SN-38 to SN-38G and any changes in the regulation of these enzymes could cause alterations in the SN-38 levels and therefore can contribute to reduced efficacy or increased toxicity upon irinotecan administration. Therefore, in this aim, we hypothesize that the downregulation of enzymes during inflammation alter irinotecan pharmacokinetics and may lead to increased toxicity.

2.4 Specific Aim 2: To determine the role of TLR2 in irinotecan-induced diarrhea and steatosis

Irinotecan (CPT-11) is a chemotherapy drug used in first- and second-line treatment of metastatic colorectal cancer. Irinotecan undergoes phase-I metabolism by hepatic and peripheral carboxylesterase to produce active metabolite, SN-38, which is 100-1000-fold more active than irinotecan and shows its cytotoxic activity by inhibiting the topoisomerase-I enzyme and causing irreversible DNA damage and cell death. The major toxicities associated with irinotecan chemotherapy in patients are gastrointestinal (GI) toxicity (diarrhea) and hepatotoxicity (steatosis or steatohepatitis). These toxicities result in life-threatening complications in patients and reduce the use of irinotecan as a chemotherapeutic agent. Toll-like receptors (TLRs) play an important role in the activation of innate immunity by recognizing specific patterns of microbial components, by which TLRs sense the invasion of pathogenic microorganisms. MyD88 serves as an adaptor linking TLRs with downstream molecules.[57] Mice lacking MyD88 do not generate TNF-α or IL-6 when exposed to IL-1 or other microbial components that activate TLR2, TLR4, TLR5, TLR7 or TLR9 and some of the recent research in our lab by Mallick et al. (unpublished) showed that MyD88 KO mice were protected from irinotecan-induced diarrhea. Some of the evidence from the literature strongly suggests that toll-like receptors (TLRs), especially TLR2 is involved in the pathogenesis of gastrointestinal and hepatotoxicity by inducing inflammation. Therefore, in this study, we hypothesized that TLR2 plays a role in irinotecan-induced diarrhea and steatosis.

2.5 Specific Aim 3: To determine the effects of soy isoflavones on irinotecan-induced diarrhea and steatosis

The major toxicities associated with irinotecan chemotherapy in patients are Diarrhea and Steatosis. The higher concentrations of the active metabolite, SN-38 in intestine and liver is believed to be the major cause of the toxicities. These toxicities result in life-threatening complications in patients and reduce the clinical use of irinotecan for the treatment of colorectal cancer. Hence, there is an urgency to develop new interventions to prevent irinotecan-induced diarrhea and steatosis. Soy isoflavones have beneficial effects on both gastrointestinal (GI) and hepatotoxicity caused by chemotherapy. Novasoy is a dietary supplement that has 40% isoflavones, including Genistein and daidzein. Therefore, our hypothesis in this aim is that Novasoy treatment in mice reduces SN-38 concentrations in the liver and intestine, and reduced the incidence of diarrhea and steatosis with irinotecan treatment in mice.

CHAPTER 3

EXPERIMENTAL METHODS

3.1 Chemicals

Irinotecan hydrochloride was purchased from Martin Surgical Supply (item no: 4434-11, Houston, TX). SN-38 was purchased from Cayman Chemical (item no: 15632, Ann Arbor, MI). Camptothecin (CPT; internal standard, 208925-50MG), Sodium fluoride (S7920-100G), sodium orthovanadate (S6508-10G), EDTA disodium salt dihydrate (E5134-50G), Ethylene glycol-bis(β-aminoethyl ether)-N,N,N′,N′-tetra acetic acid tetrasodium salt (E8145-10G), Triton™ X-100 (X100-100ML), Tris(hydroxymethyl)aminomethane (252859-100G), DL-Dithiothreitol (D9779-1G), Trizma® hydrochloride (T5941-100G), Potassium phosphate monobasic (P5655-100G), 4-Nitrophenyl acetate (N8130-25G) were purchased from Millipore Sigma (St Louis, MO). SN-38G was synthesized in Dr. Ming Hu's lab at the University of Houston, Houston, TX. NovaSoy® 400 was obtained from Archer Daniels Midland, Chicago, IL. SN-38 was purchased from Cayman chemical (item no: 15632). LPS (tlrl-3peplps) was purchased from invivogen, San Diego, CA. PCN (P0543-100MG). 4-Nitrophenyl-β-D-glucuronide (Catalog No. O-PNPBGA) was purchased from Megazyme.com. XCHT was obtained from Dr. Ming Hu's lab at the University of Houston. Unless specified, all other chemicals used were purchased from Millipore Sigma, St. Louis, MO.

3.2 Reagents

Phosphate Buffered Saline (PBS) 1x, without Ca/Mg, Ethanol (71001-628), Formalin (89370-094) and all other solvents used for chromatographic analysis were of LC-MS grade and purchased from VWR International, LLC (Suwanee, GA, USA). The Faststart Universal Probe Master Mix (04914058001) was purchased from Roche Diagnostics, Indianapolis, IN. The DNA-free DNA removal kit, 50 reactions (AM1906), High-Capacity cDNA Reverse Transcription Kit with RNase inhibitor (4374966), BCA protein assay kit (PI23225), Tris-EDTA buffer (BP24731), HBSS, no calcium, no magnesium, no phenol red (14175079), PBS, pH 7.4 (10010072), DNA-free DNA

removal kit (AM1906), RNaseZap RNase decontamination solution (AM9780), UltraPure DEPC-water (750023), LC-MS grade water (W6-4), Acetonitrile (A21-4), Methanol (A412-4) were purchased from Thermo Fisher Scientific, Waltham, MA. TRI reagent (T9424-100ML), phenol solution (P4557-100ML), Chloroform (C2432-500ML), 2-Propanol (I9516-500ML), trizol (T9424-100ML) were purchased from Millipore Sigma, St Louis, MO. Unless specified, all other reagents used were purchased from Millipore Sigma, St. Louis, MO.

3.3 Materials

Histology cassettes (18000-246), heparinized tubes (95057-409), 96-well plates are purchased from VWR International, LLC (Suwanee, GA, USA). Falcon strainers (08-771-2), 1 ml Tuberculin syringes (case of 500, 05-561-61) were purchased from Fisher Scientific, Waltham, MA. The special low-fat diet was purchased from Research Diets, New Brunswick, NJ. Cuvettes were purchased from Cole-Parmer, IL (759085D). Eppendorf tubes were purchased from Corning Inc. (MCT-175-C). Whirl-Pak for organ storage was purchased from Nasco (B01067WA).

3.4 Animals

For Specific Aim 1:

Male 5-weeks old C57BL6J mice were purchased from Jackson Laboratory (Ban Harbor, ME). The animals were kept in an environmentally controlled room (temperature 25 ± 2^0C, 12 h dark-light cycle, humidity 50 ± 5%) for at least 1 week before performing any experiments. The mice were on a regular diet ad libitum throughout the animal study. All the protocols followed for animal care and use were approved by the Institutional Animal Care and Use Committee (IACUC) at the University of Houston.

For Specific Aim 2:

Male, 5-weeks old C57BL6J and B6.129-Tlr2tm1Kir/J (TLR2 KO) mice were purchased from Jackson Laboratory, Ban Harbor, ME. The animals were kept in an environmentally controlled room (temperature 25 ± 2^0C, 12 h dark-light cycle, humidity 50 ± 5%) for at least 1 week before performing any experiments. The mice were on a special diet (low-fat diet, 35% sucrose with 10% kcal fat) ad libitum throughout the animal study. All the animal care and use protocols followed were approved by the Institutional Animal Care and Use Committee (IACUC) at the University of Houston.

For Specific Aim 3:

Male 5-weeks old C57BL6J mice were purchased from Jackson Laboratory, Ban Harbor, ME. The animals were kept in an environmentally controlled room (temperature 25 ± 2^0C, 12 h dark-light cycle, humidity 50 ± 5%) for at least 1 week before performing any experiments. The mice were on a special diet (low-fat diet, 35% sucrose with 10% kcal fat) (D12450B, Research Diets) ad libitum throughout the animal study. All the animal care and use protocols followed were approved by the Institutional Animal Care and Use Committee (IACUC) at the University of Houston.

3.5 Animal Study Design and Drug Treatments

For Specific Aim 1:

Mice (n=5) were injected with saline or LPS (2 mg/kg) intraperitoneally (i.p.) and after 16 h, a single dose of 10 mg/kg irinotecan hydrochloride was given via oral route of administration. Blood samples of approximately 20 µl were collected from the tail vein at 0 h (pre-dose) and 0.25, 0.5, 1, 2, 4, 6, 10, and 24 h post the irinotecan administration. After the 24 h sample, mouse livers were isolated, flash-frozen in liquid nitrogen and stored at -80^0C until further use.

For Specific Aim 2:

C57BL6J mice were divided into 2 groups (n = 5 per group) and treated with either saline or irinotecan. Similarly, TLR2 KO mice were divided into 2 groups and treated with saline or irinotecan. Mice were treated with either saline or irinotecan (50 mg/kg, intraperitoneal) once a day for 8 days. Mice were sacrificed on day 9, after 24 hours of last irinotecan treatment. Mouse liver and intestine were isolated immediately after sacrificing.

For Specific Aim 3:

C57BL6J mice were divided into 4 groups (n = 4 or 5 per group): saline (Sal) and NovaSoy (NS) were control groups and received either saline or NovaSoy (1 g/kg, oral gavage) from days 1 to 10. Saline and irinotecan (Sal/IRI), NovaSoy and irinotecan (NS/IRI) were the treatment groups and received either saline or NovaSoy (from days 1 to 10), along with irinotecan 50 mg/kg/day for 7 days (days 4 to 10) by oral gavage. Mice were sacrificed on day 11, after 24 hours of last drug treatment. Mouse liver and intestine were isolated immediately after sacrificing.

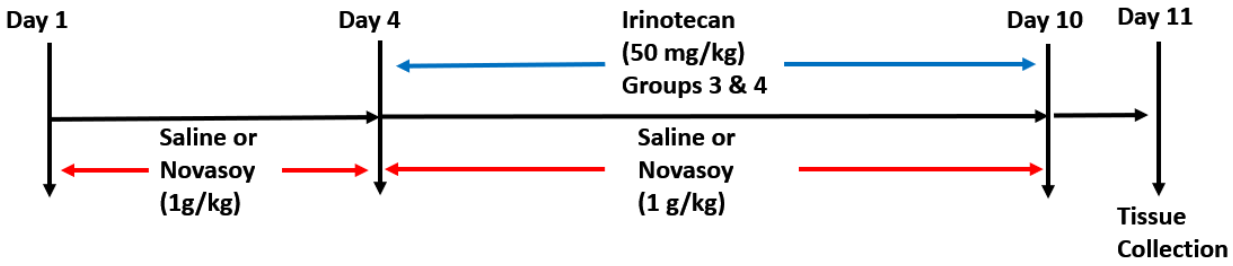

3.6 Animal PK Experiments

For animal experiments, stock solutions of saline, LPS (2 mg/kg), irinotecan (10 mg/kg or 50 mg/kg) were prepared. PK experiments were conducted by injecting saline or LPS (2 mg/kg) via i.p. route of administration and irinotecan was given orally after 16 h of saline or LPS injection to mice (n=5 per group). The injection volume was maintained at 100 µl/10 g of body weight and stock solutions were prepared accordingly. Blood samples were collected from the tail vein at 9

time points from 0-24 h and mice were sacrificed after collecting 24 h blood samples. Mice were sacrificed, liver and intestine were isolated and immediately placed liquid nitrogen and later kept at -80^{o} C.

3.7 LC-MS Sample Preparation, Analysis and Quantification

For LC-MS analysis, the frozen samples were thawed and prepared by mixing approximately 10 µl of blood samples with 10 µl of PBS. To this mixture, 200 µl of 50% of acetonitrile (ACN) containing 5 µM camptothecin (internal standard) was added as an extracting solvent. Samples were vortexed for 30 sec and centrifuged for 15 min at 18,000 ×g. After the centrifugation, one-hundred and eighty (180) µl of supernatants were collected and allowed to dry under a gentle stream of air at room temperature. The air-dried samples were then reconstituted with 100 µl of 50% acetonitrile and samples were centrifuged for 10 min at 8,000 ×g. Eighty (80) µl of the supernatant was transferred to vials and 10 µl was injected into LC-MS/MS for analysis of irinotecan, SN-38, and SN-38G.

To analyze irinotecan and metabolite concentrations, an API 5500 QTRAP triple quadrupole mass spectrophotometer (AB Sciex, USA) equipped with a Turbospray TM source was used by multiple reaction monitoring (MRM) method operated in a positive ion mode, with minor modifications to the method conditions as previously described[100]. A UPLC system, Waters Acquity™ with a diode-arrayed detector (DAD) was used. The UPLC conditions were as follows: column, Acquity UPLC BEH C18 column (50 mm × 2.1 mm I.D., 1.7 µM, Waters, Milford, MA, USA); mobile phase A - 0.1% formic acid and mobile phase B - 100% acetonitrile performed in a gradient from 0 to 4.5 min. The flow rate and sample injection volume were 0.4 ml/min and 10 µL, respectively. The following m/z transitions were selected: m/z 587.1 → 124.1 for irinotecan, m/z 393.1 → 349.1 for SN-38 m/z 569.5 → 393.1 for SN-38G and m/z 349.0 → 305.1 for CPT. The selection of the

fragment ions depended on the highest intensity of the fragment. The data collected was analyzed with Analyst 1.4.2 software (AB Sciex, USA).

3.8 Compartmental Analysis by WinNonlin

The AUC, C_{max}, and t_{max} values for saline and LPS groups were determined using compartmental analysis by WinNonlin 5.2 (Pharsight Corporation, Mountain View, CA, USA). AUC values are expressed in 'ng.h/ml'. C_{max} and t_{max} values are reported in 'ng/ml' and 'h', respectively.

3.9 PK Model Development by Phoenix

The PK model was developed based on the observed concentration vs. time data for irinotecan and SN-38 in mouse blood samples in saline and LPS groups (n = 5 per group). Initial estimates of individual compartmental PK parameters were derived using Phoenix NLME (non-linear mixed effect) (Pharsight Corp., Mountainview, CA, USA). Concentrations of irinotecan and SN-38 were fitted simultaneously. Model structures were developed based on actual dosing, sampling times and mass balance equations. Model discrimination on data was performed using Phoenix, by minimizing the Akaike Information Criterion (AIC) and by the comparison of the quality of plot fits, such as using a large amount of observed data vs. fitted data, weighted residual vs. fitted data, and weighted residual vs. time.

Different compartmental PK models were tested to describe the irinotecan and SN-38 concentrations in different compartments. Enterohepatic recycling (EHR) compartment was included in the PK model, with a linear transfer of irinotecan to EHR compartment and nonlinear transfer of SN-38 to the EHR compartment. The model was developed to establish the relationship of irinotecan and SN-38 to the EHR compartment. We omitted SN-38G data in the model in order to better describe the irinotecan and SN-38 data with high reliability and without much complexity.

Individual estimates of PK parameters were assumed to follow a log-normal distribution. Therefore, an exponential distribution model was used to account for inter-subject variability (IIV) as follows:

$$P_i = P \cdot exp(\eta_i)$$

Where P_i is the individual parameter estimate for individual i, P is the typical population parameter estimate, and η_i was assumed to be distributed N (0, ω2), with a mean of 0 and variance of ω2. Only significant IIVs in PK parameters were retained.

Residual unexplained variability was implemented as either a proportional or combined error model:

$$C_{observed,ij} = C_{pred,ij} \times (1 + \varepsilon_{p,ij}) + \varepsilon_{a,ij}$$

Where $C_{observed,ij}$ represents the observed concentration for individual i and observation j, $C_{pred,ij}$ represents the individual predicted concentration. $\varepsilon_{p,ij}$ and $\varepsilon_{a,\ ij}$ represent the proportional and additive errors distributed following N (0, σ2), with a mean of 0 and variance of σ2. The selection of an appropriate residual error model was based on the likelihood ratio test and the inspection of the goodness-of-fit plots.

3.10 Animal Body Weight Measurements and Diarrhea Evaluation

The body weight of mice was measured daily to track weight loss/gain, and the presence of diarrhea was monitored in mice daily from days 1-10. The loss in body weight from days 1 to 10 was calculated and reported in terms of % weight loss. Diarrhea was quantified according to a validated grading criterion previously described[101] with slight modification. The grading was

given based on the severity of diarrhea observed and is reported as follows: grade 0 (normal or no diarrhea), grade 1 (slightly wet and soft tool), grade 2 (wet stool with moderate perianal staining), grade 3 (severe diarrhea and staining), grade 4 (severe, life-threatening bloody diarrhea with staining and continual anal leakage).

3.11 Histological Analysis of Liver and Intestine Injury

Intestine or liver sections (n=5 per group) collected immediately after sacrificing were placed in tissue embedding cassettes and fixed in 10% neutral buffered formalin (vol/vol) for histological examination. The samples were then embedded in paraffin and stained with hematoxylin and eosin (H&E) at Pathology Core and Lab, Baylor College of Medicine (BCM), Houston, TX. The H&E stained slides of intestine and liver were evaluated by an experienced pathologist in a blinded fashion and morphological observations of intestine and liver injury were recorded. The liver injury was assessed based on the percentage of hepatocytes showing fat accumulation (steatosis). The severity of steatosis in control and irinotecan-treated groups was reported as previously described[101] with slight modifications. The grading was as follows: score 0 (no steatosis), score 1 (minimal fat accumulation, < 5% steatosis), score 2 (5-30% steatosis), score 3 (30-65% steatosis), score 4 (severe fat accumulation, > 65% steatosis). The final score reported was an average of scores observed individually for each slide in a group. To evaluate the intestinal injury, criteria such as shortening of villi and disruption of crypt cells were considered.

3.12 RNA Isolation from Mouse Liver Tissues

Reagents:

Chloroform, TRIzol, 70% Ethyl alcohol, RNA Zap, Milli Q water, isopropyl alcohol, RNase free water or DEPC water, TE Buffer, pH 8.8)

Method:

Liver tissues (~ 0.1g) stored in -80 °C were collected in 2 mL microcentrifuge tubes and 0.75 mL of cold TRIzol reagent was added per tube. The tubes were placed on ice and homogenized using hand-held Beckman Polytron homogenizer (highest setting) for ~45-60 seconds. After each tube is homogenized, the homogenizer was washed in RNA Zap, 70% Ethanol, MilliQ H2O and Trizol reagent in the same order to prevent contamination. Care was taken to avoid the generation of too much froth or bubbles during homogenization. Homogenized samples were incubated for 5 min at room temperature. After 5 min, 0.2 ml of cold chloroform was added and tubes were shaken vigorously by hand for 15 seconds and again incubated at room temperature for 15 mins. After 15 min, samples were centrifuged at 12000 rpm/15 mins/4 ºC. After centrifugation, the mixture separates into a lower red, phenol-chloroform phase, interphase, and a colorless upper aqueous phase. The volume of the aqueous phase is about 70% of the volume of TRIzol reagent used for homogenization. Then the aqueous phase was transferred into a clean tube. To the tube, 0.5 ml of isopropyl alcohol was added, mixed by vigorous shaking, and incubated at room temperature for 10 mins. The samples were centrifuged at 12000 rpm/10 mins/4 ºC. After the centrifugation, the supernatant was removed and 1 ml of 75% ethanol was added to the pellet, mixed the sample by vortexing, and centrifuged again at 12000rpm/5 mins/4 ºC. After the centrifugation, all the Ethanol was pipetted out and RNA pellet was allowed to dry. Later, the RNA sample was dissolved in 50 µl of DEPC water by passing the solution several times through a pipette tip. For RNA quantification, 600 µl of Tris-EDTA buffer was taken into new centrifuge tubes and 1.2 µl of dissolved RNA was added (diluting with TE buffer 500 times). From the 600 µl, 500 µl was transferred into a cuvette and the absorbance of RNA was measured by using Beckman-Coulter DU800 spectrophotometer.

3.13 DNase Digestion

Reagents:

DNase reaction buffer (10X), DNase enzyme (1 U/µl), DEPC water, phenol, chloroform, ethanol, 3M sodium acetate (pH 5.2).

Method:

DNase Reaction was set by mixing RNA sample (100 µl), DNase reaction buffer (20 µl) and DNase enzyme (10 µl) to make up a total reaction volume of 200 µl. The reaction mixture was incubated at 37 °C for 30 min. After 30 min, 50 µl of RNase-free water was added to the digest followed by 125 µl phenol and 125 µl chloroform. Tubes were mixed by vigorous shaking by hand for 30 sec. The samples were then centrifuged for 15 min at 12000 rpm/4 ºC. After centrifugation, the aqueous upper phase was transferred to a new RNase-free tube. To the tube, 250 µl of chloroform was added and tubes were shaken by hand for 30 secs and centrifuged for 15 min at 12000 rpm/4 ºC. After centrifugation, the aqueous upper phase was transferred to a new RNase-free tube. For 100 µl of supernatant collected, 3X (300 µl) the volume of the absolute ethanol was added along with 10 µl of 3M sodium acetate, pH 5.2. The samples were then gently mixed by inversion and incubated at -70 °C for 30 min. After 30 min, the samples were centrifuged for 15 min at 12000 rpm. Following the centrifugation, the supernatant was carefully removed without disturbing the pellet. To the pellet, 1 ml of cold 70% ethanol was added and centrifuged again for 15 min at 12000 rpm/4 ºC. After the centrifugation, the alcohol was carefully removed, and the RNA sample was allowed to dry. Once the pellet was dried, it was dissolved in 30 µl of DEPC water and RNA was quantified using spectrophotometer as described earlier.

3.14 cDNA synthesis

Reagents:

10X RT buffer, 25X dNTP mix (100 mM), 10X Random Primers, Multiscribe Reverse Transcriptase, RNase inhibitor (20u/µl), DEPC water.

Method:

A high capacity Reverse Transcription Kit obtained from Thermo Fisher Scientific was used for the cDNA synthesis. For the reaction, a 40 µl of total reaction volume was used (20 µl of RNA sample and 20 µl of cDNA reaction mix). For each reaction, the 20 µl of reaction mix contained 4 µl of 10x RT buffer, 1.6 µl of 25x dNTP mix (100 mM), 4 µl of 10x Random primers, 2 µl of multiscribe reverse transcriptase, 2 µl of RNase inhibitor, and 6.4 µl of DEPC water. Once the RNA sample was mixed with the reaction mix, the 40 µl of total volume was transferred to a microcentrifuge tube and the tubes were placed in an Applied Biosystems PCR Thermal Cycler to synthesize the cDNA. The temperature conditions used for the thermal cycler were: 25°C for 0-10 min, 37° C for 11-70 min, held constant at 37° C from 71-130 min, 85° C for 5 sec, then cooled down to 4° C for 90 min.

3.15 Real-time PCR

Reagents and Materials:

Roche master mix, cyclophilin and gene-specific forward and reverse primers, Taqman probe, DEPC water, 96-well plate.

Method:

Firstly, 26 µl of DEPC water was added to 2 µl of cDNA sample to dilute it to 14 times. The tubes were spun down and then tapped to mix the reaction contents. Each sample was prepared in duplicate and transferred 20 µl of diluted cDNA sample to 2 wells (10 µl per each well) of a 96-well plate. For each gene, the reagent mix was prepared separately using gene-specific primers and probes. The total volume of the reagent mix for each sample was 15 µl. For each reaction, the 15 µl of reaction mix contained Roche master mix (11.25 µl), forward primer (0.075 µl), Reverse primer (0.075 µl), Taqman probe (0.05 µl), and Milli-Q water (3.55 µl). The primer sequence (5'-3') of the genes studied were as follows: Cyclophilin (Forward GGCCGATGACGAGCCC, Reverse TGTCTTTGGAACTTTGTCTGCA, Probe 6TGGGCCGCGTCTCCTTCGA), Cyp3a11 (Forward GGATGAGATCGATGAGG CTCTG, Reverse CAGGTATTCCATCTCCATCACA - GT, Probe CCAACAAGGCACCTCCCACGTATGA), Ugt1a1 (Forward TCTGAGCCCTGCA - TCTATCTG, Reverse CCCCAGAGGCGTTGACATA, Probe TGGTATAAATTGCCTTCAG - AAAAAGCCCCTATC), TNF-α (Forward CATCTTCTCAAAATTCGAGTGACAA, Reverse TGGGAGTAGACAAGGTACAACCG, Probe CACGTCGTAGCAAACCACCAAGTGGA). The 15 µl of the reaction mixture was added to the 10 µl of diluted cDNA sample in the well plate. The total volume for each reaction was 25 µl. After the addition of the reaction mix, the well plate was sealed with PCR sealing film and the plate was gently tapped to mix the reaction contents. The well plate was then spin down for 15 sec. An Applied Biosystems RTPCR system was used for the analysis. The experiment conditions were 50°C for 2 min (stage 1), denaturing at 95°C for 10 min (stage 2), denaturing at 95°C for 15 sec and annealing at 60°C for 1 min (stage 3, 50 cycles). Cyclophilin was used as the housekeeping gene to normalize the quantitative expression values.

The threshold cycle (Ct) values were of each sample was determined by the PCR instrument. ΔΔCt method was used to calculate relative gene expression.

3.16 Analysis of Liver and Intestine Concentrations

Reagents:

Acetonitrile, Phosphate Buffered Saline, camptothecin (Internal standard), 0.1% formic acid.

Method:

Liver and intestinal concentrations of irinotecan, SN-38, and SN-38G in saline and Novasoy treated groups were determined using LC-MS/MS analysis. For the analysis, the liver or intestine sample was homogenized and further processed to extract compounds. A 10 µl of tissue homogenate was mixed with 10 µl of PBS and to this mixture, 200 µl of 50% of acetonitrile (ACN) containing 5 µM camptothecin (internal standard) was added as an extracting solvent. Samples were vortexed for 30 sec and centrifuged for 15 min at 15000 rpm. After the centrifugation, 180 µl of supernatants were collected and allowed to dry under a gentle stream of air at room temperature. The air-dried samples were then reconstituted with 100 µl of 50% acetonitrile and samples were centrifuged for 10 min at 10000 rpm. 80 µl of the supernatant was transferred to vials and 10 µl was injected into LC-MS/MS for the analysis of irinotecan, SN-38, and SN-38G.

To analyze irinotecan and metabolite concentrations, an API 5500 QTRAP triple quadrupole mass spectrophotometer (AB Sciex, USA) equipped with a Turbospray TM source was used by multiple reaction monitoring (MRM) method operated in a positive ion mode, with minor modifications to the method conditions as previously described[100]. A UPLC system, Waters Acquity™ with a diode-arrayed detector (DAD) was used. The UPLC conditions were as follows: column, Acquity UPLC BEH C18 column (50 mm × 2.1 mm I.D., 1.7 µM, Waters, Milford, MA, USA); mobile

phase A - 0.1% formic acid; mobile phase B - 100% acetonitrile performed in a gradient from 0 to 4.5 min. The flow rate and the sample injection volume were 0.4 ml/min and 10 µL, respectively. The following m/z transitions were selected: m/z 587.1 → 124.1 for irinotecan; m/z 393.1 → 349.1 for SN-38; m/z 569.5 → 393.1 for SN-38G; m/z 349.0 → 305.1 for CPT. The selection of the fragment ions depended on the highest intensity of the fragment. The data collected was analyzed with Analyst 1.4.2 software (AB Sciex, USA).

3.17 Preparation of Whole Cell Extracts

Reagents and Stock solutions:

Tris HCl, pH 7.5 (1M), NaCl (5M), EDTA (0.5), EGTA (1M), Triton X-100, Deoxycholate (10%), MilliQ water, DTT, Sodium Fluoride (NaF) (200 mM), Sodium vanadate (Na3VO4) (200 mM), Dithiothreitol (DTT) (1 M).

Method:

A 500 ml of homogenization buffer was prepared by mixing Tris HCl, pH 7.5 (25 ml), NaCl (50 ml), EDTA (2 ml), EGTA (1 ml), Triton X-100 (5 ml), deoxycholate (12.5 ml), and Milli-Q water (404.5 ml). Immediately before the use, NaF (200 mM), Na3Vo4, DTT were added to the homogenization buffer. The whole-cell extracts were prepared from mouse liver tissues by taking approximately 0.1 g of liver tissue in 1 ml of homogenization buffer. The liver sample in the buffer was kept in a glass tube and homogenized by 10 strokes of Dounce A and 10 strokes of Dounce B glass homogenizers. The homogenate was then transferred to Eppendorf tube and centrifuged at 13000 rpm for 10 min at 4^{o}C. After the centrifugation, the supernatant was collected. The whole-cell extracts were stored at 80^{o}C in Eppendorf tubes until the protein quantification by BCA assay.

3.18 BCA Assay for Protein Quantification

Reagents and Materials:

Pierce BCA assay kit (Thermo Fisher Scientific, 23225) with working reagents A and B, Albumin (BSA), MilliQ water, 96-well flat bottom plate (Corning Inc.), BioTek Plate Reader (BioTek, Winooski, VT, USA)

Method:

The whole-cell extract samples were kept on ice and allowed to thaw. A 30 µl of BSA standard concentrations of 0, 0.1, 0.2, 0.3, 0.4, 0.6, 0.8, and 1 mg/ml were prepared using the stock concentration of 2 mg/ml and Milli-Q water. The BSA stock solution of 2 mg/ml was diluted to 1 mg/ml to prepare standard concentrations. 30 µl of samples were prepared in 1:20 and 1:40 dilution by mixing re required amount of protein to milli-Q water. Then, 200 µl per each well of working reagent was prepared by mixing 50 parts of working reagent A to 1 part of working reagent B as per the recommendations in the protocol from the manufacturer. 10 µl of standards and unknown samples were added to wells in preplanned order and to the standards and samples, the 200 µl of working reagent was added. The well plate was then covered with aluminum foil and incubated for 30 min at 37^{o}C. After measuring the absorbance at 570 nm using a BioTek plate reader, the standard curve was plotted with average OD values for each sample and the protein concentration of each unknown sample in µg/ml was calculated.

3.19 Carboxylesterase Activity Assay

Reagents and Materials:

P-nitrophenyl acetate (PNPA), 96-well flat bottom plate (Corning, 3585), Biotek plate reader

(BioTek, Winooski, VT, USA)

Method:

Whole cell extracts were prepared from mouse livers and protein concentration was determined by BCA assay according to the manufacturer's protocol (Pierce Chemical, Rockford, IL), as described previously. Total carboxylesterase activity was monitored by measuring the absorbance using a BioTek plate reader in a 96-well plate. The whole cell extracts containing CEs enzyme (100 μg/ml) was incubated with the substrate P-nitrophenyl acetate (PNPA) (750 μM) at 37 ºC. 50 μl of protein solution was added to the wells and 150 μl of P-nitrophenyl acetate (PNPA) to make a 200 μl reaction volume. The reaction time was 30 min. The absorbance was measured for 10 min at 405 nm using Biotek plate reader ((BioTek, Winooski, VT, USA). The assay was set up in the instrument with 2 min intervals. The enzyme specific activity was calculated using the following equation:

Specific activity: [Absorbance (slope) x reaction volume in well (0.0002 L) x 106 (to convert moles of epsilon to μM)]/ [epsilon of p-nitrophenolate at pH 7.4 (15.3 mM) x time of reaction (12 min) x Sample volume (0.05 ml) x total amount of protein in each well (0.1 mg/ml) x light path length (mostly 1cm). The specific activity of carboxylesterase was expressed as the μmoles of PNP formed per min per mg of protein.

3.20 Ugt1a1 Activity Assay

Reagents and Materials:

SN-38, SN-38 Glucuronide, acetonitrile, 0.1% formic acid, camptothecin (internal standard), Solution A (3.6 mM UDPGA triammonium salt), solution B (4 mM saccharolactone, 0.88 mM MgCl2 and 0.022 mg/ml alamethacin), Potassium phosphate (Cat # P5655, Sigma).

Method:

Ugt1a1 activity in control and irinotecan-treated groups was determined by measuring the formation of SN-38 glucuronide by LC-MS/MS analysis using SN-38 as a substrate. Briefly, whole cell extracts from the mouse liver tissue were prepared, and protein concentration was determined using the BCA assay kit according to the manufacturer's protocol (Pierce Chemical, Rockford, IL). To measure the enzyme activity, a reaction containing 1 mg/ml protein, 10 µM of SN-38, solution A (25 mM UDPGA Triammonium salt) and solution B (25 mM Saccharolactone, 5 mM $MgCl_2$ and 0.022 mg/ml Alamethicin) in 0.05 M KPi buffer was used. The total reaction volume was 170 µl. The reaction was conducted in a water bath at 37 ^{o}C for 60 min. The reaction was terminated by adding 7 µl of acetonitrile (ACN) containing 1 µg/ml CPT (internal standard). Samples were then processed and analyzed by LC-MS/MS to determine the ugt1a1 activity. The specific enzyme activity was expressed as nM of SN-38G formed.

3.21 Toxicokinetic Experiments

Reagents and Materials:

Novasoy, irinotecan hydrochloride, saline, heparin, SN-38, and SN-38 glucuronide, camptothecin (internal standard).

Method:

Toxicokinetic (TK) studies were conducted in C57BL6 mice to determine the effects of NovaSoy treatment on the toxicokinetics of irinotecan. For the TK study, a total of 12 mice were used and divided into 2 groups (n=6 per group). Mice were pre-treated with either saline or NovaSoy (1 g/kg, oral gavage) for 3 days. From day 4, mice groups received either saline or Novasoy, along with irinotecan (50 mg/kg/day, oral gavage) until day 8 and mice were sacrificed 24 h after the last

dose of irinotecan. For the TK analysis, approximately 20 µl of blood samples were collected from the tail vein of mice on day 4 (1^{st} dose of irinotecan) and day 7 (4^{th} dose of irinotecan) from 0-24 h at predetermined time points. In addition, 0 h (pre-dose), 2 h (post-dose) blood samples were collected on days 0, 5, and 8 following irinotecan administration. Blood concentrations of irinotecan, SN-38, and SN-38G were determined using LC-MS/MS using the method conditions described in section 3.7. AUC, C_{max}, and t_{max} values were determined using NCA analysis by WinNonlin 5.2 software.

3.22 Statistical Analysis

For Specific Aim 1:

Data are expressed as mean ± standard deviation for all the experiments. Statistical analysis was performed using the t-test to compare the significance between saline and LPS groups. GraphPad Prism 8.0 software was used for the analysis and a P-value of < 0.05 was considered as statistically significant.

For Specific Aim 2:

Data are expressed as mean ± standard deviation for all the experiments. One-way ANOVA was performed using GraphPad Prism 8.0 software to determine the significance of differences between control and treatment groups. P-value of < 0.05 was considered as statistically significant.

For Specific Aim 3:

Data are expressed as mean ± standard deviation for all the experiments. One-way ANOVA was performed using GraphPad Prism 8.0 software to determine the significance of differences between control and treatment groups. P-value of < 0.05 was considered as statistically significant.

CHAPTER 4

Effects of Inflammation on Irinotecan Pharmacokinetics and Development of a Best-fit PK Model

Abstract

Irinotecan is a chemotherapeutic drug used in the treatment of advanced colorectal cancer and elevated blood concentrations of its active metabolite, SN-38 leads to increased gastrointestinal (GI) toxicity and diarrhea in patients. In this study, we investigated the effects of inflammation on the pharmacokinetics (PK) of irinotecan (CPT-11) and its active metabolite, SN-38. Mice were i.p.-injected with either saline or lipopolysaccharide (LPS) to induce inflammation. After 16 h, irinotecan was administered orally. Blood was collected from the tail vein of mice from 0-24 h after dosing. Concentrations of irinotecan, SN-38 and SN-38G were analyzed using LC-MS/MS. The AUC, C_{max}, and t_{max} were derived using WinNonlin® 5.2. A PK model was developed using Phoenix NLME® to describe the PK of irinotecan and SN-38 during inflammation. Results indicated a significant increase in the blood concentrations of irinotecan and SN-38 in mice during inflammation. The AUC of irinotecan and SN-38 in the LPS group were 2.6 and 2-folds, respectively, of those in control saline-treated mice. The C_{max} of irinotecan and SN-38 in LPS treated mice were 2.4 and 2.3-folds of those in saline-treated mice. The PK model was successfully developed and validated. The best-fit plots of individual PK analysis showed a good correlation between observed and predicted concentrations of irinotecan and SN-38. Together, this study reveals that SN-38 concentrations are elevated during inflammation, which may increase the GI toxicity and diarrhea in patients who receive irinotecan; and the developed PK model can quantitatively describe the PK of irinotecan and SN-38 during inflammation.

4.1 INTRODUCTION

Irinotecan (CPT-11) is a first-line chemotherapeutic drug for advanced colorectal cancer[102,103]. Irinotecan is a pro-drug to the active metabolite, 7-ethyl-10-hydroxycamptothecin (SN-38), which is approximately 100 to 1000-fold more cytotoxic than the parent compound[12,104–106]. SN-38 shows its anticancer activity by inhibiting the topoisomerase-I enzyme[107–109], which is involved in DNA replication. The SN-38 metabolite is formed from irinotecan by the carboxylesterase enzyme and is further conjugated to an inactive glucuronide (SN-38G) metabolite by the UGT1A1 enzyme[110]. Enterohepatic recycling (EHR) occurs when SN-38G is deconjugated back to SN-38 by bacterial β-glucuronidases produced in the intestine, followed by reabsorption of SN-38[111]. The CYP3A4 enzyme metabolizes irinotecan to inactive, non-toxic metabolites APC and NPC[112–115].

Irinotecan-induced gastrointestinal (GI) toxicity has been extensively studied[116–119], and the major dose-limiting toxicity is diarrhea. Generally, diarrhea caused by irinotecan is the result of increased exposure of intestinal epithelium to the active metabolite, SN-38. Delayed diarrhea is observed in up to 87% of patients, with 30-40% experiencing severe diarrhea (grade 3 or 4)[120,121]. Due to severe diarrhea caused by irinotecan, the dose given to patients is reduced, which limits the use of irinotecan as a chemotherapeutic agent, resulting in limited efficacy of the drug in approximately 40% patients[122].

Well-established studies have shown that during inflammation, the expression and activities of many drug-metabolizing enzymes (DMEs) and transporters were significantly altered[41,48–50,123–126]; the enzymes involved in irinotecan metabolism are primarily down-regulated. Specifically, cyp3a11 RNA levels are reduced in mouse liver by lipopolysaccharide (LPS), or lipoteichoic acid (LTA), which are components of gram-negative and gram-positive bacteria, respectively[49,50].

Treatment with LPS was shown to decrease the expression and hydrolytic activity of human carboxylesterase 1 and 2 (HCE 1 and HCE 2) *in vitro* and *in vivo*[51]. Hepatic expression of the phase-II enzyme, ugt1a1 was also reduced by LPS treatment for 16 h in mice[52]. Therefore, it is likely that irinotecan metabolism and PK will be altered during infection or inflammation due to the reduced expression and activity of several key enzymes.

A strong correlation exists in the literature between the incidence of irinotecan-induced diarrhea and the area under the plasma concentration versus time curve (AUC) of its active metabolite, SN-38. For instance, Sasaki et al. showed that the episodes of diarrhea had a better correlation with the AUC of SN-38 than that of irinotecan[117], and with multivariate analysis, concluded that the AUC of SN-38 is a significant variable for the incidence of diarrhea[117]. Similarly, few other studies also showed a significant correlation with the blood concentrations of SN-38 and the development of diarrhea[118,119]. Therefore, in the present study, we have investigated the PK of irinotecan and its metabolites, SN-38 and SN-38G in mice treated with LPS. We determined the AUC, C_{max}, and t_{max} for irinotecan, SN-38, and SN-38G. In addition, we developed a PK model using Phoenix NLME® to predict irinotecan and SN-38 concentrations during inflammation. Together, this study aims to identify and characterize the effects of inflammation on the PK of irinotecan and SN-38.

4.2 MATERIALS & METHODS

4.2.1 Chemicals

Camptothecin (CPT; internal standard) was purchased from Millipore Sigma (St Louis, MO). Irinotecan hydrochloride was purchased from Martin Surgical Supply (item no: 4434-11, Houston, TX). SN-38 was purchased from Cayman Chemical (item no: 15632, Ann Arbor, MI). SN-38G was synthesized in Dr. Ming Hu's lab at the University of Houston, Houston, TX. All

solvents used for chromatographic analysis were of LC-MS grade and purchased from VWR International, LLC (Suwanee, GA, USA). Unless specified, all other chemicals and reagents were purchased from Millipore Sigma (St. Louis, MO).

4.2.2 Animals

Male 5-weeks old C57BL6J mice were purchased from Jackson Laboratory (Ban Harbor, ME). The animals were kept in an environmentally controlled room (temperature 25 ± 2^0C, 12 h dark-light cycle, humidity 50 ± 5%) for at least 1 week before performing any experiments. The mice were on a regular diet ad libitum throughout the animal study. All the protocols followed for animal care and use were approved by the Institutional Animal Care and Use Committee (IACUC) at the University of Houston.

4.2.3 Study Design and Drug Treatments

Mice (n=5) were injected with saline or LPS (2 mg/kg) intraperitoneally (i.p.) and after 16 h, a single dose of 10 mg/kg irinotecan hydrochloride was given via oral route of administration. Blood samples of approximately 20 µl were collected from the tail vein at 0 h (pre-dose) and 0.25, 0.5, 1, 2, 4, 6, 10, and 24 h post the irinotecan administration. After the 24 h sample, mouse livers were isolated, flash-frozen in liquid nitrogen and stored at -80^0C until further use.

4.2.4 Sample Preparation, LC-MS/MS Quantification, and PK Studies

For LC-MS analysis, the frozen samples were thawed and prepared by mixing approximately 10 µl of blood samples with 10 µl of PBS. To this mixture, 200 µl of 50% of acetonitrile (ACN) containing 5 µM camptothecin (internal standard) was added as an extracting solvent. Samples were vortexed for 30 sec and centrifuged for 15 min at 18,000 ×g. After the centrifugation, one-hundred and eighty (180) µl of supernatants were collected and allowed to dry under a gentle

stream of air at room temperature. The air-dried samples were then reconstituted with 100 µl of 50% acetonitrile and samples were centrifuged for 10 min at 8,000 ×g. Eighty (80) µl of the supernatant was transferred to vials and 10 µl was injected into LC-MS/MS for analysis of irinotecan, SN-38, and SN-38G.

To analyze irinotecan and metabolite concentrations, an API 5500 QTRAP triple quadrupole mass spectrophotometer (AB Sciex, USA) equipped with a Turbospray TM source was used by multiple reaction monitoring (MRM) method operated in a positive ion mode, with minor modifications to the method conditions as previously described[100]. A UPLC system, Waters Acquity™ with a diode-arrayed detector (DAD) was used. The UPLC conditions were as follows: column, Acquity UPLC BEH C18 column (50 mm × 2.1 mm I.D., 1.7 µM, Waters, Milford, MA, USA); mobile phase A - 0.1% formic acid and mobile phase B - 100% acetonitrile performed in a gradient from 0 to 4.5 min. The flow rate and sample injection volume were 0.4 ml/min and 10 µL, respectively. The following m/z transitions were selected: m/z 587.1 → 124.1 for irinotecan, m/z 393.1 → 349.1 for SN-38 m/z 569.5 → 393.1 for SN-38G and m/z 349.0 → 305.1 for CPT. The selection of the fragment ions depended on the highest intensity of the fragment. The data collected was analyzed with Analyst 1.4.2 software (AB Sciex, USA).

4.2.5 Determination of AUC, C_{max}, t_{max} by WinNonlin

The AUC, C_{max}, and t_{max} values for saline and LPS groups were determined using compartmental analysis by WinNonlin 5.2 (Pharsight Corporation, Mountain View, CA, USA). AUC values are expressed in 'ng.h/ml'. C_{max} and t_{max} values are reported in 'ng/ml' and 'h', respectively.

4.2.6 PK Co-modeling of Irinotecan and SN-38

The PK model was developed based on the observed concentration vs. time data for irinotecan and SN-38 in mouse blood samples in saline and LPS groups (n = 5 per group). Initial estimates of individual compartmental PK parameters were derived using Phoenix NLME (non-linear mixed effect) (Pharsight Corp., Mountainview, CA, USA). Concentrations of irinotecan and SN-38 were fitted simultaneously. Model structures were developed based on actual dosing, sampling times and mass balance equations. Model discrimination on data was performed using Phoenix, by minimizing the Akaike Information Criterion (AIC) and by the comparison of the quality of plot fits, such as using a large amount of observed data vs. fitted data, weighted residual vs. fitted data, and weighted residual vs. time.

Different compartmental PK models were tested to describe the irinotecan and SN-38 concentrations in different compartments. Enterohepatic recycling (EHR) compartment was included in the PK model, with a linear transfer of irinotecan to EHR compartment and nonlinear transfer of SN-38 to the EHR compartment. The model was developed to establish the relationship of irinotecan and SN-38 to the EHR compartment. We omitted SN-38G data in the model in order to better describe the irinotecan and SN-38 data with high reliability and without much complexity.

Individual estimates of PK parameters were assumed to follow a log-normal distribution. Therefore, an exponential distribution model was used to account for inter-subject variability (IIV) as follows:

$$P_i = P \cdot exp(\eta_i)$$

Where P_i is the individual parameter estimate for individual i, P is the typical population parameter estimate, and η_i was assumed to be distributed N (0, ω2), with a mean of 0 and variance of ω2. Only significant IIVs in PK parameters were retained.

Residual unexplained variability was implemented as either a proportional or combined error model:

$$C_{observed,ij} = C_{pred,ij} \times (1 + \varepsilon_{p,ij}) + \varepsilon_{a,ij}$$

Where $C_{observed,ij}$ represents the observed concentration for individual i and observation j, $C_{pred,ij}$ represents the individual predicted concentration. $\varepsilon_{p,ij}$ and $\varepsilon_{a,\ ij}$ represent the proportional and additive errors distributed following N (0, σ2), with a mean of 0 and variance of σ2. The selection of an appropriate residual error model was based on the likelihood ratio test and the inspection of the goodness-of-fit plots.

4.2.7 Statistical Analysis

Data are expressed as mean ± standard deviation for all the experiments. Statistical analysis was performed using the t-test to compare the significance between saline and LPS groups. GraphPad Prism 8.0 software was used for the analysis and a P-value of < 0.05 was considered as statistically significant.

4.3 RESULTS

4.3.1 PK of Irinotecan and Metabolites

The observed concentration-time profiles for irinotecan, SN-38, and SN-38G obtained from 0 to 24 h after irinotecan administration in saline or LPS mice groups are shown in Figure 4.1. When compared to the saline group, the blood concentrations of irinotecan and SN-38 were significantly higher in the LPS group from 0.25-10 h. On the other hand, the blood concentrations of SN-38G in the LPS group were significantly elevated only at 2, 4, and 6 h. Interestingly, the SN-38 concentration-time profile showed a significant second peak at 6 h in the LPS group, while the second peak was much lower in the saline group. This suggests that inflammation may increase the EHR and reabsorption of SN-38 in the LPS group.

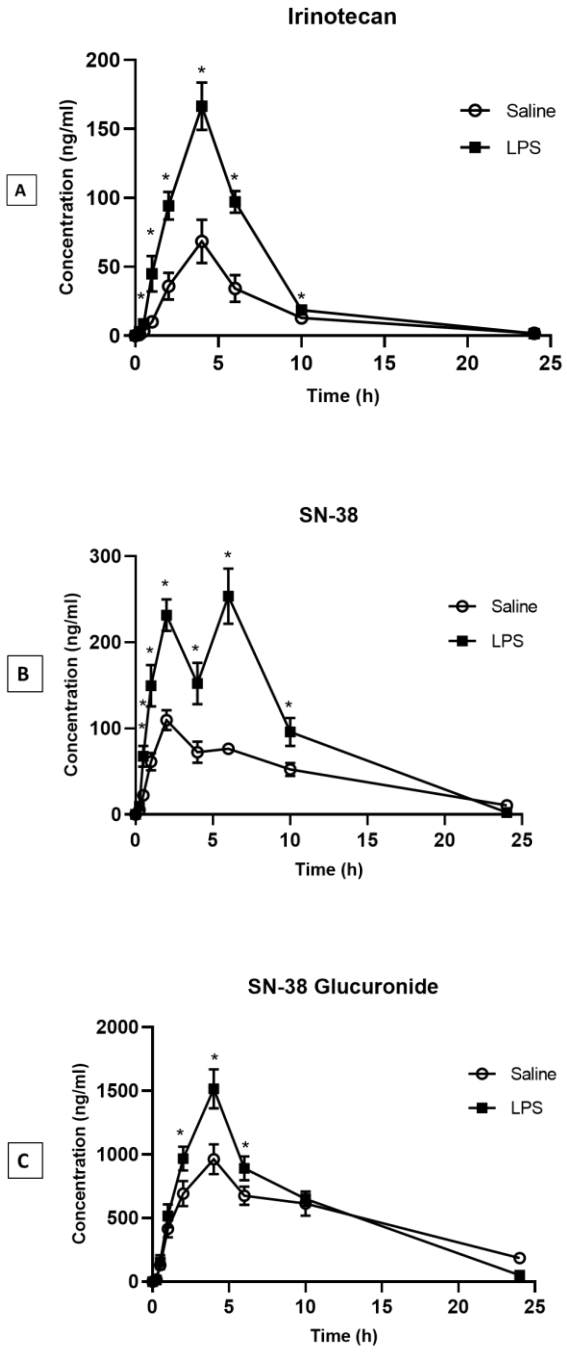

Figure 4.1. Observed blood concentration-time profiles of irinotecan **(A)**, its pharmacologically active metabolite, SN-38 **(B)**, and inactive glucuronic acid conjugate SN-38G **(C)** after a single dose oral administration of 10 mg/kg irinotecan.

PK values of Irinotecan, SN-38, and SN-38G in Saline (Group 1) and LPS (Group 2) Mice groups

Group 1: Irinotecan concentrations (ng/ml)							
Time point	Mouse 1	Mouse 2	Mouse 3	Mouse 4	Mouse 5	Average	STDEV
0	0	0	0	0	0	0	0
15	0.458	0.816	0.792	0.864	2.06	0.998	0.615012
30	1.65	4.75	4.03	3.45	2.13	3.202	1.294342
60	9.47	7.92	11.1	14	7.99	10.096	2.540242
120	40	28.5	31.7	28	51.1	35.86	9.780746
240	78.9	51.9	59.3	61.7	90.2	68.4	15.69586
360	26.3	25.8	32.2	49	37.9	34.24	9.613688
600	15.8	10.3	13.4	14.4	10.4	12.86	2.444995
1440	2.22	2.46	1.7	0.855	1.69	1.785	0.617657

Group 2: Irinotecan concentrations (ng/ml)							
Time point	Mouse 1	Mouse 2	Mouse 3	Mouse 4	Mouse 5	Average	STDEV
0	0	0	0	0	0	0	0
15	3.05	2.74	3.99	3.17	1.36	2.862	0.958316
30	5.66	6.07	6.89	14.4	10.1	8.624	3.669323
60	39	36.7	40.7	67.9	40.5	44.96	12.92316
120	93.7	79.3	91.5	103	104	94.3	10.03718
240	188	168	144	156	176	166.4	17.1114
360	95.8	107	103	88.8	90.7	97.06	7.815881
600	16.7	18.4	17.5	22.9	17.4	18.58	2.489377
1440	1.92	1.18	2	1.59	0.879	1.5138	0.479997

Group 1: SN-38 concentrations (ng/ml)							
Time point	Mouse 1	Mouse 2	Mouse 3	Mouse 4	Mouse 5	Average	STDEV
0	0	0	0	0	0	0	0
15	3.44	6.81	4.29	7.4	4.84	5.356	1.685654
30	19.4	22.1	25.3	24.9	20	22.34	2.715327
60	55.6	46.4	66.1	70.4	68	61.3	10.06529
120	119	101	123	109	95.6	109.52	11.59966
240	73.8	66.7	56	75.4	89.7	72.32	12.36596
360	83.4	75.6	75.9	68.4	78.2	76.3	5.410176
600	53.9	62.8	43.8	55.2	46.2	52.38	7.59355
1440	8.32	12.8	6.59	11.7	14.3	10.742	3.198346

Group 2: SN-38 concentrations (ng/ml)							
Time point	Mouse 1	Mouse 2	Mouse 3	Mouse 4	Mouse 5	Average	STDEV
0	0	0	0	0	0	0	0
15	5.93	7.45	11.7	15.2	8.46	9.748	3.709834
30	62.7	77.7	61	82.6	54	67.6	12.03682
60	135	174	173	119	147	149.6	23.97499
120	215	234	216	260	233	231.6	18.25651
240	131	124	180	158	168	152.2	23.98333
360	298	238	221	276	235	253.6	32.11386
600	107	114	71.7	95	91.1	95.76	16.28045
1440	2.84	3.24	1.97	2.31	1.98	2.468	0.558005

Group 1: SN-38G concentrations (ng/ml)							
Time point	Mouse 1	Mouse 2	Mouse 3	Mouse 4	Mouse 5	Average	STDEV
0	0	0	0	0	0	0	0
15	8.53	18.3	19.5	30.3	14.4	18.206	8.000917
30	133	153	127	119	118	130	14.24781
60	413	372	336	455	505	416.2	66.68358
120	617	828	601	657	760	692.6	97.78701
240	861	977	823	1080	1070	962.2	117.6168
360	719	769	584	674	629	675	72.74957
600	561	606	524	603	775	613.8	96.19615
1440	176	184	147	238	184	185.8	32.912

Group 2: SN-38G concentrations (ng/ml)							
Time point	Mouse 1	Mouse 2	Mouse 3	Mouse 4	Mouse 5	Average	STDEV
0	0	0	0	0	0	0	0
15	21.3	12.5	22.5	8.53	9.53	14.872	6.593366
30	161	141	238	146	83.9	153.98	55.34439
60	434	606	613	427	510	518	89.67999
120	826	996	947	1080	988	967.4	92.6434
240	1460	1490	1780	1380	1470	1516	153.3949
360	918	741	871	929	993	890.4	94.17431
600	697	664	603	708	583	651	55.81666
1440	44.3	47.7	42.9	70.8	49.5	51.04	11.35421

The $AUC_{0\text{-}24}$, C_{max}, and t_{max} were determined by WinNonlin 5.2 (Table 4.1). The AUC, C_{max}, and t_{max} values for irinotecan, SN-38, and SN-38G were derived based on their concentrations and

the estimates of parameters from the established compartmental model. The compartmental analysis showed that the AUC of irinotecan (994.2 ± 34.7 ng.h/ml) in the LPS group with inflammation was approximately 2.6-fold of that in the saline group (381.4 ± 60.1 ng.h/ml). In addition, the C_{max} of irinotecan in the LPS group (144.3 ± 10.1 ng/ml) was 2.4-fold of those in the saline group (59.6 ± 12.8 ng/ml). Similarly, the AUC of SN-38 in LPS group (2,364.3 ± 275.1 ng.h/ml) was significantly higher with a 2-fold increase compared to that in the saline group (1,194.4 ± 139.2 ng.h/ml), and the C_{max} of SN-38 in the LPS group (226.5 ± 8.7 ng/ml) was 2.3-fold higher to that of the saline group (96.6 ± 6.1 ng/ml). On the other hand, no significant difference was observed in the AUC or C_{max} of SN-38G between saline and LPS groups. The AUCs of SN-38G in saline and LPS groups were 13,895.4 ± 1,795.4 ng.h/ml and 12,428.5 ± 660.4 ng.h/ml, respectively. The t_{max} was not apparently altered with inflammation.

	Irinotecan		**SN-38**		**SN-38G**	
	Saline	*LPS*	*Saline*	*LPS*	*Saline*	*LPS*
AUC (ng.h/ml)	381.4 ± 60.1	994.2 ± 34.7*	1194.4 ± 139.2	2364.3 ± 275.1*	13895.4 ± 1795.4	12428.5 ± 660.4
C_{max} (ng/ml)	59.6 ± 12.8	144.3 ± 10.1*	96.6 ± 6.1	226.5 ± 8.7*	857.7 ± 84.0	1289 ± 68.0
t_{max} (h)	3.4 ± 0.2	3.3 ± 0.2	2.4 ± 0.3	3.5 ± 0.4	3.8 ± 0.2	3.7 ± 0.3

Note: * indicates a statistical significance ($p < 0.05$)

Table 4.1. AUC, C_{max}, t_{max} of irinotecan, SN-38, SN-38G in saline and LPS groups, derived using WinNonlin 5.2.

AUC, C_{max} and T_{max} values from Compartment Analysis for mice in Saline and LPS Groups:

SALINE_GROUP2_PK								
CPT11_pk parameter	unit	LPS-M1	LPS-M2	LPS-M3	LPS-M4	LPS-M5	MEAN	SD
AUC	hr*ng/ml	394.13	297.06	361.01	391.58	463.05	381.37	60.13
Cmax	ng/ml	63.42	44.24	50.34	62.65	77.39	59.61	12.86
Tmax	hr	3.21	3.35	3.46	3.84	3.16	3.40	0.27
T1/2	hr	1.58	1.71	1.84	1.59	1.52	1.65	0.13
Tlag	hr	0.92	0.88	0.82	1.54	0.96	1.02	0.29
Ka	1/hr	0.44	0.40	0.38	0.43	0.45	0.42	0.03
CL_F	ml/hr/kg	25372.19	33662.72	27700.21	25537.55	21596.07	26773.75	4433.32
V_F	ml/kg	57903.46	82928.42	73468.90	58720.12	47464.18	64097.01	14021.20

SALINE_GROUP2_PK								
sn38_pk parameter	unit	LPS-M1	LPS-M2	LPS-M3	LPS-M4	LPS-M5	MEAN	SD
AUC	hr*ng/ml	1207.16	1376.23	984.27	1195.78	1208.54	1194.40	139.27
Cmax	ng/ml	102.21	86.47	100.09	95.60	98.54	96.58	6.14
Tmax	hr	2.45	2.95	2.02	2.34	2.47	2.44	0.33

SALINE_GROUP2_PK								
sn38G_pk parameter	unit	LPS-M1	LPS-M2	LPS-M3	LPS-M4	LPS-M5	MEAN	SD
AUC	hr*ng/ml	13013.55	13839.38	11536.60	14797.00	16290.55	13895.41	1795.43
Cmax	ng/ml	806.05	928.34	736.98	888.05	929.10	857.70	84.04
Tmax	hr	4.04	3.66	3.82	3.77	3.51	3.76	0.20

LPS_GROUP2_PK								
CPT11_pk parameter	unit	LPS-M1	LPS-M2	LPS-M3	LPS-M4	LPS-M5	MEAN	SD
AUC	hr*ng/ml	1035.74	1018.60	945.86	986.93	983.79	994.18	34.71
Cmax	ng/ml	155.94	141.61	133.01	137.20	153.98	144.35	10.18
Tmax	hr	3.28	3.47	3.34	3.07	3.15	3.26	0.16
T1/2	hr	1.69	1.84	1.80	1.83	1.65	1.76	0.09
Tlag	hr	0.83	0.82	0.73	0.42	0.80	0.72	0.17
Ka	1/hr	0.41	0.38	0.38	0.38	0.43	0.39	0.02
CL_F	ml/hr/kg	9654.93	9817.37	10572.45	10132.47	10164.76	10068.39	354.06
V_F	ml/kg	23496.10	26040.32	27436.35	26782.27	24218.52	25594.71	1680.67

LPS_GROUP2_PK								
sn38_pk parameter	unit	LPS-M1	LPS-M2	LPS-M3	LPS-M4	LPS-M5	MEAN	SD
AUC	hr*ng/ml	2559.44	2683.64	2005.05	2390.19	2182.98	2364.26	275.08
Cmax	ng/ml	226.13	213.65	227.03	238.35	227.13	226.46	8.75
Tmax	hr	4.16	2.95	3.25	3.68	3.53	3.52	0.46
LPS_GROUP2_PK								
sn38G_pk parameter	unit	LPS-M1	LPS-M2	LPS-M3	LPS-M4	LPS-M5	MEAN	SD
AUC	hr*ng/ml	12388.4	12315.83	12216.75	13510.42	11711.01	12428.48	660.3955
Cmax	ng/ml	1215.76	1253.81	1390.14	1264.10	1321.21	1289.00	67.99
Tmax	hr	4.12	3.31	3.57	3.62	3.70	3.66	0.29

4.3.2 PK Model Development and Validation

A best-fit model to describe the PK of irinotecan and SN-38 in blood was developed. The model consisted of one compartment each for irinotecan and SN-38 connected with a rate constant K12 of the conversion process, and a third compartment connected with irinotecan and SN-38 for EHR. The final model structure is presented in Figure 4.2. The model was described by the mass balance equations listed below:

A1 for irinotecan = - (A1 * K1e) + (Aa * Ka)- (A1 * k12)- (A1 * K13- A3 * K31)

A2 for SN38= (A1 * k12)- (A2 * K2e) - (V_{max} * SN38 / (SN38 + Km))

A3 = (V_{max} * SN38 / (SN38 + Km)) + (A1 * K13- A3 * K31)

$A_{irinotecan}$ = (A1 * K1e)

Aa = - (Aa * Ka)

A_{sn38} = (A2 * K2e)

The results indicate that the inclusion of non-linear PK transferring from SN-38 to the EHR compartment significantly improved the model fitting.

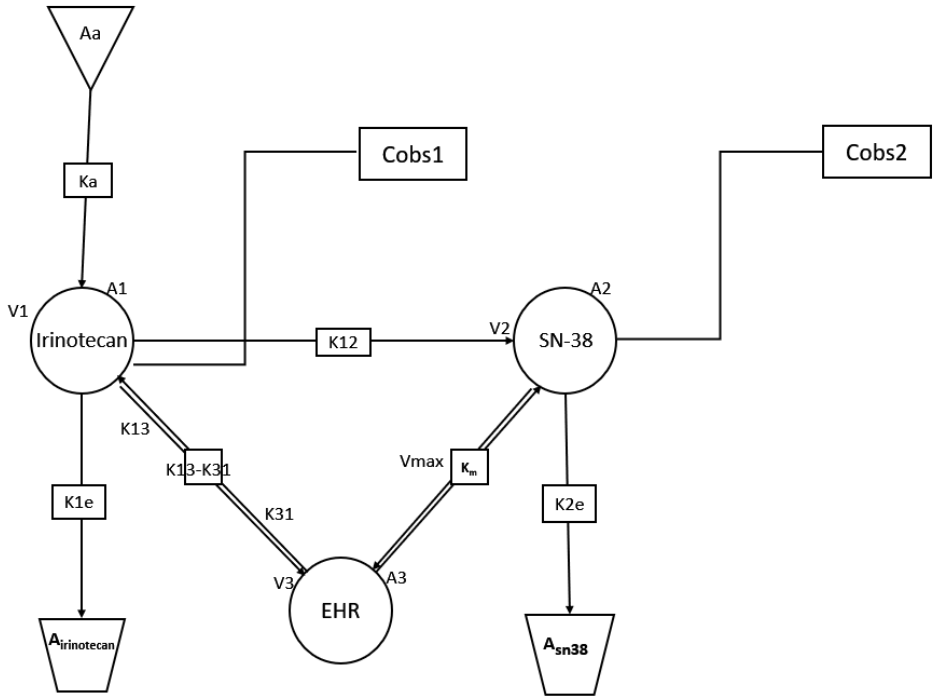

Figure 4.2. The model structure and parameters of the best fit PK Model of irinotecan and SN-38 with EHR

Ka: absorption rate constant, irinotecan compartment

K12: rate constant, irinotecan to SN-38

K1e: elimination rate constant, irinotecan compartment

K2e: elimination rate constant, SN-38 compartment

V_{max}: maximum rate, the saturable process between SN-38 and EHR compartment

K_m: the Michaelis Menten constant, the saturable process between SN-38 and EHR compartment

K13: rate constant, irinotecan to EHR compartment

V1: volume distribution in irinotecan compartment

V2: volume distribution in SN-38 compartment

Cobs1: concentrations observed for compartment 1 (irinotecan)

Cobs2: concentrations observed for compartment 2 (SN-38)

$A_{irinotecan}$: elimination phase of irinotecan

A_{sn38}: elimination phase of SN-38

Based on the best-fit PK model developed, individual PK analysis of irinotecan and SN-38 was performed using observed blood concentrations-time data of irinotecan and SN-38 in each mouse to derive the PK parameters of individual mice. The average values of each PK parameter for saline and LPS groups are reported and compared with Student's t-test in Table 4.2. The model also revealed a nonlinear PK process of SN-38 transferring to the EHR compartment with V_{max} and K_m characterized. The inflammation resulted in a significant reduction of conversion rate (K12) of irinotecan to SN38 and increased Km in the EHR of SN38.

Parameter	Unit	Saline Group	LPS Group	p-value
K12	1/h	0.53±0.08	0.36±0.11*	0.023
Km	ng/mL	183.13±71.12	610.96±186.91*	0.004
V_{max}	mg/h	2.49±0.90	2.96±1.07	0.232
Ka	1/h	0.17±0.03	0.19±0.07	0.478
V1	L	40.85±8.90	21.16±9.47	0.129
K1e	1/h	0.23±0.31	0.03±0.05	0.246
V2	L	0.006±0.004	0.005±0.003	0.314
K2e	1/h	0.11±0.06	0.10±0.15	0.428
K13	1/h	0.04±0.07	0.03±0.02	0.222
K31	1/h	0.60±0.84	0.0003±0.0004	0.091

Note: * indicates a statistical significance ($p < 0.05$)

Table 4.2. PK parameters of irinotecan and SN-38 in saline and LPS groups predicted individually from developed PK model.

Predicted individual PK profiles of irinotecan and SN-38 were simulated using the best-fit model and derived PK parameters. (Figure 4.3a). Good correlations were observed between observed and predicted values of irinotecan and SN-38 in all mice (Figure 4.3b).

Predicted PK parameters from Individual Modeling:

Experiment 2-Saline Mice-Table for Individual PK										
Parameter	Units	Mouse 1	Mouse2	Mouse3	Mouse4	Mouse 5	Mean estimate	SD	CV%	p-value
tvV1	L	26.40	48.35	45.36	45.86	38.31	40.85	8.90	21.79	0.478
tvK1e	1/h	0.001	0.560	0.588	0.001	0.001	0.23	0.31	136.35	0.129
tvKa	1/h	0.13	0.14	0.20	0.19	0.18	0.17	0.03	18.82	0.246
tvV2	L	0.0092	0.0037	0.0048	0.0107	0.0028	0.0062	0.0035	56.58	0.314
tvk12	1/h	0.62	0.44	0.51	0.61	0.46	0.53	0.08	15.59	0.023
tvK2e	1/h	0.05	0.07	0.07	0.17	0.18	0.11	0.06	55.91	0.428
tvVmax	mg/h	1.13	2.10	2.78	3.05	3.39	2.49	0.90	35.96	0.232
tvKm	ng/mL	69.68	204.70	209.68	170.76	260.83	183.13	71.12	38.84	0.004
tvK13	1/h	0.164	0.012	0.010	0.015	0.014	0.043	0.068	156.64	0.222
tvK31	1/h	0.003	1.214	1.771	0.027	0.0002	0.60	0.84	138.58	0.091

Experiment 2-LPS Mice-Table for Individual PK									
Parameter	Units	Mouse 1	Mouse2	Mouse3	Mouse4	Mouse 5	Mean estimate	SD	CV%
tvV1	L	21.64	20.25	35.15	111.88	20.29	21.16	9.47	44.77
tvK1e	1/h	0.010	0.007	0.013	0.119045	0.010	0.032	0.049	152.72
tvKa	1/h	0.17	0.17	0.31	0.113435	0.19	0.19	0.07	37.06
tvV2	L	0.002	0.004	0.009	2.68E-03	0.006	0.005	0.003	58.97
tvk12	1/h	0.26	0.37	0.26	0.528913	0.39	0.36	0.11	30.80
tvK2e	1/h	0.036	0.023	0.022	0.36085	0.038	0.096	0.148	153.81
tvVmax	mg/h	2.56	3.12	4.19	1.37359	3.57	2.96	1.07	36.13
tvKm	ng/mL	690.45	633.32	771.09	288.966	670.96	610.96	186.91	30.59
tvK13	1/h	0.07	0.03	0.01	0.0080835	0.01	0.03	0.02	95.62
tvK31	1/h	0.00017	0.00032	0.00098	0.0001248	0.00006	0.00033	0.00037	113.24
stdev0		35.61	30.30	23.02	24.2921	30.09	28.66	5.10	17.78
stdev1		55.74	48.11	28.82	43.7106	33.35	41.95	10.93	26.05

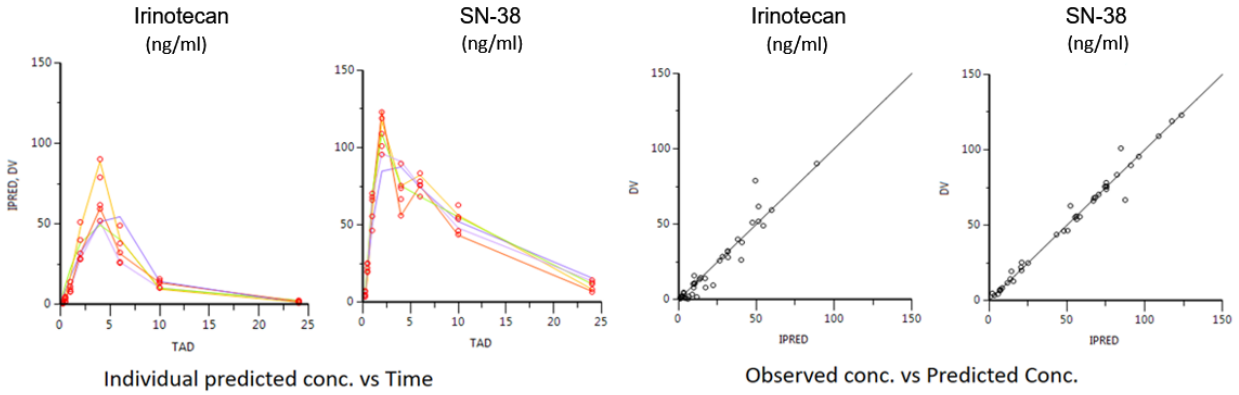

Figure 4.3. Plots of individual predicted concentration (IPRED) vs time after dose (TAD) **(4.3a)** and observed concentration vs predicted concentration **(4.3b)** for irinotecan and SN-38.

Figure 4.4 represents the diagnostic plots of individual weighted residuals (IWRES) versus individual predicted concentration (IPRED) profiles, in which, all weighted residuals fall within the narrow range of -2 to 2 of IWRES and distributed around the line of 0 on Y-axis for irinotecan and SN-38 compartments. The diagnostic plots of IWRES versus time (TAD) profiles in irinotecan and SN-38 compartments are presented in Figure 4.5. These diagnostic plots from PK modeling indicated that the best fit model of irinotecan and SN-38 could simultaneously describe the blood concentration profiles of irinotecan and SN-38, with reliability and stability for all mice in the saline and LPS treated groups.

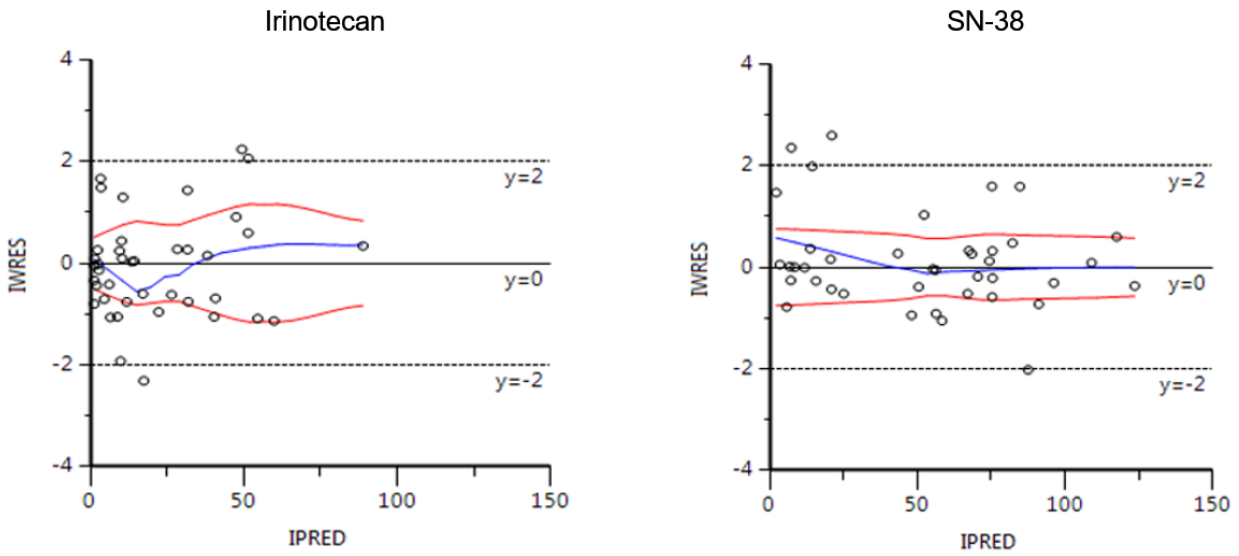

Figure 4.4. Diagnostic plots of individual weighted residual (IWRES) vs individual predicted concentration (IPRED) for irinotecan and SN-38.

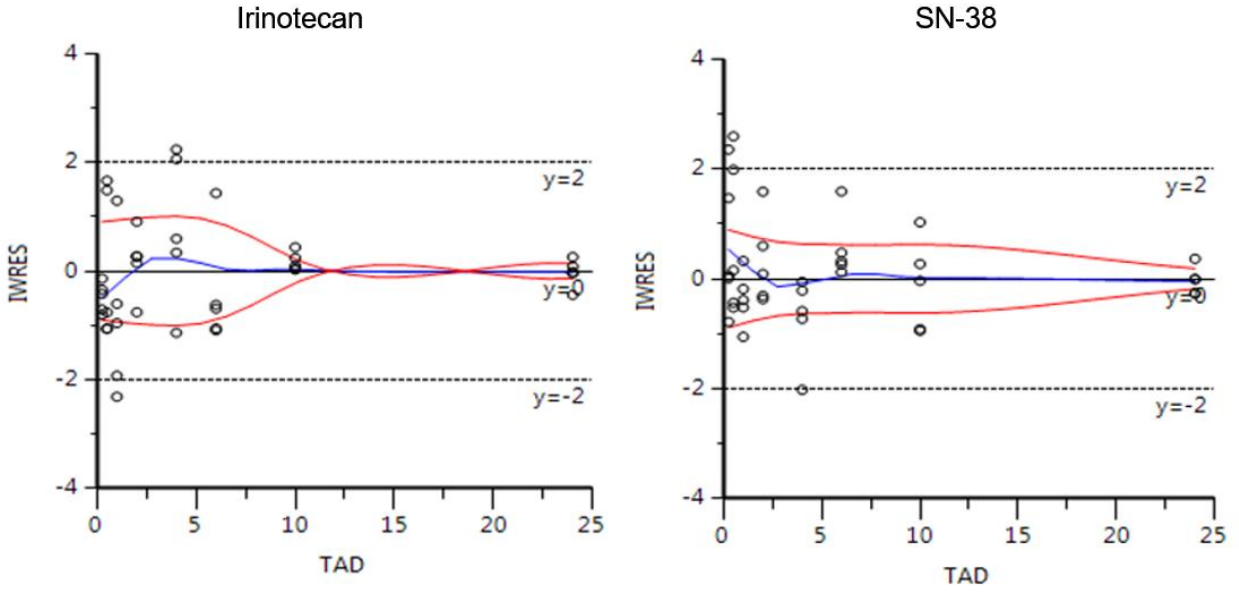

Figure 4.5. Diagnostic plots of individual weighted residual (IWRES) vs time after dose (TAD) for irinotecan and SN-38.

4.4 DISCUSSION

To our knowledge, this is the first study that describes the PK of irinotecan, SN-38, and SN-38G during inflammation. In this study, we (1) investigated the effects of inflammation on the PK of irinotecan, SN-38, and SN-38G, and (2) developed a co-model to simultaneously describe the PK of irinotecan and SN-38 during inflammation with parameters characterized. It is well known that during inflammation, the expression and activity of drug-metabolizing enzymes (DMEs) and transporters are reduced, mainly due to transcriptional suppression or as a result of post-translational protein modification, induced by mediators such as pro-inflammatory cytokines (IL-6, TNF-α, IL-1β) [42,44,47,123,127–129]. The reduction in the expression and activity significantly alters drug metabolism, pharmacokinetics, and pharmacodynamics (PK/PD) of drugs, and therefore poses a risk for toxicity and drug-drug interactions[39,41,56,130,131]. As reported in our results, the AUC of irinotecan and SN-38 were significantly elevated in mice after LPS treatment, with an increase of 2.6-folds for irinotecan and 2-folds for SN-38 when compared with the saline group. The significant increase in irinotecan concentrations could be due to the downregulation of carboxylesterase enzyme expression during inflammation, as reported by Mao et al (2011)[51], and confirmed with the decreased conversion rate constant, k12 in our developed PK model. The downregulation of CEs expression and activity could result in reduced phase-I metabolism of irinotecan, which converts the parent compound to SN-38.

As it is known that irinotecan chemotherapy causes severe diarrhea in patients, the 2-fold elevation of SN-38 concentrations during inflammation presents a higher risk of toxicity that may warrant dosage modifications in these patients who receive irinotecan. As ugt1a1 is known to be down-regulated during inflammaton[52,132,133], a possible mechanism for the elevation of SN-38 during inflammation could be the reduction in the expression and activity of ugt1a1.

Furthermore, the reduced expression and activity of UGT1A1 during inflammation may have contributed to the reduction in phase-II metabolism and conversion of SN-38 to inactive SN-38G, which results in a decreased clearance and increased accumulation of SN-38. This observation suggests that patients who receive irinotecan during inflammation may have an increased risk of experiencing severe, life-threatening diarrhea due to the significant elevation of SN-38 concentrations. On the other hand, there is limited evidence present on the regulation of intestinal β-glucuronidase enzyme expression and activity during inflammation *in vivo*. A recent study shows that LPS increases β-glucuronidase activity in liver cells[134]. Based on the elevated concentrations of SN-38 and the observation of a second peak in the PK profile of SN-38, a possible mechanism could also be the increase in the activity of β-glucuronidase enzyme during inflammation, which may have increased the reconversion of inactive SN-38G to active SN-38. This is consistent with our observation that SN-38G blood concentrations were unchanged by LPS treatment. Together, the downregulation of UGT1A1 and upregulation of β-glucuronidase enzymes might have played significant roles in the elevated blood SN-38 concentrations and AUC during inflammation.

As we observed a significant increase in SN-38 concentrations and AUC in mice with LPS treatment, we aimed to develop a PK model that can describe the correlation between irinotecan and SN-38 concentrations during inflammation. To date, a number of pharmacokinetic models were developed and published in various studies to describe irinotecan and SN-38 PK [110,117,135–138]. However, the co-modeling approach used in this study is novel, as for the first time, the effect of inflammation is incorporated in the PK model building. The proposed and validated PK model in this study can be used to accurately predict the plasma concentration of irinotecan and SN-38. The best fit structural model consisted of compartments for irinotecan, SN-38 and EHR

compartment connected with different rate constants. The model fitting exercises revealed a nonlinear PK process of SN-38 transferring between the EHR compartment with V_{max} and K_m. After the inclusion of non-linear PK for SN-38 and EHR compartments, the model was developed and model discrimination was performed on data using Phoenix, by minimizing the Akaike Information Criteria (AIC) and by comparison of the quality of fit plots. With the best fit model of irinotecan and SN-38, good correlations between observed and predicted concentrations were obtained in irinotecan and SN-38 compartments. The PK parameters described in the model were derived from 10 mice (5 mice per group). The standard deviation of PK parameter estimates (Table 4.2) revealed a small variation among 5 mice in each group, which reflected in the stability of the model. The rate constant K12 was significantly decreased, indicating that the conversion of irinotecan to SN-38 is reduced during inflammation. The K_m was significantly increased in the LPS group, indicating that the affinity of SN-38 to transporters involved in the recycling process was decreased during inflammation. Moreover, it is apparent with our model that during inflammation, the EHR increased with a higher Km and resulted in a significant second peak in the SN-38 profile.

The diagnostic plots from the developed model indicate that the best-fit PK model of irinotecan and SN-38 was highly stable to simultaneously describe the PK of irinotecan and SN-38 data with reliability in mice during inflammation. In addition to the effects of inflammation, the model also allowed us to successfully evaluate the effects of enterohepatic recycling in describing the PK of irinotecan and SN-38. The therapeutic implication of our research is that patients with inflammation should receive lower doses of irinotecan to achieve the same exposure as normal patients without inflammation. Using the developed model, we documented the impact of

inflammation on irinotecan PK quantitatively, which is useful to rationally adjust the dose of irinotecan to minimize the toxicity.

A limitation of this study is that only 10 mice were employed. A large sample size would have enhanced the predictive performance of our modeling results. Further studies focusing on irinotecan metabolism should be conducted and the mechanism of EHR elimination should be clearly demonstrated in the future.

4.5 Conclusion

The present study investigated the effects of inflammation on the PK of irinotecan and its metabolites SN-38, and SN-38G. Our research showed that during inflammation, the concentrations of irinotecan and SN-38 were elevated, likely because inflammation altered the expression and activities of phase-I and phase-II enzymes that are involved in irinotecan metabolism. This study also found that the AUC and C_{max} of irinotecan and SN-38 were significantly higher in mice with inflammation, which indicates that the patients with inflammation may experience severe toxicity in the form of diarrhea due to the increased exposure to SN-38. This research suggests a need for the adjustment of irinotecan dose in patients during inflammation. We further developed a PK model using Phoenix, which may be useful in predicting the PK of irinotecan and SN-38 during therapeutic drug monitoring or for establishing PK/PD relationships of irinotecan during inflammation.

CHAPTER 5

Role of TLR2 in Irinotecan-induced Diarrhea and Steatosis

Abstract:

Irinotecan (CPT-11) is a chemotherapy drug used in first- and second-line treatment of metastatic colorectal cancer. Irinotecan undergoes phase-I metabolism by hepatic and peripheral carboxylesterase to produce active metabolite, SN-38, which is 100-1000-fold more active than irinotecan and shows its cytotoxic activity by inhibiting the topoisomerase-I enzyme and causing irreversible DNA damage and cell death. The major toxicities associated with irinotecan chemotherapy in patients are gastrointestinal (GI) toxicity (diarrhea) and hepatotoxicity (steatosis or steatohepatitis). These toxicities result in life-threatening complications in patients and reduce the use of irinotecan as a chemotherapeutic agent. Evidence from the literature strongly suggests that toll-like receptors (TLRs), especially TLR2 is involved in the pathogenesis of gastrointestinal and hepatotoxicity. Therefore, in this study, we investigated the role of TLR2 in irinotecan-induced toxicity. Specifically, we used TLR2 WT and KO mice and treated with either saline (control) or irinotecan (treatment group) for 8 days and sacrificed the mice on day 9. To measure the extent of GI toxicity in TLR2 WT and KO mice, we conducted body weight measurements, the incidence of diarrhea, blood concentration analysis, and histological analysis of intestinal damage. Similarly, to determine the role of TLR2 in irinotecan-induced hepatotoxicity, H&E and Oil-Red-O histological analysis of liver sections, gene expression of enzymes and pro-inflammatory cytokines, and enzyme activity assays were conducted. The results indicate that the TLR2 KO mice with irinotecan treatment showed significantly lower damage both in terms of diarrhea and steatosis. Together, the results indicate a key role of TLR2 in the pathogenesis of irinotecan-induced toxicity. In the future, pharmacological inhibition or KO of TLR2 may help in healing irinotecan-induced GI and hepatotoxicity.

5.1 Introduction

Irinotecan (CPT-11) is a chemotherapy drug used in first- and second-line treatment of metastatic colorectal cancer[122,139,140]. Irinotecan undergoes phase-I metabolism by hepatic and peripheral carboxylesterase to form SN-38 (active & toxic metabolite)[141], which is glucuronidated by ugt1a1 to inactive SN-38 Glucuronide (SN-38G) [140]. Cyp3a4 also converts irinotecan to inactive APC and NPC metabolites[141]. SN-38 is 100-1000 fold more active than irinotecan and shows its cytotoxic activity by inhibiting topoisomerase-I enzyme[30,142,143], which causes irreversible DNA damage and cell death[30,141,144].

Patients who receive irinotecan chemotherapy experience severe side effects. Life-Threatening toxicity associated with irinotecan is gastrointestinal (GI) toxicity in the form of acute or delayed diarrhea[65,140,142–144]. Due to severe diarrhea, the dose of irinotecan is decreased, which results in reduced efficacy of the drug[65,145]. In addition, the fluid/electrolyte imbalance caused by diarrhea can lead to additional side effects such as renal insufficiency, malnutrition, and dehydration[65]. The National Cancer Institute (NCI) has issued a scale to assess the severity of diarrhea induced by chemotherapy in humans. This scale ranges from grade 1-5 based on the number of stools patients experience in a day over the baseline and an increase in ostomy output compared with baseline[29]. Although it is believed that the free intestinal luminal SN-38, either from bile or deconjugation of SN-38G, is responsible for irinotecan-induced diarrhea[140,144], the precise mechanisms underlying the toxicity remain unclear and effective interventions to prevent diarrhea are limited[65].

Toll-like receptors (TLRs) play an important role in the activation of innate immunity by recognizing specific patterns of microbial components, by which TLRs sense the invasion of pathogenic microorganisms. After binding with the ligand, TLRs dimerize and experience a conformational change, which then recruits downstream signaling molecules. The downstream

molecules include the adaptor molecule myeloid differentiation primary response protein 88 (MyD88), IRAKs, and TAK-1.[57] MyD88 serves as an adaptor linking TLRs with downstream molecules Mice lacking MyD88 do not generate TNF-α or IL-6 when exposed to IL-1 or other microbial components that activate TLR2, TLR4, TLR5, TLR7 or TLR9.[57] Among the toll-like receptors, TLR2 plays a key role in the initiation and maintenance of innate immune responses and previous research has shown that TLRs expression may be altered after chemotherapy treatment and correlate well with gastrointestinal mucositis.[61] Several studies have found an increased mRNA expression and protein levels of TLR2 along with TLR4 in samples of patients with gastrointestinal inflammatory diseases such as coeliac disease, inflammatory bowel disease and ulcerative colitis .[62–64] These studies suggest a potential mechanism that TLRs mediate gastrointestinal dysfunction and pain. Specifically, a study by Wardill et al. identified that TLR4 mediates the irinotecan-induced gut toxicity and pain and suggest that TLR4 can be a target for improved toxicity outcomes.[65] Moreover, the intestinal permeability and LPS translocation were higher in wild-type mice than mice with TLR4 deletion.[65] Another study by Frolova et al. investigated the expression of TLR2 and TLR4 in Biopsy samples of patients with inflammatory bowel diseases.[64] Specifically, small intestine and colon samples were obtained from patients with Crohn's disease and Ulcerative colitis and performed a immunohistochemical analysis of cryostat sections using polyclonal and monoclonal antibodies specific for TLR2 and TLR4 and found that the TLR2 expression in the terminal ileum of the collected patient's samples was significantly upregulated compared to controls.[64] A more recent study by Fakiha et al., 2019 showed that Amitriptyline, which is known to inhibit TLR2 and TLR4 activity in in vitro models, also inhibited diarrhea and colonic apoptosis caused by chemotherapy treatment in rats.[66] TLR mediated inflammatory pathways have also been linked with chemotherapy-induced gut toxicity and pain.[67]

The alimentary mucositis caused by chemotherapy is also heavily linked with the human gut microbiome and bacteria and these bacteria is tightly regulated by the TLR family, because TLRs play a vital role in the gut homeostasis and bacterial regulation.[68] A review by Ribeiro et al. suggests that TLR2 is a potential therapeutic target to modulate or minimize the toxicity associated with chemotherapy, and also to optimize cancer treatment dosing and clinical outcomes. Another review by Stringer reports that TLR2 along with TLR4, TLR5, and TLR9 are involved in intestinal mucositis.[69] TLR-2/GSK-3β signaling pathway also has been suggested to play a key role in the development of intestinal mucositis caused by doxorubicin.[70] More importantly, a study investigated the involvement of TLRs and MyD88 in the pathogenesis of intestinal mucositis caused by anticancer regimens using MyD88- and TLR2-knock out mice. This study found that genetic deletion of TLR2 and MyD88 effectively controlled the signs of intestinal injury when compared with wild-type control mice.[71]

Toll-like receptors have also been suggested to play a role in the development of steatosis. For example, metabolic syndrome is well known to induce fat accumulation in hepatocytes and one study by Himes et al. reported that mice lacking TLR2 are protected from hepatic steatosis and these mice also showed diminished inflammatory cytokine expression.[59] Gut-derived bacterial endotoxins also may play a role in the development of non-alcoholic fatty liver disease (NAFLD).

Given the amount of evidence in the literature suggesting a key role of TLR2 in the pathogenesis of gastrointestinal diseases as well as hepatotoxicity, in this study, we aimed to investigate the role of TLR2 in irinotecan-induced GI and hepatotoxicity using TLR2 wild-type and knockout mice.

5.2 Materials and Methods

5.2.1 Chemicals

Irinotecan hydrochloride was purchased from Martin Surgical Supply, Houston, TX (item no: 4434-11). SN-38 was purchased from Cayman chemical (item no: 15632). SN-38G was synthesized in Dr. Ming Hu's lab at the University of Houston, Houston, TX. Camptothecin (CPT; internal standard) was purchased from Millipore Sigma, St Louis, MO. 4-Nitrophenyl-β-D-glucuronide (Catalog No. O-PNPBGA) was purchased from Megazyme.com. The special low-fat diet was purchased from Research Diets, New Brunswick, NJ. Formalin and all other solvents used for chromatographic analysis were of LC-MS grade and purchased from VWR International, LLC (Suwanee, GA, USA). Unless specified, all other chemicals and reagents used were purchased from Millipore Sigma, St. Louis, MO.

5.2.2 Animals

Male, 5-weeks old C57BL6J and B6.129-Tlr2tm1Kir/J (TLR2 KO) mice were purchased from Jackson Laboratory, Ban Harbor, ME. The animals were kept in an environmentally controlled room (temperature 25 ± 2^0C, 12 h dark-light cycle, humidity 50 ± 5%) for at least 1 week before performing any experiments. The mice were on a special diet (low-fat diet, 35% sucrose with 10% kcal fat) ad libitum throughout the animal study. All the animal care and use protocols followed were approved by the Institutional Animal Care and Use Committee (IACUC) at the University of Houston.

5.2.3 Study Design and Drug Treatments

C57BL6J mice were divided into 2 groups (n = 5 per group) and treated with either saline or irinotecan. Similarly, TLR2 KO mice were divided into 2 groups and treated with saline or

irinotecan. Mice were treated with either saline or irinotecan (50 mg/kg, intraperitoneal) once a day for 8 days. Mice were sacrificed on day 9, after 24 hours of last irinotecan treatment. Mouse liver and intestine were isolated immediately after sacrificing.

5.2.4 Evaluation of Body Weight and Incidence of Diarrhea

The body weight of mice was measured daily to track weight loss/gain, and the presence of diarrhea was monitored in mice daily from days 1-9. The loss in body weight from days 1 to 9 was calculated and reported in terms of % weight loss. Diarrhea was quantified according to a validated grading criterion previously described[101] with slight modification. The grading was given based on the severity of diarrhea observed and is reported as follows: grade 0 (normal or no diarrhea), grade 1 (slightly wet and soft tool), grade 2 (wet stool with moderate perianal staining), grade 3 (severe diarrhea and staining), grade 4 (severe, life-threatening bloody diarrhea with staining and continual anal leakage).

5.2.5 Histological Analysis of Intestine and Liver injury

Intestine or liver sections (n=5 per group) collected immediately after sacrificing were placed in tissue embedding cassettes and fixed in 10% neutral buffered formalin (vol/vol) for histological examination. The samples were then embedded in paraffin and stained with hematoxylin and eosin (H&E) at Pathology Core and Lab, Baylor College of Medicine (BCM), Houston, TX. The H&E stained slides of intestine and liver were evaluated by an experienced pathologist in a blinded fashion and morphological observations of intestine and liver injury were recorded. The liver injury was assessed based on the percentage of hepatocytes showing fat accumulation and hepatic inflammation (steatosis or steatohepatitis). The severity of steatosis in control and irinotecan-treated groups was reported as previously described[101] with slight modifications. The grading was

as follows: score 0 (no steatosis), score 1 (minimal fat accumulation, < 5% steatosis), score 2 (5-30% steatosis), score 3 (30-65% steatosis), score 4 (severe fat accumulation, > 65% steatosis). The final score reported was an average of scores observed individually for each slide in a group. To evaluate the intestinal injury, criteria such as shortening of villi and disruption of crypt cells were considered.

5.2.6 Analysis of Blood Concentrations

The whole blood concentrations of irinotecan, SN-38, and SN-38G in TLR2 WT and KO treatment groups were determined using LC-MS/MS analysis. For the analysis, a 10 µl of the blood sample was mixed with 10 µl of PBS and to this mixture, 200 µl of 50% of acetonitrile (ACN) containing 5 µM camptothecin (internal standard) was added as an extracting solvent. Samples were vortexed for 30 sec and centrifuged for 15 min at 15000 rpm. After the centrifugation, 180 µl of supernatants were collected and allowed to dry under a gentle stream of air at room temperature. The air-dried samples were then reconstituted with 100 µl of 50% acetonitrile and samples were centrifuged for 10 min at 10000 rpm. 80 µl of the supernatant was transferred to vials and 10 µl was injected into LC-MS/MS for the analysis of irinotecan, SN-38, and SN-38G.

To analyze irinotecan and metabolite concentrations, an API 5500 QTRAP triple quadrupole mass spectrophotometer (AB Sciex, USA) equipped with a Turbospray TM source was used by multiple reaction monitoring (MRM) method operated in a positive ion mode, with minor modifications to the method conditions as previously described[100]. A UPLC system, Waters Acquity™ with a diode-arrayed detector (DAD) was used. The UPLC conditions were as follows: column, Acquity UPLC BEH C18 column (50 mm × 2.1 mm I.D., 1.7 µM, Waters, Milford, MA, USA); mobile phase A - 0.1% formic acid; mobile phase B - 100% acetonitrile performed in a gradient from 0 to 4.5 min. The flow rate and the sample injection volume were 0.4 ml/min and 10 µL, respectively.

The following m/z transitions were selected: m/z 587.1 → 124.1 for irinotecan; m/z 393.1 → 349.1 for SN-38; m/z 569.5 → 393.1 for SN-38G; m/z 349.0 → 305.1 for CPT. The selection of the fragment ions depended on the highest intensity of the fragment. The data collected was analyzed with Analyst 1.4.2 software (AB Sciex, USA).

5.2.7 Gene Expression of Enzymes and Proinflammatory Cytokines

Relative gene expression of TNF-α and Ugt1a1 was determined by RT-PCR. Briefly, total RNA from mouse liver tissue was isolated using TRIzol reagent according to the manufacturer's protocol. RNA samples were assessed for quality and quantity using a spectrophotometer (Beckman Coulter DU 800). The RNA samples were then treated with DNase digestion enzyme and buffer to remove any contaminating DNA from the RNA preparation. A 5 µg of total RNA was used for the cDNA synthesis using a High Capacity Reverse Transcription Kit from Applied Biosystems. RT-PCR was performed using an Applied Biosystems 7300 system. For RT-PCR, the reaction mixture contained about 50-100 ng of cDNA, 300 nM of gene-specific forward primer, 300 nM reverse primer, and 200 nM probe and a 15 µl of Taqman Universal PCR Master Mix from Roche. Cyclophilin was used as the housekeeping gene to normalize the quantitative expression values. The threshold cycle (Ct) values were of each sample was determined by the PCR instrument. The ΔΔCt method was used to calculate relative gene expression.

5.2.8 Carboxylesterase Activity

Whole cell extracts were prepared from mouse livers and protein concentration was determined by BCA assay according to the manufacturer's protocol (Pierce Chemical, Rockford, IL). Total carboxylesterase activity was monitored by measuring the absorbance using a BioTek plate reader in a 96-well plate. Briefly, whole cell extracts containing CEs enzyme was incubated with the

substrate P-nitrophenyl acetate (PNPA) at 37 ^{o}C, and absorbance was measured for 10 min at 405 nm. The assay was run for 10 min with 2 min intervals. The specific activity of carboxylesterase was expressed as the µmoles of PNP formed per min per mg of protein.

5.2.9 Ugt1a1 Activity

Ugt1a1 activity in control and irinotecan-treated groups was determined by measuring the formation of SN-38 glucuronide by LC-MS/MS analysis using SN-38 as a substrate. Briefly, whole cell extracts from the mouse liver tissue were prepared, and protein concentration was determined using the BCA assay kit according to the manufacturer's protocol (Pierce Chemical, Rockford, IL). To measure the enzyme activity, a reaction containing 1 mg/ml protein, 10 µM of SN-38, solution A (25 mM UDPGA Triammonium salt) and solution B (25 mM Saccharolactone, 5 mM $MgCl_2$ and 0.022 mg/ml Alamethicin) in 0.05 M KPi buffer was used. The total reaction volume was 170 µl. The reaction was conducted in a water bath at 37 ^{o}C for 60 min. The reaction was terminated by adding 7 µl of acetonitrile (ACN) containing 1 µg/ml CPT (internal standard). Samples were then processed and analyzed by LC-MS/MS to determine the ugt1a1 activity. The specific enzyme activity was expressed as nM of SN-38G formed.

5.2.10 Statistical Analysis

Data are expressed as mean ± standard deviation for all the experiments. One-way ANOVA was performed using GraphPad Prism 8.0 software to determine the significance of differences between control and treatment groups. P-value of < 0.05 was considered as statistically significant.

5.3 Results

5.3.1 Evaluation of Body Weight and Diarrhea

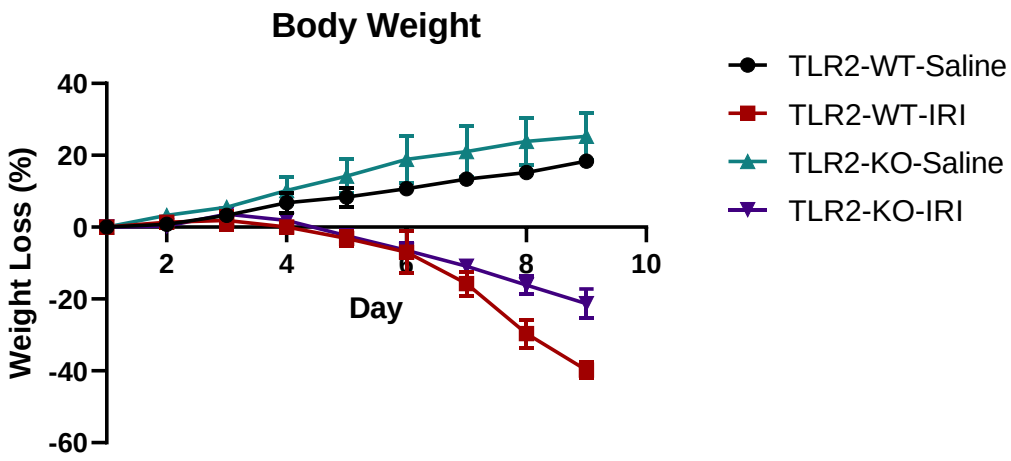

Figure 5.1. Percentage Body Weight (BW%) change in control and treatment groups measured from days 1-10.

Experimental values of body weight change in TLR2 WT and KO mice from day 1 – 9

	Change in Weight (%)			
	TLR2-WT-SAL	TLR2-WT-IRI	TLR2KO-SAL	TLR2KO-IRI
Day 1	0.0	0.0	0.0	0.0
Day 2	0.8	1.4	3.3	0.3
Day 3	3.3	1.9	5.5	3.6
Day 4	6.8	0.0	10.2	1.9
Day 5	8.4	-3.1	14.2	-2.4
Day 6	10.7	-7.0	18.9	-6.5
Day 7	13.4	-15.7	21.0	-10.9
Day 8	15.2	-29.6	23.9	-16.1
Day 9	18.4	-39.8	25.3	-21.3

	STDEV			
	TLR2-WT-SAL	TLR2-WT-IRI	TLR2KO-SAL	TLR2KO-IRI
Day 1	0.00	0.00	0.00	0.00
Day 2	1.84	1.08	1.45	1.55
Day 3	1.12	2.81	1.87	1.04
Day 4	2.83	1.97	3.80	1.53
Day 5	2.66	2.21	4.86	1.97
Day 6	1.44	5.96	6.64	2.24
Day 7	1.41	3.38	7.16	1.44
Day 8	1.64	3.94	6.53	2.45
Day 9	1.98	2.18	6.63	4.12

The body weights in mice treated with saline and irinotecan in TLR2 WT and KO mice were recorded each day over the course of 9 days and reported as the % weight change during the treatment period (Figure 5.1). Results showed that there was a slight increase in the body weight from day 1-4 in all the groups of mice, although the saline-treated groups showed an even higher increase than the irinotecan treated mice in both TLR2 WT and KO groups. The slight increase in body weight remained constant in both the mice groups with saline treatment until the end of the treatment period (day 9). However, after day 4, a significant decline in the body weight was

observed with irinotecan treatment in both TLR2 WT and KO mice. By day 9 of the treatments (7^{th} dose of irinotecan), the TLR 2 WT mice group showed severe weight loss with an average of 39.8% reduction due to bloody diarrhea, whereas in the TLR2 KO group, the average weight loss was 21.3% when compared to the body weight of mice on day 1. Although the weight loss from day 1 to 9 was higher in the TLR2 WT group with irinotecan treatment, the statistical analysis by ANOVA followed by a posthoc Tukey test did not show a significant difference in the weight loss between TLR WT and KO groups. No body weight loss was observed in the control groups with saline treatment in both TLR2 WT and KO mice groups throughout the treatment period.

Treatment Groups	Mice Number per Group	Diarrhea Score								
		Day 1	Day 2	Day 3	Day 4	Day 5	Day 6	Day 7	Day 8	Day 9
Group 1 (TLR2 WT-Saline)	n=5	No Diarrhea	No Diarrhea	No Diarrhea	No Diarrhea	No Diarrhea	No Diarrhea	No Diarrhea	No Diarrhea	No Diarrhea
Group 2 (TLR2 WT-Irinoecan)	n=5	No Diarrhea	No Diarrhea	No Diarrhea	No Diarrhea	Symptoms of diarrhea, normal movement	Grade 1 visible bloody diarrhea, slight weakness,	Grade 2 Increased bloody diarrhea, blood stains, weak mice, less movement, slightly crunched position	Grade 3 Severely weak mice in crunched position, reduced movemet; however able to move. Cages covered with bloody stains.	Grade 4 Severe bloody diarrhea, severe weakness.
Group 3 (TLR2 KO-Saline)	n=5	No Diarrhea	No Diarrhea	No Diarrhea	No Diarrhea	No Diarrhea	No Diarrhea	No Diarrhea	No Diarrhea	No Diarrhea
Group 4 (TLR2 KO-Irinotecan)	n=5	No Diarrhea	No Diarrhea	No Diarrhea	No Diarrhea	No Diarrhea	symptoms of diarrhea, no bloody diarrhea	Grade 1 Slight bloody diarrhea, normal movemet of mice	Grade 1 visible bloody stains in cage, reduced movement in mice, weak mice, slightly crunched position while moving	Grade 2-3 Reduced movement of mice, reduced intake of food, visible weakness, crunched position, bloody diarrhea.

Table 5.1. Incidence of diarrhea and diarrhea grade observed from days 1-10 in control and irinotecan treated mice groups.

The incidence and severity of diarrhea were monitored in both control and irinotecan treated mice in TLR2 WT and KO groups for 9 days (Table 5.1). No diarrhea was observed in saline-treated mice in TLR2 WT and KO groups throughout the treatment period. TLR2 WT group showed signs of diarrhea on day 5 of irinotecan treatment and the severity of diarrhea steadily increased in this group of mice until day 9. On day 9, TLR2 WT group mice showed a grade 4 diarrhea with severe diarrhea and weakness with no movement. On the other hand, the TLR2 KO

mice treated with irinotecan showed only a grade 2 diarrhea on day 9 with signs of reduced movement in mice, reduced intake of food, visible weakness, and bloody diarrhea. However, the severity of bloody diarrhea observed in the TLR2 KO group is less severe when compared to TLR2 WT group mice.

5.3.2 Histological Analysis of Intestine and Liver Damage

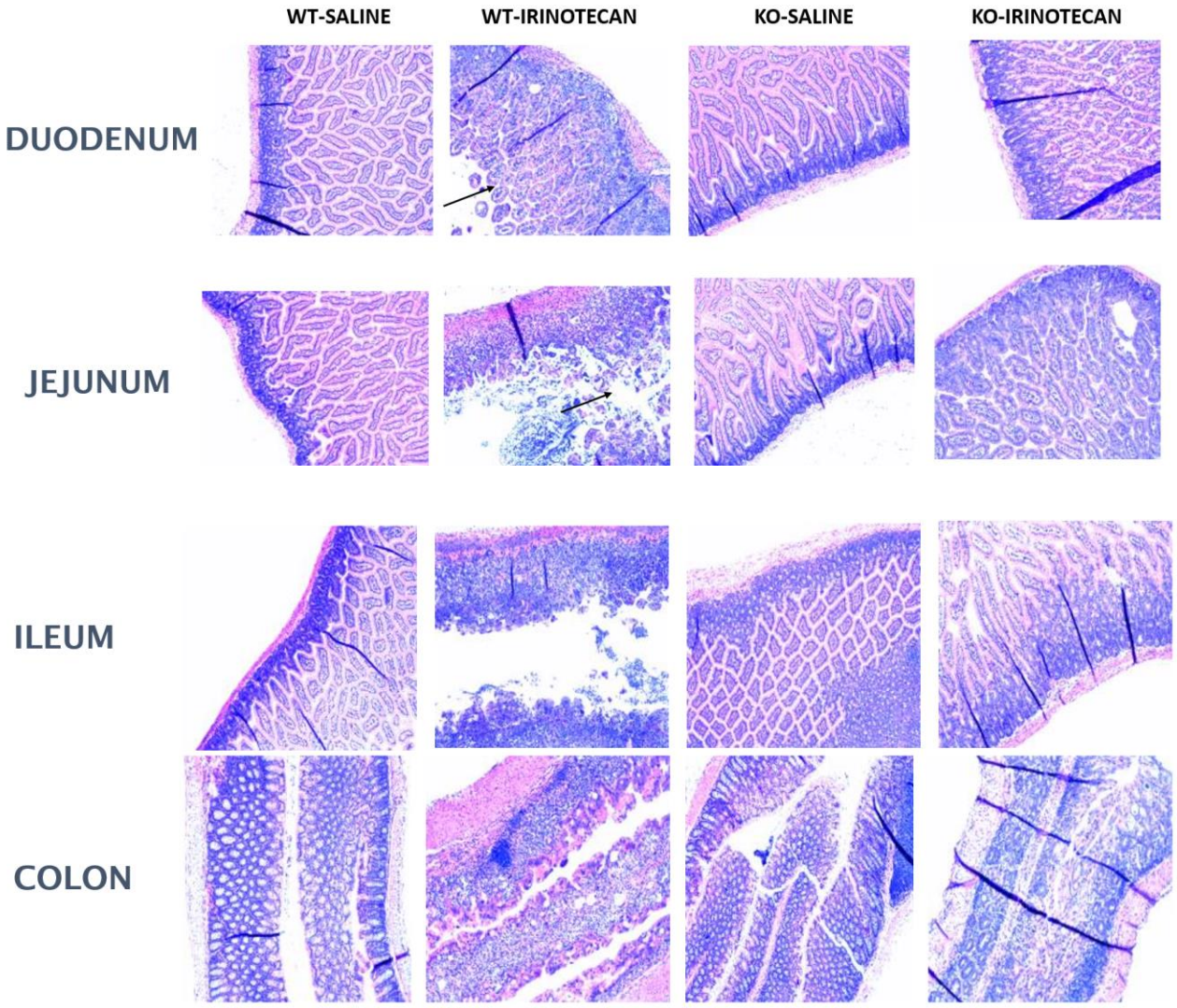

Figure 5.2. H&E stained images Duodenum, Jejunum, Ileum, and Colon of mice groups: WT-Saline, WT-Irinotecan, KO-Saline, KO-Irinotecan

The intestinal tissues duodenum, jejunum, ileum, and colon collected from saline and irinotecan-treated TLR2 WT and KO groups were fixed in 10% buffered formalin, and subsequently, paraffin-embedded and stained with H&E. Histological analysis was performed on paraffin-embedded sections following H&E staining and the images were evaluated by a pathologist for the presence of intestinal injury. The images of TLR4-WT with irinotecan treatment showed severe damage of all parts of the small intestine and colon, with a total disruption of crypts, obvious shortening of villi (Figure 5.2), whereas TLR2 WT and KO groups with saline treatment did not show any indications of morphological changes in the intestine. On the other hand, a moderate change in the morphology of intestinal tissue was observed in TLR2 KO group treated with irinotecan; however, significantly less damage and fewer changes to the villi and crypts were noticed in comparison with the intestinal damage observed in the TLR2 WT mice treated with irinotecan. The intestinal damage observed by histological analysis in control and irinotecan treated groups is well-correlated with the trends in body weight loss and incidence of diarrhea observed. Specifically, the TLR2 WT mice, which showed severe intestinal damage also was found to have the highest loss in body weight.

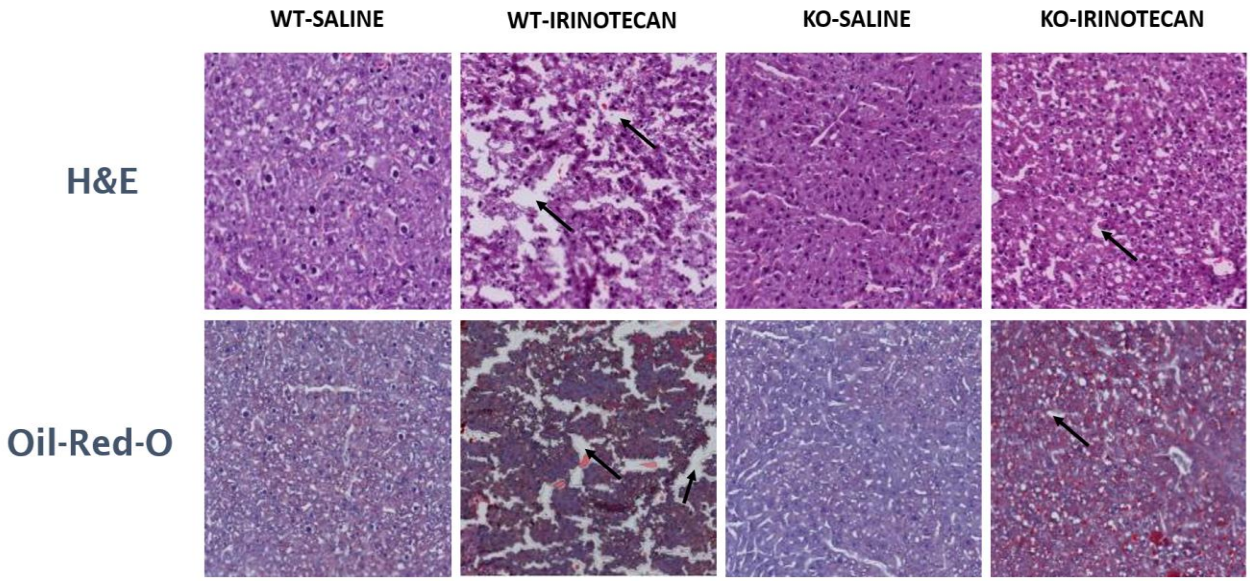

Figure 5.3. H&E and Oil-Red-O stained liver images of mice groups, WT-Saline, WT-Irinotecan, KO-Saline, KO-Irinotecan

H&E and Oil-Red-O stained liver sections were examined for indications of fat accumulation and signs of hepatic inflammation (steatosis and steatohepatitis) and a score were assigned by a pathologist based on the extent of fat accumulation observed with saline and irinotecan treatments in TLR2 WT and KO mice. As expected, the saline-treated mice in both TLR2 WT and KO groups did not show any fat accumulation (Figure 5.3). When compared to the irinotecan treated mice, extensive fat accumulation was seen in the TLR2 WT group with up to 80% fat accumulation with a steatosis score of 4. Although TLR2 KO mice also showed a clear fat accumulation, the severity of steatosis was less in comparison with the TLR2 WT group.

5.3.3 Gene Expression of Enzymes and Pro-inflammatory Cytokines

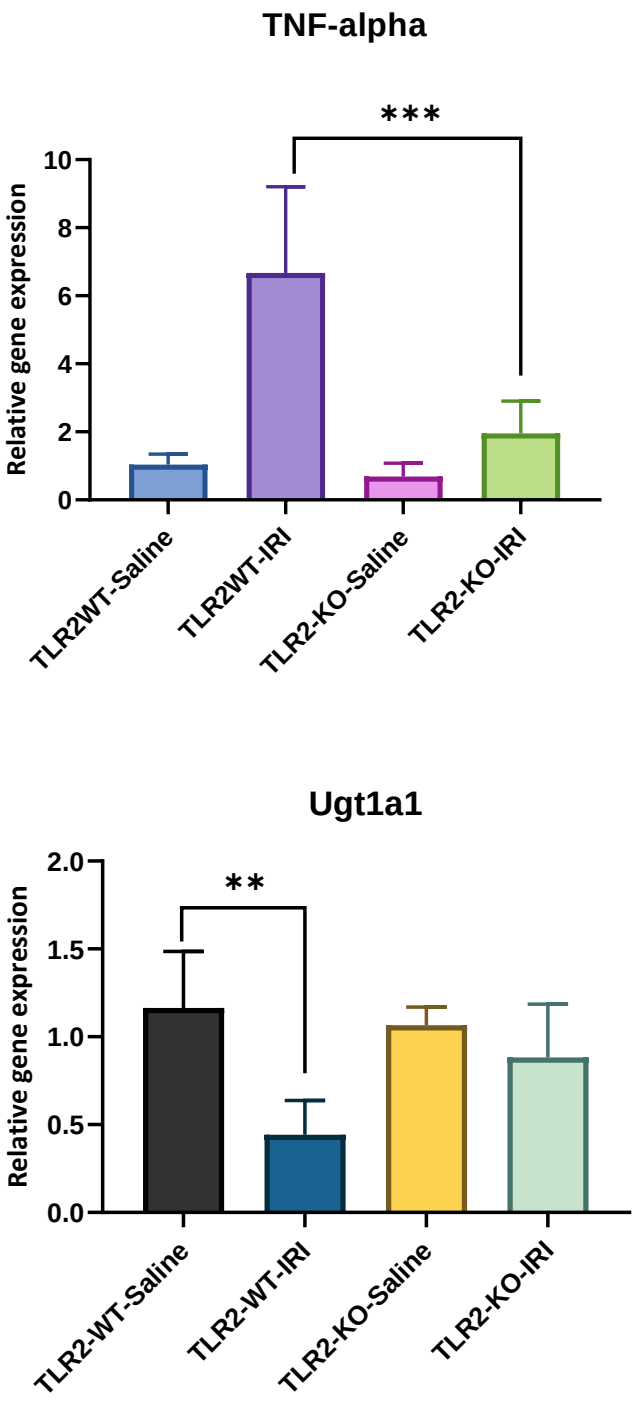

Figure 5.4. Gene Expression of TNF-α and Ugt1a1 in livers of mice groups: WT-Saline, WT-Irinotecan, KO-Saline, KO-Irinotecan.

TNF-a Gene Expression Ct values and Fold Change Calculations:

TNF-a											
Sample	Ct 1	Ct 2	Ave Ct	SD Ct	ΔCt	ΔCtAve	ΔΔCt	2(-ΔΔCt)		Corrected	SD 2(-ΔΔCt)
WT-SAL-M1	26.4738	26.2415	26.3577	0.1643	7.3187		-0.3104	1.2401			
WT-SAL-M2	26.8573	26.3848	26.6211	0.3341	7.2324		-0.3967	1.3165			
WT-SAL-M3	27.1425	27.3155	27.2290	0.1223	7.3337	7.62907	-0.2954	1.2272	1.0395	1.0000	0.3060
WT-SAL-M4	28.0245	27.956	27.9903	0.0484	8.1824		0.5533	0.6815			
WT-SAL-M5	27.3844	27.4908	27.4376	0.0752	8.0783		0.4492	0.7325			
WT-IRI-M1	24.9583	25.0135	24.9859	0.0390	5.5381		-2.0910	4.2605			
WT-IRI-M2	24.6783	24.1459	24.4121	0.3765	5.1102		-2.5189	5.7315			
WT-IRI-M3	23.8948	23.4371	23.6660	0.3236	4.4147	4.97407	-3.2144	9.2819	6.6734	6.4197	2.5316
WT-IRI-M4	24.8841	24.741	24.8126	0.1012	5.4234		-2.2057	4.6130			
WT-IRI-M5	23.9432	23.8461	23.8947	0.0687	4.3842		-3.2449	9.4802			
KO-SAL-M1	27.3746	27.3459	27.3603	0.0203	7.9646		0.3355	0.7925			
KO-SAL-M2	26.6621	26.3748	26.5185	0.2032	7.2626		-0.3665	1.2892			
KO-SAL-M3	28.5558	28.99	28.7729	0.3070	9.3464	8.34733	1.7173	0.3041	0.6894	0.6632	0.3868
KO-SAL-M4	27.4587	27.8463	27.6525	0.2741	8.2478		0.6187	0.6513			
KO-SAL-M5	28.5738	28.4749	28.5244	0.0699	8.9155		1.2864	0.4100			
KO-IRI-M1	26.3389	26.1483	26.2436	0.1348	6.7207		-0.9084	1.8769			
KO-IRI-M2	27.194	27.4348	27.3144	0.1703	7.9058		0.2767	0.8255			
KO-IRI-M3	25.4839	25.3844	25.4342	0.0704	5.9881	6.8181	-1.6410	3.1189	1.9554	1.8811	0.9465
KO-IRI-M4	26.9472	27.0338	26.9905	0.0612	7.2614		-0.3677	1.2903			
KO-IRI-M5	25.6879	25.9457	25.8168	0.1823	6.2147		-1.4144	2.6655			

Ugt1a1 Gene Expression Ct values and Fold Change Calculations:

Ugt1a1											
Sample	Ct 1	Ct 2	Ave Ct	SD Ct	ΔCt	ΔCtAve	ΔΔCt	2(-ΔΔCt)		Corrected	SD 2(-ΔΔCt
WT-SAL-M1	21.2345	21.3975	21.3160	0.1153	2.2770		0.0540	0.9633			
WT-SAL-M2	21.7428	21.4829	21.6129	0.1838	2.2242		0.0012	0.9992			
WT-SAL-M3	21.3445	21.4587	21.4016	0.0808	1.5063	2.22299	-0.7167	1.6434	1.0517	1.0000	0.3753
WT-SAL-M4	21.9753	21.9424	21.9589	0.0233	2.1510		-0.0720	1.0512			
WT-SAL-M5	22.2468	22.3849	22.3159	0.0977	2.9565		0.7335	0.6014			
WT-IRI-M1	23.4729	23.8492	23.6611	0.2661	4.2132		1.9902	0.2517			
WT-IRI-M2	21.6458	21.3479	21.4969	0.2106	2.1949		-0.0281	1.0197			
WT-IRI-M3	22.2578	22.2479	22.2529	0.0070	3.0016	3.25007	0.7786	0.5829	0.5580	0.5305	0.3087
WT-IRI-M4	22.3414	22.1839	22.2627	0.1114	2.8735		0.6505	0.6371			
WT-IRI-M5	23.4831	23.4724	23.4778	0.0076	3.9673		1.7443	0.2985			
KO-SAL-M1	21.4748	21.3485	21.4117	0.0893	2.0160		-0.2070	1.1543			
KO-SAL-M2	21.5435	21.5367	21.5401	0.0048	2.2842		0.0612	0.9585			
KO-SAL-M3	21.3435	21.4458	21.3947	0.0723	1.9681	2.13542	-0.2549	1.1932	1.0665	1.0141	0.1031
KO-SAL-M4	21.6575	21.4849	21.5712	0.1220	2.1665		-0.0565	1.0400			
KO-SAL-M5	21.5678	22.1348	21.8513	0.4009	2.2424		0.0194	0.9866			
KO-IRI-M1	21.7284	21.4729	21.6007	0.1807	2.0778		-0.1452	1.1059			
KO-IRI-M2	22.4488	22.2489	22.3489	0.1414	2.9402		0.7172	0.6083			
KO-IRI-M3	21.3487	21.389	21.3689	0.0285	1.9228	2.47667	-0.3002	1.2313	0.8831	0.8397	0.3035
KO-IRI-M4	22.0927	22.0123	22.0525	0.0569	2.3234		0.1004	0.9328			
KO-IRI-M5	22.7645	22.6784	22.7215	0.0609	3.1193		0.8963	0.5373			

The gene expression analysis results of pro-inflammatory cytokine TNF-α and Ugt1a1 enzyme are shown in Figure 5.4. As the literature suggests, with irinotecan induced steatohepatitis, there is typically hepatic inflammation present in the liver. Moreover, the conversion from SN-38 to SN-

38G by the Ugt1a1 enzyme determines the concentration levels of SN-38 and the associated gut and liver toxicity. Therefore, we aimed to measure the gene expression of TNF-α cytokine and Ugt1a1 in livers of TLR2 WT and KO mice treated with saline or irinotecan. Interestingly, we found that with the irinotecan treatment, the TNF-α expression was significantly induced in the TLR2 WT mice, with a 6.4-fold increase when compared to TLR2 WT mice with saline treatment (control). The expression of TNF-α in TLR2 KO mice with either saline or irinotecan was not significantly altered. Most importantly, we found that the TNF-α expression in TLR2WT mice was significantly higher compared to TLR2 KO mice with irinotecan treatment (6.4 vs 1.8-fold increase, respectively). These results suggest that irinotecan upregulates pro-inflammatory cytokine (TNF-α) expression in the liver and therefore may contribute to steatohepatitis.

In contrast to the TNF-α gene expression results, we observed that irinotecan treatment itself downregulated the Ugt1a1 expression in TLR2 WT mice compared with saline treatment. However, we did not find any statistically significant difference in the Ugt1a1 expression between TLR2 WT and KO mice with irinotecan treatment (0.55 vs 0.88-folds).

5.3.4 Analysis of Blood Concentrations

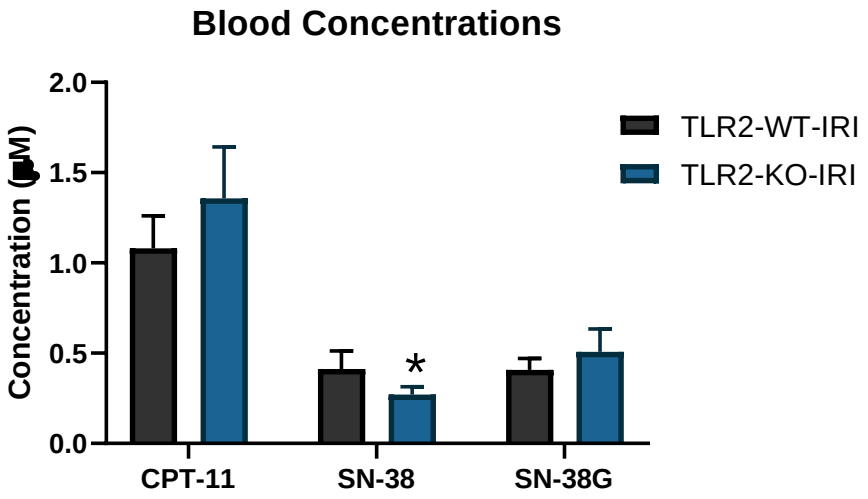

Figure 5.5. Blood Concentrations of Irinotecan, SN-38, and SN-38G in TLR2 WT and KO mice groups treated with Irinotecan.

Blood concentration values of irinotecan, SN-38, and SN-38G.

Concentrations (uM)					
Irinotecan	SN-38	SN-38G	SD		
1.08025	0.41175	0.407	0.181292	0.10031409	0.063650085
1.3578	0.2706	0.5076	0.284102	0.043142786	0.125941653
CPT-11	SN-38	SN-38G			
0.135622524	0.024003	0.19222			

The blood concentrations of irinotecan, SN-38, and SN-38G were measured in both the irinotecan treated mice groups (TLR2 WT and KO) using LC-MS/MS analysis and the concentrations were shown in figure 5.5. The concentrations of irinotecan and metabolites were measured in μM. The parent compound, irinotecan blood concentrations were not altered between TLR2 WT and KO mice. However, we found significantly lower SN-38 blood concentrations in the TLR2 KO group. Similar to the parent compound, the SN-38G inactive

metabolite concentrations were not altered between the TLR2 WT and KO groups with irinotecan treatment.

5.3.5 Carboxylesterase and Ugt1a1 Enzyme Activity

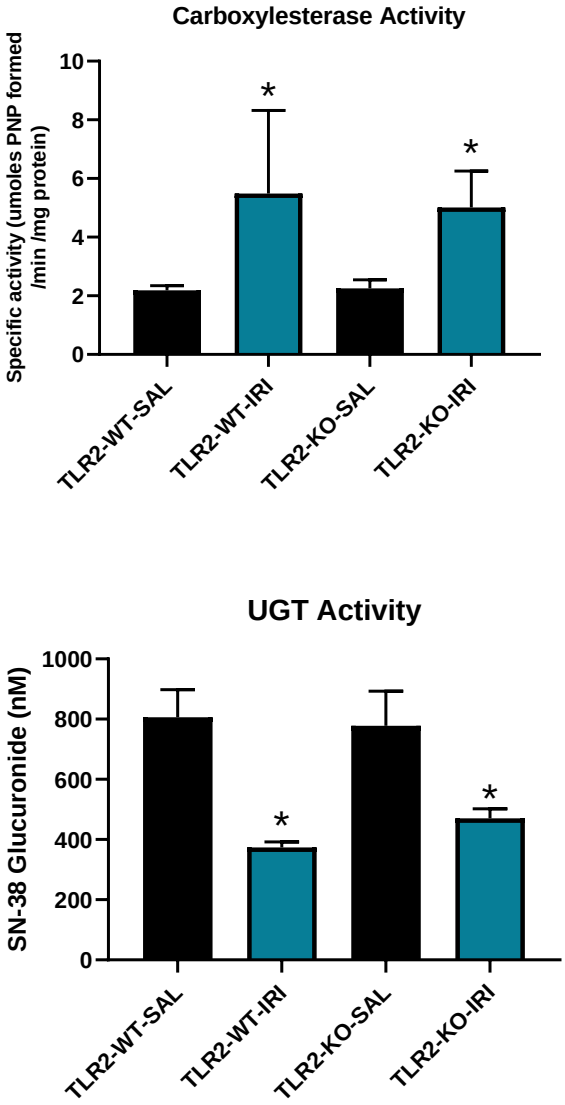

Figure 5.7. Activity of liver carboxylesterase enzyme in mice treated with Saline, NovaSoy, Sal/IRI, or NS/IRI.

Carboxylesterase Specific Activity Values and Calculations

Sample	0	2	4	6	8	10	Slope	R-square	PNP Concentration (moles/L)	PNP Concentration (moles/L/min)	PNP concentration (mMoles/ml/min)
Buffer	0.053	0.058	0.055	0.057	0.059	0.059	0.001	0.607	0.00003	0.000003	0.000003
Buffer +PNPA	0.044	0.044	0.046	0.047	0.049	0.051	0.001	0.957	0.00004	0.000004	0.000004
WT-SAL-M1	0.410	0.446	0.464	0.488	0.502	0.524	0.011	0.982	0.00059	0.000059	0.000059
WT-SAL-M2	0.413	0.436	0.456	0.476	0.489	0.502	0.009	0.988	0.00048	0.000048	0.000048
WT-SAL-M3	0.426	0.444	0.469	0.495	0.500	0.526	0.010	0.983	0.00054	0.000054	0.000054
WT-SAL-M4	0.398	0.434	0.455	0.475	0.492	0.507	0.011	0.975	0.00057	0.000057	0.000057
WT-SAL-M5	0.390	0.428	0.443	0.462	0.481	0.497	0.010	0.976	0.00055	0.000055	0.000055
WT-IRI-M1	0.340	0.423	0.495	0.543	0.621	0.689	0.034	0.996	0.00185	0.000185	0.000185
WT-IRI-M2	0.214	0.234	0.243	0.268	0.298	0.315	0.010	0.982	0.00056	0.000056	0.000056
WT-IRI-M3	0.313	0.348	0.373	0.385	0.404	0.439	0.012	0.977	0.00063	0.000063	0.000063
WT-IRI-M4	0.363	0.453	0.535	0.600	0.650	0.673	0.031	0.964	0.00171	0.000171	0.000171
WT-IRI-M5	0.240	0.256	0.274	0.297	0.238	0.343	0.007	0.412	0.00037	0.000037	0.000037
KO-SAL-M1	0.383	0.423	0.445	0.469	0.484	0.505	0.012	0.976	0.00063	0.000063	0.000063
KO-SAL-M2	0.379	0.433	0.455	0.477	0.491	0.507	0.012	0.932	0.00065	0.000065	0.000065
KO-SAL-M3	0.386	0.442	0.457	0.474	0.485	0.494	0.010	0.876	0.00053	0.000053	0.000053
KO-SAL-M4	0.392	0.424	0.442	0.455	0.470	0.487	0.009	0.975	0.00049	0.000049	0.000049
KO-SAL-M5	0.402	0.438	0.453	0.475	0.483	0.503	0.009	0.965	0.00051	0.000051	0.000051
KO-IRI-M1	0.360	0.453	0.497	0.560	0.596	0.633	0.027	0.972	0.00144	0.000144	0.000144
KO-IRI-M2	0.390	0.463	0.493	0.549	0.578	0.650	0.024	0.984	0.00132	0.000132	0.000132
KO-IRI-M3	0.347	0.377	0.397	0.422	0.449	0.487	0.013	0.992	0.00073	0.000073	0.000073
KO-IRI-M4	0.409	0.488	0.541	0.593	0.649	0.695	0.028	0.993	0.00152	0.000152	0.000152
KO-IRI-M5	0.401	0.456	0.488	0.541	0.592	0.636	0.023	0.997	0.00126	0.000126	0.000126

PNP concentration (µmoles/ml/min)	PNP Concentration (umoles/actual reaction volume/min)	Amount of protein in each reaction well (mg)	Specific Activity (uMoles/min/mg)	Average Specific Activity	STDEV	P Value
0.003	0.001	0.005	0.108			
0.004	0.001	0.005	0.158			
0.059	0.012	0.005	2.352			
0.048	0.010	0.005	1.936			
0.054	0.011	0.005	2.148	2.185	0.158758	
0.057	0.011	0.005	2.280			
0.055	0.011	0.005	2.209			
0.185	0.037	0.005	7.403			
0.056	0.011	0.005	2.241			
0.063	0.013	0.005		5.490	2.828418	0.032728261
0.171	0.034	0.005	6.826			
0.037	0.007	0.005				
0.063	0.013	0.005	2.538			
0.065	0.013	0.005	2.593			
0.053	0.011	0.005	2.135	2.253	0.294074	0.661528447
0.049	0.010	0.005	1.943			
0.051	0.010	0.005	2.055			
0.144	0.029	0.005	5.748			
0.132	0.026	0.005	5.269			
0.073	0.015	0.005	2.923	5.015	1.235825	0.000955019
0.152	0.030	0.005	6.077			
0.126	0.025	0.005	5.057			

Ugt1a1 Specific Activity Values

Group	Concentration (nM)	Average	stdev
WT-SAL-M1	906.6666667		
WT-SAL-M2	866.3333333		
WT-SAL-M3	681.3333333		
WT-SAL-M4	831.3333333		
WT-SAL-M5	746	806.3333	91.5927
WT-IRI-M1	372.3333333		
WT-IRI-M2	364.6666667		
WT-IRI-M3	349.3333333		
WT-IRI-M4	397.6666667		
WT-IRI-M5	383.6666667	373.5333	18.37662
KO-SAL-M1	761.6666667		
KO-SAL-M2	869.3333333		
KO-SAL-M3	911		
KO-SAL-M4	626.3333333		
KO-SAL-M5	721.3333333	777.9333	114.5769
KO-IRI-M1	499.6666667		
KO-IRI-M2	500.3333333		
KO-IRI-M3	455.6666667		
KO-IRI-M4	425.6666667		
KO-IRI-M5	470.6666667	470.4	31.50697

Group	Concentration	STDEV
WT-SAL	806.3333333	91.5927
WT-IRI	373.5333333	18.37662
KO-SAL	777.9333333	114.5769
KO-IRI	470.4	31.50697

P value	
WT-SAL vs WT-IRI	0.00001
WT-SAL vs KO-SAL	0.676504794
WT-SAL vs KO-IRI	0.0001
WT-IRI vs KO-IRI	0.000346453

The specific activity of liver carboxylesterase (CE) was measured in TLR2 WT and KO groups with saline or irinotecan treatments and the specific activity were expressed as µmoles of PNP/min/mg of protein (Figure 5.7). The activity was compared among the 4 groups and we

observed a significantly higher carboxylesterase activity in both TLR2 WT and KO mice with irinotecan treatment compared to saline, which indicates that irrespective of TLR2, irinotecan treatment alone significantly increases the activity of carboxylesterase and may lead to increased conversion of irinotecan to SN-38. However, we did not find any significant change between the TLR2 WT and KO mice with either saline or irinotecan treatment, which signifies the finding that TLR2 is not involved in altering the carboxylesterase activity either with or without irinotecan treatment. On the other hand, the activity of Ugt1a1 is significantly downregulated in both TLR2 WT and KO mice with irinotecan treatment, which suggests a less conversion of SN-38 to inactive SN-38G. Although irinotecan downregulated the Ugt1a1 activity in both TLR2 WT and KO mice, similar to the carboxylesterase activity, we did not find any significant difference in the Ugt1a1 activity between TLR2 WT and KO mice with either saline or irinotecan treatment, which further suggests that TLR2 may not be involved in regulating Ugt1a1 activity.

5.4 Discussion

Gastrointestinal (GI) toxicity is a common complication associated with chemotherapy. GI toxicity presents a severe problem; however, it remains untreatable, resulting in a lower quality of life and in some cases, higher morbidity of patients receiving chemotherapy. Specifically, Irinotecan treatment induces severe GI toxicity, especially late-onset diarrhea. Diarrhea is a common adverse reaction and dose-limiting toxicity of irinotecan therapy and therefore limiting the clinical application of irinotecan.[22] The intestinal toxicity of irinotecan is regulated by its active metabolite, SN-38.[26] Although the SN-38 induced toxicity has been explained by various mechanisms, the explanations are controversial and the underlying pathophysiology is still under investigation.

The pathogenesis of GI toxicity is thought to be mediated by Toll-like receptor family members, leading to epithelial cell apoptosis.[29] Toll-like receptor 2 (TLR2) is a pattern recognition receptor

and a member of the TLR family that recognizes the molecular patterns of gram-negative or gram-positive bacteria.[146] In this study, we investigated the role of TLR2 in irinotecan-induced gut and liver toxicity. According to our hypothesis, we conducted animal studies using TLR2 WT and KO mice and irinotecan treatment to determine if TLR2 plays any role in irinotecan-induced toxicity. TLR2 WT and KO mice were divided into 4 groups and treated with either saline or irinotecan. Our results provide evidence that during the irinotecan treatment period, TLR2 WT mice showed a higher loss in body weight. Although the higher weight loss in the TLR2 WT group is statistically not significant compared with TLR2 KO, the incidence of bloody diarrhea, weakness and less food intake in TLR WT mice were more severe, which suggests that the presence of TLR2 in the WT group is contributing to the GI toxicity induced by irinotecan. Similarly, the histological images of TLR4-WT with irinotecan treatment showed severe damage of all parts of the small intestine, including duodenum, jejunum, ileum as well as colon, with a total disruption of crypts, obvious shortening of villi (Figure 5.2), whereas TLR2 WT and KO groups with saline treatment did not show any indications of morphological changes in the intestine. Our study also showed that the intestinal damage observed by histological analysis in control and irinotecan treated groups is well-correlated with the trends in body weight loss and incidence of diarrhea observed.

Our data showing that TLR2 KO mice showed less severe damage is well correlated with the previous studies suggesting a role of TLR2 in chemotherapy-induced GI toxicity or intestinal mucositis. TLR2 has been shown to play a key role in the initiation and maintenance of innate immune responses and previous research has shown that TLRs expression may be altered after chemotherapy treatment and correlate well with gastrointestinal mucositis.[61] Several studies have found an increased mRNA expression and protein levels of TLR2 along with TLR4 in samples of patients with gastrointestinal inflammatory diseases such as coeliac disease, inflammatory bowel

disease and ulcerative colitis .[62–64] These studies suggest a potential mechanism that TLRs mediate gastrointestinal dysfunction and pain. TLR4 has been identified as a mediator of irinotecan-induced gut toxicity and pain, suggesting that TLR4 can be a target for improved toxicity outcomes.[65] The expression of TLR2 and TLR4 in Biopsy samples of patients with inflammatory bowel diseases revealed that TLR2 expression in the terminal ileum of the collected patients' samples was significantly upregulated compared to controls.[64] Similarly, Amitriptyline, an inhibitor of TLR2 and TLR4 activity in in vitro models, also inhibited diarrhea and colonic apoptosis caused by chemotherapy treatment in rats.[66] TLR mediated inflammatory pathways have also been linked with chemotherapy-induced gut toxicity and pain.[67] The alimentary mucositis caused by chemotherapy is also heavily linked with the human gut microbiome and bacteria and these bacteria are tightly regulated by the TLR family, because TLRs play a vital role in the gut homeostasis and bacterial regulation.[68] A review reports that TLR2 is a potential therapeutic target to modulate or minimize the toxicity associated with chemotherapy, and also to optimize cancer treatment dosing and clinical outcomes. Stringer et al. report that TLR2 along with TLR4, TLR5, and TLR9 are involved in intestinal mucositis.[69] It is also shown that TLR2 regulates the severity of intestinal toxicity caused by another chemotherapy drug, doxorubicin.[70] More importantly, TLRs and MyD88 were found to be involved in the pathogenesis of intestinal mucositis caused by anticancer regimens using MyD88- and TLR2-knock out mice. It is also found that genetic deletion of TLR2 and MyD88 effectively controlled the signs of intestinal injury when compared with wild-type control mice.[71]

In patients who have borderline resectable liver disease are typically given irinotecan as neoadjuvant chemotherapy for tumor regression. Irinotecan chemotherapy in this case also presents with a high risk of mortality post resection of colorectal liver metastasis due to the

hepatotoxicity induced by irinotecan in the forms of steatosis or steatohepatitis. Toll-like receptors have also been suggested to play a role in the development of steatosis. Therefore, we also studied the role of TLR2 in the development of steatosis after irinotecan treatment in mice. The H&E and Oil-Red-O stained liver sections showed extensive fat accumulation in the TLR2 WT group with up to 80% fat accumulation with a steatosis score of 4. This finding is in good agreement with past studies suggesting TLR2 is involved in the development of steatosis. For example, metabolic syndrome is well known to induce fat accumulation in hepatocytes and a study by Himes et al. reported that mice lacking TLR2 are protected from hepatic steatosis and these mice also showed diminished inflammatory cytokine expression.[59] As the literature suggests, with irinotecan induced steatohepatitis, there is typically hepatic inflammation present in the liver. Moreover, the conversion of SN-38 to SN-38G is mediated by the Ugt1a1 enzyme, which determines the concentration levels of SN-38 and probably the associated gut and liver toxicity. Therefore, we aimed to measure the gene expression of TNF-α cytokine and Ugt1a1 in livers of TLR2 WT and KO mice treated with saline or irinotecan. Interestingly, we found that with the irinotecan treatment, the TNF-α expression was significantly induced in the TLR2 WT mice when compared to TLR2 WT mice with saline treatment (control). Most importantly, we found that the TNF-α expression in TLR2WT mice was significantly higher compared to TLR2 KO mice with irinotecan treatment, which suggests that irinotecan upregulates pro-inflammatory cytokine (TNF-α) expression in the liver and therefore may contribute to steatohepatitis. We observed that the irinotecan treatment itself significantly downregulated the Ugt1a1 expression in TLR2 WT mice compared with saline treatment. Overall, the gene expression results of TNF-a and Ugt1a1 indicate that TLR2 may be involved in inducing the inflammation in mice liver due to the increased TNF-a expression levels observed in the TLR2 WT mice treated with irinotecan.

We measured the specific activity of liver carboxylesterase (CE) in TLR2 WT and KO groups with saline or irinotecan treatments and compared the activity among 4 groups. We observed a significantly higher carboxylesterase activity in both TLR2 WT and KO mice with irinotecan treatment compared to saline, which indicates that irrespective of TLR2, irinotecan treatment alone significantly increases the activity of carboxylesterase and may lead to increased conversion of irinotecan to SN-38. However, we did not find any significant change between the TLR2 WT and KO mice with either saline or irinotecan treatment, which signifies the finding that TLR2 is not involved in altering the carboxylesterase activity with or without irinotecan treatment. On the other hand, the activity of Ugt1a1 is significantly reduced in both TLR2 WT and KO mice with irinotecan treatment compared to saline treatment. This suggests that irinotecan treatment by itself reduces the ugt1a1 activity in both TLR2 WT and KO mice and therefore leads to less conversion of SN-38 to inactive SN-38G. However, we did not find any significant difference in the Ugt1a1 activity between TLR2 WT and KO mice with irinotecan treatment, which further suggests that TLR2 may not be involved in regulating Ugt1a1 activity. Altogether, our results strongly suggest that the TLR2 is involved in both gastrointestinal and hepatotoxicity induced by irinotecan, as evidenced by the incidence of diarrhea, histological analysis, and the gene expression of pro-inflammatory cytokines in the liver.

5.5 Conclusion

The results suggest that TLR2 KO mice treated with irinotecan showed reduced incidence of diarrhea, more severe bloody diarrhea, fat accumulation in the liver and intestinal damage when compared with the control group mice and TLR2 WT mice treated with irinotecan. In addition, TLR2 KO mice also showed lower SN-38 blood concentrations and liver TNF-α expression. Together, these results suggest that TLR2 is involved in both diarrhea and hepatotoxicity caused

by irinotecan. The evidence from this study suggests that the pharmacological inhibition of TLR2 may contribute to the healing of GI toxicity following irinotecan chemotherapy.

CHAPTER 6

Effects of Soy Isoflavone Treatment on Irinotecan-induced Diarrhea and Steatosis in Mice

Abstract

Irinotecan (CPT-11) is a potent anti-cancer drug primarily used for the treatment of metastatic colorectal cancer. The major toxicities associated with irinotecan chemotherapy in patients are gastrointestinal (GI) toxicity (diarrhea) and hepatotoxicity (steatosis or steatohepatitis). Elevated concentrations of the active metabolite SN-38 in the intestine and liver is believed to be the major cause of the toxicities. These toxicities result in life-threatening complications in patients and reduce the use of irinotecan as a chemotherapeutic agent. Therefore, there is an urgency to develop new interventions to prevent diarrhea and steatosis associated with irinotecan. Soy isoflavones have been shown to have beneficial effects on both gastrointestinal (GI) and hepatotoxicity caused by chemotherapy. Here, we studied the effects of NovaSoy, a soy-based isoflavone concentrate with a total isoflavone of 40% (20% genistein, ~18% daidzein, ~2% other isoflavones), on irinotecan-induced diarrhea and steatosis in mice. Results showed that the mice treated with Novasoy and irinotecan (NS/IRI) showed significantly less bodyweight loss and incidence of diarrhea compared to mice treated with saline and irinotecan (Sal/IRI). Histopathological analysis of liver and intestine sections revealed a less severe fat accumulation (<10% steatosis) and intestinal damage in NS/IRI group. Analysis of liver and intestine concentrations showed less accumulation of SN-38 concentrations in the NS/IRI group compared to the Sal/IRI group. Enzyme activity assays exhibited a significant increase in the activity of carboxylesterase, whereas ugt1a1 activity is reduced. Toxicokinetic (TK) studies showed no significant changes in blood concentrations of irinotecan and metabolites. Together, the results suggested that soy isoflavone treatment could delay the incidence of diarrhea and steatosis caused by irinotecan and can be used as an intervention to reduce the toxicities associated with irinotecan.

6.1 Introduction

Irinotecan (CPT-11) is a chemotherapeutic agent used in first- and second-line treatment of metastatic colorectal cancer[122,139,140]. Irinotecan is metabolized by hepatic and peripheral carboxylesterase to SN-38 (active & toxic metabolite)[141], which is glucuronidated by ugt1a1 to inactive SN-38G[140]. Cyp3a4 also converts irinotecan to inactive APC and NPC metabolites[141]. SN-38 shows its cytotoxic activity by inhibiting topoisomerase-I enzyme[30,142,143], which causes irreversible DNA damage and cell death[30,141,144].

The life-threatening side effect associated with irinotecan chemotherapy is gastrointestinal (GI) toxicity in the form of acute or delayed diarrhea[65,140,142–144]. Due to the occurrence of severe diarrhea, the dose of irinotecan is reduced, which results in reduced efficacy of the drug[65,145]. In addition, the fluid/electrolyte imbalance caused by diarrhea can lead to additional side effects such as renal insufficiency, malnutrition, and dehydration[65]. The National Cancer Institute (NCI) has published a scale to assess the severity of diarrhea caused by chemotherapy in humans. This scale is divided into grades 1-5 based on the increase in the number of stools over the baseline and an increase in ostomy output compared with baseline[29]. Although it is believed that the free intestinal luminal SN-38, either from bile or deconjugation of SN-38G, is responsible for irinotecan-induced diarrhea[140,144], the precise mechanisms underlying the toxicity remain unclear and effective interventions to prevent diarrhea are limited[65].

Irinotecan is also used in the treatment of unresectable or recurrent colorectal cancer[147]. Irinotecan chemotherapy improves the prognosis and allows for resection of the tumor. However, the use of irinotecan is associated with the development of hepatotoxicity (steatosis or steatohepatitis)[148]. A study reported a clear association between irinotecan use and development of steatohepatitis[149]. Research has shown an increase in postoperative mortality with irinotecan treatment due to liver

failure from steatosis or steatohepatitis[141]. The mechanism of irinotecan-induced hepatotoxicity is unclear; however, the process is believed to include the accumulation of fat within the hepatocytes resulting from the oxidative stress caused by irinotecan chemotherapy, which later develops into hepatotoxicity[141]. In addition, mitochondrial dysfunction and production of reactive oxygen species (ROS), lipid peroxidation, and release of pro-apoptotic and pro-fibrotic cytokines by Kupffer cells are also thought to be involved in the development of hepatotoxicity[141].

Due to the incidence of life-threatening gut and liver toxicities associated with irinotecan and the lack of effective strategies to prevent these toxicities, there is an urgency to develop interventions that can limit the toxicities associated with irinotecan and as well as to improve the therapeutic outcomes of the treatment. Moreover, evidence suggests that soy isoflavones have beneficial effects on GI and hepatotoxicity[74,150–152]. Therefore, in the present study, we evaluated whether a soy isoflavone concentrate (NovaSoy), can exert a beneficial effect on the occurrence of diarrhea and steatosis caused by irinotecan treatment in mice.

6.2 Materials & Methods

6.2.1 Chemicals

Irinotecan hydrochloride was purchased from Martin Surgical Supply, Houston, TX (item no: 4434-11). NovaSoy® 400 was obtained from Archer Daniels Midland, Chicago, IL. Novasoy contained 40% of total isoflavones (20% Daidzein, 18-20% Genistein, 2% Glycitein, and <1% other isoflavones). The composition of NovSoy is presented in the below. SN-38 was purchased from Cayman chemical (item no: 15632). SN-38G was synthesized in Dr. Ming Hu's lab at the University of Houston, Houston, TX. Camptothecin (CPT; internal standard) was purchased from Millipore Sigma, St Louis, MO. 4-Nitrophenyl-β-D-glucuronide (Catalog No. O-PNPBGA) was purchased from Megazyme.com. The special low-fat diet was purchased from Research Diets,

New Brunswick, NJ. Formalin. All other solvents used for chromatographic analysis were of LC-MS grade and purchased from VWR International, LLC (Suwanee, GA, USA). Unless specified, all other chemicals and reagents used were purchased from Millipore Sigma, St. Louis, MO.

Specifications of Novasoy	
Total isoflavones, %, as is**	40. min.
Moisture, %	7.0, max.
Heavy Metals, ppm, as lead*	5.0, max.
Standard plate count, per g	3,000 max.
Yeast & mold, per g	300 max.
Salmonella, per 100 g	Neg.
E. Coli, per 40 g	Neg.

Isoflavone	**Approximate %**
Daidzein	20%
Genistein	18-20%
Glycitein	2%
Other isoflavones	<1%

Figure 6.0. Tables of Novaosoy composition and the percentage of individual constituents. (Information obtained from Archers Daniel Midland webite and via personal communication with the company).

6.2.2 Animals

Male 5-weeks old C57BL6J mice were purchased from Jackson Laboratory, Ban Harbor, ME. The animals were kept in an environmentally controlled room (temperature 25 ± 2^0C, 12 h dark-light cycle, humidity 50 ± 5%) for at least 1 week before performing any experiments. The mice were on a special diet (low-fat diet, 35% sucrose with 10% kcal fat) ad libitum throughout the animal study. All the animal care and use protocols followed were approved by the Institutional Animal Care and Use Committee (IACUC) at the University of Houston.

6.2.3 Study Design and Drug Treatments

C57BL6J mice were divided into 4 groups (n = 4 or 5 per group): saline (Sal) and NovaSoy (NS) were control groups and received either saline or NovaSoy (1 g/kg, oral gavage) from days 1 to 10. Saline and irinotecan (Sal/IRI), NovaSoy and irinotecan (NS/IRI) were the treatment groups and received either saline or NovaSoy (from days 1 to 10), along with irinotecan 50 mg/kg/day for 7 days (days 4 to 10) by oral gavage. Mice were sacrificed on day 11, after 24 hours of last drug treatment. Mouse liver and intestine were isolated immediately after sacrificing.

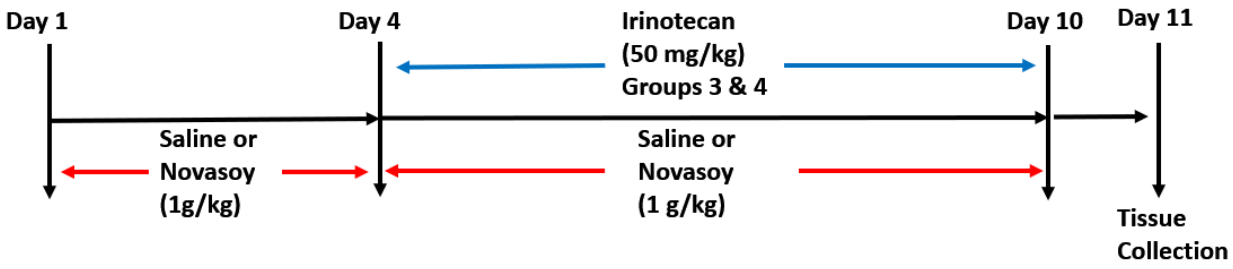

Figure 6.1 Study design and drug treatments.

6.2.4 Evaluation of Body Weight and Diarrhea

The body weight of mice was measured daily to track weight loss/gain, and the presence of diarrhea was monitored in mice daily from days 1-10. The loss in body weight from days 1 to 10 was calculated and reported in terms of % weight loss. Diarrhea was quantified according to a validated grading criterion previously described[101] with slight modification. The grading was given based on the severity of diarrhea observed and is reported as follows: grade 0 (normal or no diarrhea), grade 1 (slightly wet and soft tool), grade 2 (wet stool with moderate perianal staining), grade 3 (severe diarrhea and staining), grade 4 (severe, life-threatening bloody diarrhea with staining and continual anal leakage).

6.2.5 Histological Analysis of Intestine and Liver injury

Intestine or liver sections (n=5 per group) collected immediately after sacrificing were placed in tissue embedding cassettes and fixed in 10% neutral buffered formalin (vol/vol) for histological examination. The samples were then embedded in paraffin and stained with hematoxylin and eosin (H&E) at Pathology Core and Lab, Baylor College of Medicine (BCM), Houston, TX. The H&E stained slides of intestine and liver were evaluated by an experienced pathologist in a blinded fashion and morphological observations of intestine and liver injury were recorded. The liver injury was assessed based on the percentage of hepatocytes showing fat accumulation (steatosis). The severity of steatosis in control and irinotecan-treated groups was reported as previously described[101] with slight modifications. The grading was as follows: score 0 (no steatosis), score 1 (minimal fat accumulation, < 5% steatosis), score 2 (5-30% steatosis), score 3 (30-65% steatosis), score 4 (severe fat accumulation, > 65% steatosis). The final score reported was an average of

scores observed individually for each slide in a group. To evaluate the intestinal injury, criteria such as shortening of villi and disruption of crypt cells were considered.

6.2.6 Analysis of Liver and Intestine Concentrations

Liver and intestinal concentrations of irinotecan, SN-38, and SN-38G in saline and NovaSoy treated groups were determined using LC-MS/MS analysis. For the analysis, the liver or intestine sample was homogenized and further processed to extract compounds. A 10 µl of tissue homogenate was mixed with 10 µl of PBS and to this mixture, 200 µl of 50% of acetonitrile (ACN) containing 5 µM camptothecin (internal standard) was added as an extracting solvent. Samples were vortexed for 30 sec and centrifuged for 15 min at 15000 rpm. After the centrifugation, 180 µl of supernatants were collected and allowed to dry under a gentle stream of air at room temperature. The air-dried samples were then reconstituted with 100 µl of 50% acetonitrile and samples were centrifuged for 10 min at 10000 rpm. 80 µl of the supernatant was transferred to vials and 10 µl was injected into LC-MS/MS for the analysis of irinotecan, SN-38, and SN-38G.

To analyze irinotecan and metabolite concentrations, an API 5500 QTRAP triple quadrupole mass spectrophotometer (AB Sciex, USA) equipped with a Turbospray TM source was used by multiple reaction monitoring (MRM) method operated in a positive ion mode, with minor modifications to the method conditions as previously described[100]. A UPLC system, Waters Acquity™ with a diode-arrayed detector (DAD) was used. The UPLC conditions were as follows: column, Acquity UPLC BEH C18 column (50 mm × 2.1 mm I.D., 1.7 µM, Waters, Milford, MA, USA); mobile phase A - 0.1% formic acid; mobile phase B - 100% acetonitrile performed in a gradient from 0 to 4.5 min. The flow rate and the sample injection volume were 0.4 ml/min and 10 µL, respectively. The following m/z transitions were selected: m/z 587.1 → 124.1 for irinotecan; m/z 393.1 → 349.1 for SN-38; m/z 569.5 → 393.1 for SN-38G; m/z 349.0 → 305.1 for CPT. The selection of the

fragment ions depended on the highest intensity of the fragment. The data collected was analyzed with Analyst 1.4.2 software (AB Sciex, USA).

6.2.7 Carboxylesterase Activity

Whole cell extracts were prepared from mouse livers and protein concentration was determined by BCA assay according to the manufacturer's protocol (Pierce Chemical, Rockford, IL). Total carboxylesterase activity was monitored by measuring the absorbance using a BioTek plate reader in a 96-well plate. Briefly, whole cell extracts containing CEs enzyme was incubated with the substrate P-nitrophenyl acetate (PNPA) at 37 ^{o}C, and absorbance was measured for 10 min at 405 nm. The specific activity of carboxylesterase was expressed as the µmoles of PNP formed per min per mg of protein.

6.2.8 Ugt1a1 Activity

Ugt1a1 activity in control and irinotecan-treated groups was determined by measuring the formation of SN-38 glucuronide by LC-MS/MS analysis using SN-38 as a substrate. Briefly, whole cell extracts from the mouse liver tissue were prepared, and protein concentration was determined using the BCA assay kit according to the manufacturer's protocol (Pierce Chemical, Rockford, IL). To measure the enzyme activity, a reaction containing 1 mg/ml protein, 10 µM of SN-38, solution A (25 mM UDPGA Triammonium salt) and solution B (25 mM Saccharolactone, 5 mM $MgCl_2$ and 0.022 mg/ml Alamethicin) in 0.05 M KPi buffer was used. The total reaction volume was 170 µl. The reaction was conducted in a water bath at 37 ^{o}C for 60 min. The reaction was terminated by adding 7 µl of acetonitrile (ACN) containing 1 µg/ml CPT (internal standard). Samples were then processed and analyzed by LC-MS/MS to determine the ugt1a1 activity. The specific enzyme activity was expressed as nM of SN-38G formed.

6.2.9 Toxicokinetic Studies

Toxicokinetic (TK) studies were conducted in C57BL6 mice to determine the effects of NovaSoy treatment on the toxicokinetics of irinotecan. For the TK study, a total of 12 mice were used and divided into 2 groups (n=6 per group). Mice were pre-treated with either saline or NovaSoy (1 g/kg, oral gavage) for 3 days. From day 4, mice groups received either saline or Novasoy, along with irinotecan (50 mg/kg/day, oral gavage) until day 8 and mice were sacrificed 24 h after the last dose of irinotecan. For the TK analysis, approximately 20 µl of blood samples were collected from the tail vein of mice on day 4 (1^{st} dose of irinotecan) and day 7 (4^{th} dose of irinotecan) from 0-24 h at predetermined time points. In addition, 0 h (pre-dose), 2 h (post-dose) blood samples were collected on days 0, 5, and 8 following irinotecan administration. Blood concentrations of irinotecan, SN-38, and S-38G were determined using LC-MS/MS using the method conditions described in section 2.6. AUC, C_{max}, and t_{max} values were determined using NCA analysis by WinNonlin 5.2 software.

6.2.10 Statistical Analysis

Data are expressed as mean ± standard deviation for all the experiments. One-way ANOVA was performed using GraphPad Prism 8.0 software to determine the significance of differences between control and treatment groups. P-value of < 0.05 was considered as statistically significant.

6.3 Results

6.3.1 Body Weight and Incidence of Diarrhea

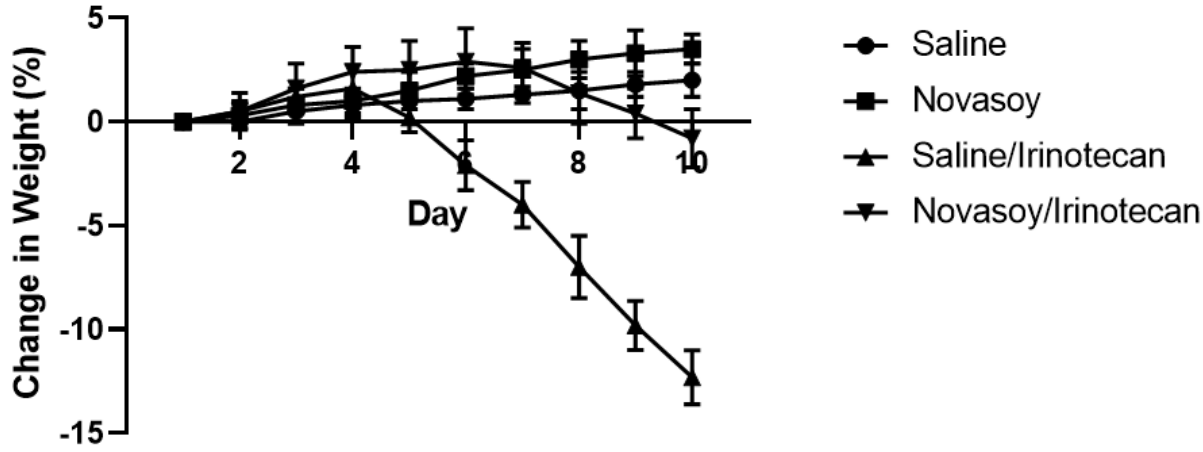

Figure 6.2. Percentage Body Weight (BW%) change in control and treatment groups measured from days 1-10.

Body weights of each mouse in control and treatment groups from day 1-10.

Day	Group 1 (Sal/Sal)				Group 2 (Sal/Novasoy)			
	M1	M2	M3	M4	M1	M2	M3	M4
Day 1	27.6	25.1	23.7	26.9	22.5	28.1	29.3	24.7
Day 2	27.6	25.1	23.8	26.8	22.7	28	29.3	24.9
Day 3	27.8	25.1	24	26.9	22.8	28.1	29.4	25.1
Day 4	27.7	25.3	24.1	27	22.9	28.2	29.5	25
Day 5	27.9	25.4	24	27	22.9	28.2	29.7	25.3
Day 6	28.1	25.4	23.9	27.1	23	28.5	30.1	25.3
Day 7	28	25.3	24.1	27.2	23.2	28.4	30.1	25.5
Day 8	28.1	25.4	24.3	27	23.3	28.6	30.2	25.6
Day 9	28.3	25.5	24.2	27.2	23.4	28.7	30.1	25.8
Day 10	28.3	25.4	24.4	27.3	23.4	28.8	30.3	25.7

Day	Group 3 (Sal/Irinotecan)					Group 4 (Novasoy/Irinotecan)				
	M1	M2	M3	M4	M5	M1	M2	M3	M4	M5
Day 1	24.8	27.4	29.1	23.9	29.8	26.4	22.1	23.9	21.2	28.4
Day 2	24.9	27.6	29.3	23.8	30.1	26.3	22	24.1	21.5	28.7
Day 3	25.1	27.7	29.3	24.2	30.3	26.4	22.3	24.4	21.9	28.9
Day 4	25.2	27.8	29.5	24.3	30.3	26.7	22.5	24.5	22.1	29
Day 5	24.7	27.2	29.3	24	30.1	26.6	22.5	24.7	22.1	29
Day 6	24.1	26.4	28.5	23.7	29.5	26.6	22.8	24.6	22.3	29.1
Day 7	23.5	26	28.2	23.1	28.9	26.7	22.9	24.6	22	28.8
Day 8	22.6	25.1	27.3	22.5	28.1	26.4	22.7	24.1	21.9	28.4
Day 9	22.1	24.3	26.4	21.7	27.3	26.2	22.5	23.9	21.5	28.2
Day 10	21.5	23.7	26.1	21	26.2	26.2	22.2	23.6	21.3	27.6

The irinotecan-induced body weight loss in mice was measured each day over the course of 10 days and reported as the % weight change during the treatment period (Figure 6.2). Results showed that there was a slight increase in body weight from day 1-4 in all the groups of mice. The slight increase in body weight remained constant in both the mice groups without irinotecan treatment (Saline and NovaSoy). However, after the irinotecan treatment on day 4, a significant decline in the body weight was observed in the Sal/IRI group until day 10. By day 10 of the treatments (7^{th} dose of irinotecan), the Sal/IRI mice group showed severe weight loss with an average of 12.3% reduction due to bloody diarrhea. On the other hand, NS/IRI group mice did not show any decline in their body weight until day 7 (4^{th} dose of irinotecan). Notably, by day 10, an average of only 0.8% decrease in body weight was observed in NS/IRI group, as compared to the 12.3% decrease in Sal/IRI group. No loss in the bodyweight was observed in the control groups (Sal or NS) throughout the experiment. Statistical analysis showed a significant difference in the bodyweight loss between Sal/IRI and NS/IRI groups during the course of 10 days treatment period.

Treatment Groups	n number	Incidence of Diarrhea / Diarrhea Grade									
		Day 1	**Day 2**	**Day 3**	**Day 4**	**Day 5**	**Day 6**	**Day 7**	**Day 8**	**Day 9**	**Day 10**
Saline	4	N/D	N/D	N/D	N/D	N/D	N/D	N/D	N/D	N/D	N/D
Novasoy	4	N/D	N/D	N/D	N/D	N/D	N/D	N/D	N/D	N/D	N/D
Sal/IRI	5	N/D	N/D	N/D	N/D	N/D	N/D	N/D	Signs of Diarrhea (less mobility, sluggishness, weakness)	Grade 2 (liquid stools, weakness, less mobility)	Grade 3 (liquid stools, signs of bloody diarrhea, severe weakness)
NS//IRI	5	N/D	N/D	N/D	N/D	N/D	N/D	N/D	N/D	N/D	Slight weakness, less movement, no diarrhea

N/D: No Diarrhea

Table 6.1. Incidence of Diarrhea and Diarrhea grade observed from days 1-10 in control and irinotecan treated mice groups.

The occurrence and severity of diarrhea were monitored in both control and irinotecan treated mice for 10 days (Table 6.1). No diarrhea was observed in both the Saline and NS group throughout the treatment period. Sal/IRI group showed signs of diarrhea on day 8 of the experiment (day 5 of irinotecan treatment) and the severity of diarrhea steadily increased in this group of mice until day 10. On day 10, Sal/IRI group showed a grade 3 diarrhea with liquid stools, bloody diarrhea and signs of severe weakness. On the other hand, mice treated with NS/IRI did not show any signs of diarrhea until day 9. On day 10, signs of slight weakness, reduced movement of mice were observed. However, no diarrhea was observed in this group of mice.

6.3.2 Histological Analysis of Intestinal and Liver Damage

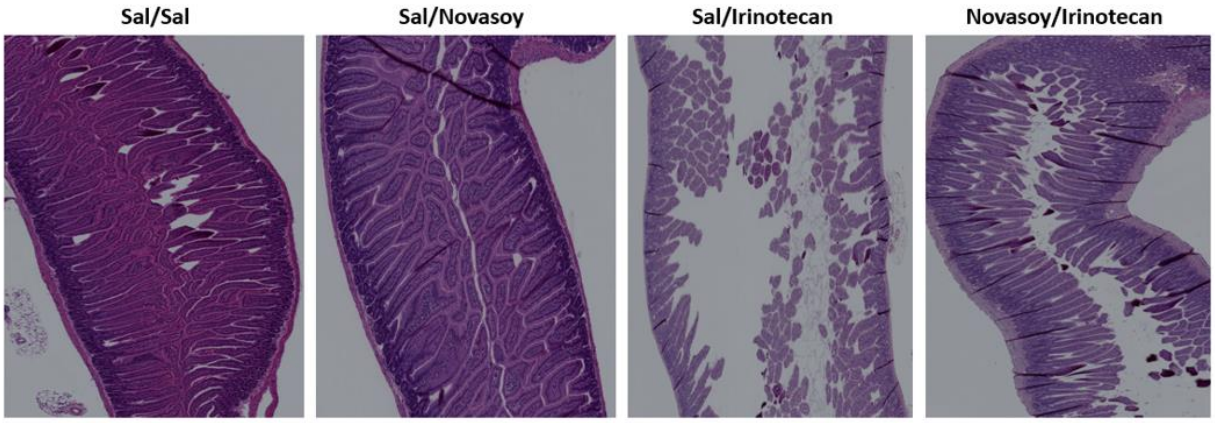

Figure 6.3. H&E stained intestine images of mice treated with A) Saline B) Novasoy 3) Sal/IRI and 4) NS/IRI.

Intestinal Histology Observations:

Intestine Histology Observations			
Saline	**Novasoy**	**Saline/Irinotecan**	**Novasoy/Irinotecan**
No morphological changes observed	Normal morphology, except some shortening of villi	Dilated crypts; No ulceration; No necrosis	Slightly Dilated crypts; No ulceration; No necrosis

The intestinal tissues collected from control and irinotecan-treated groups were fixed in 10% buffered formalin, and subsequently, paraffin-embedded and stained with H&E. Histological analysis was performed on paraffin-embedded sections following H&E staining and the images were evaluated by a pathologist for the presence of intestinal injury. The images of Sal/IRI treated mice intestine showed severe damage of intestine with a total disruption of crypts, obvious shortening of villi (Figure 6.3), whereas control groups (saline and NovaSoy) did not show any indications of morphological changes in the intestine. On the other hand, a moderate change in the

morphology of intestinal tissue was observed in NS/IRI group; however, significantly less damage and fewer changes to the villi and crypts in comparison with the damage in Sal/IRI treated mice. The intestinal damage observed by histological analysis in control and irinotecan treated groups is well-correlated with the bodyweight loss and incidence of diarrhea observed. Especially, the mice with severe intestinal damage (Sal/IRI group) also showed the most loss in body weight.

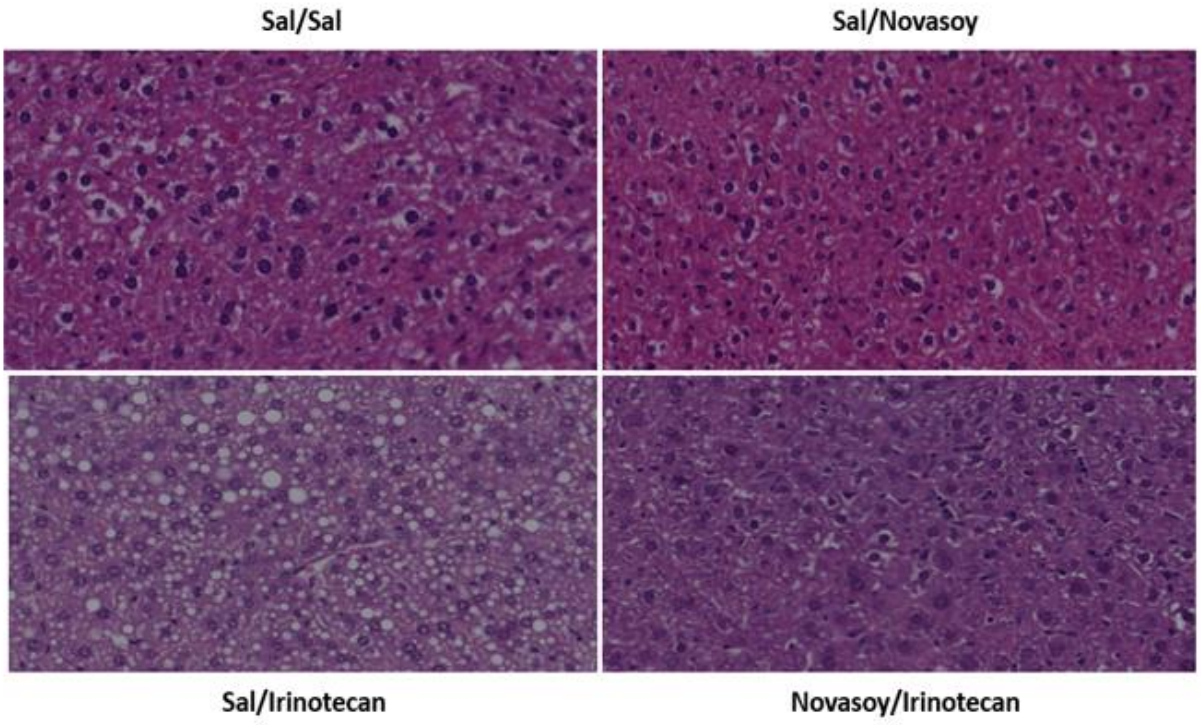

Figure 6.4. Images of H&E stained liver tissue sections treated with A) Saline B) Novasoy 3) Sal/IRI and 4) NS/IRI.

Liver Histology Observations of individual mice in a group and Steatosis score:

Sal/Sal			Sal/Novasoy		
M1	M2	M3	M1	M2	M3
Score 0 (No Steatosis)	Score 0 (No Steatosis)	Score 0 (No Steatosis)	Score 0 (No Steatosis)	Score 0 (No Steatosis)	Score 0 (No Steatosis); Glycogen formation

Sal/Irinotecan			Novasoy/Irinotecan		
M1	M2	M3	M1	M2	M3
Score 3+; Micro and Macrovescular steatosis; 90% fat accumulation in cells; No necrosis	Score 3+; Macrovescular steatosis; 99% fat accumulation in cells	Score 3+; Minor macrovescular steatosis; 80% fat accumulation in cells	Score 0 (No Steatosis) Mild Inflammation	Score 0 (No Steatosis) Mild Inflammation	Score 0 (No Steatosis) Mild/Chronic Inflammation

Liver Histology Observations			
Saline	**Novasoy**	**Saline/Irinotecan**	**Novasoy/Irinotecan**
Score 0 (No Steatosis)	Score 0 (No Steatosis); Glycogen formation	Score 3+ Micro and macrovescular steatosis; 90% fat accumulation; No necrosis	Score 0 (No Steatosis) Mild Inflammation

H&E stained liver sections were examined for indications of fat accumulation (steatosis) and a score was assigned based on the extent of fat accumulation observed. As expected, the saline and Novasoy treated mice groups did not show any fat accumulation (Figure 6.4); however, signs of mild inflammation were observed in mice treated NovaSoy alone. Sal/IRI showed extensive fat accumulation (up to 90%) with a steatosis score of 4. This observation was seen in all the mice in

the Sal/IRI group (n=5). Surprisingly, NS/IRI treated mice livers showed no presence of steatosis despite the irinotecan treatment in this group for 7 days.

6.3.3 Intestine and Liver Concentrations of Irinotecan and Metabolites

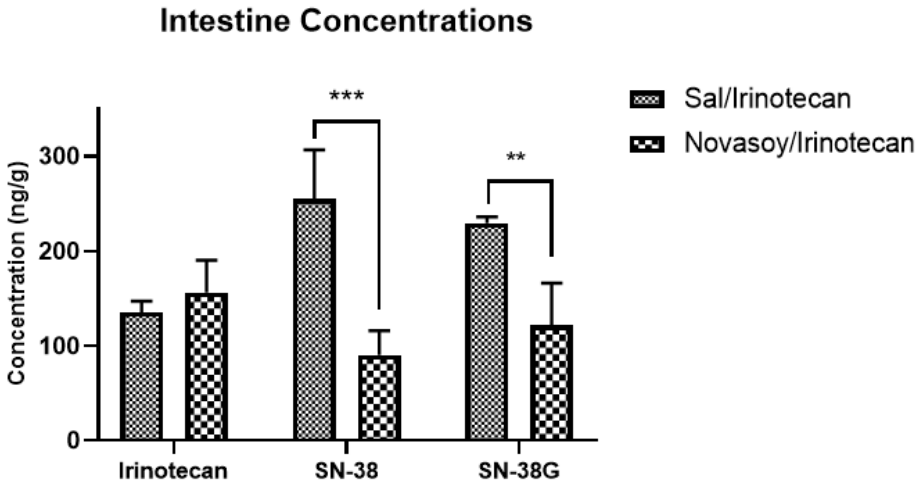

Figure 6.5. Intestine Concentrations of Irinotecan, SN-38, and SN-38G in mice treated with Sal/IRI or NS/IRI

Intestine concentration values of irinotecan, SN-38, and SN-38G

	Concentrations (ng/ml)			SD		
	Irinotecan	SN-38	SN-38G	Irinotecan	SN-38	SN-38G
Sal/IRI	135.6	255	229.4	11.58878768	51.74456493	6.73052747
Novasoy/IRI	156.2	90.64	121.64	34.20087718	25.21513434	44.6065914

The concentrations of irinotecan and its metabolites SN-38 and SN-38G were measured in the intestine and liver tissues of mice in treatment groups (Sal/IRI and NS/IRI) using LC-MS/MS analysis and the concentrations were reported as ng/g of tissue (Figure 6.5 and 6.6). The intestinal concentrations revealed a significant increase of both the metabolites SN-38 and SN-38G in the Sal/IRI group in comparison with the NS/IRI group, whereas the parent compound irinotecan concentrations were unchanged.

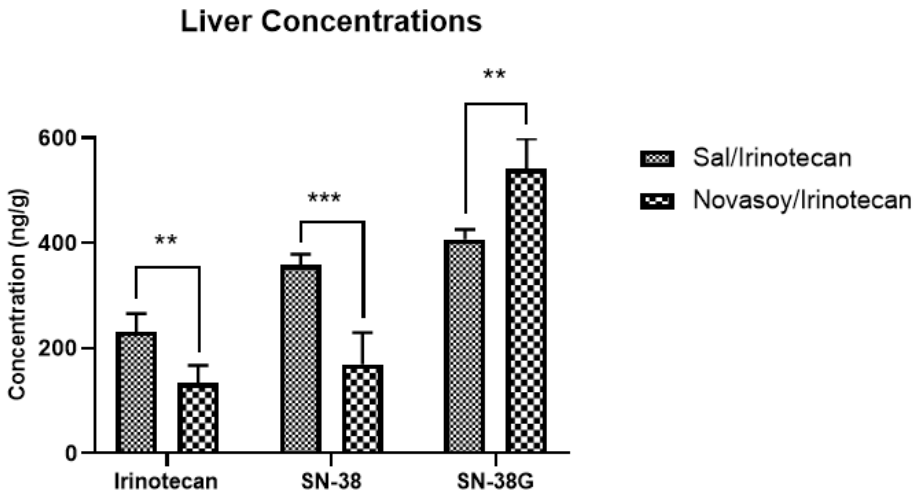

Figure 6.6. Liver Concentrations of Irinotecan, SN-38, and SN-38G in mice treated with Sal/Irinotecan or Novasoy/Irinotecan.

Liver concentration values of irinotecan, SN-38, and SN-38G

	Concentrations (ng/ml)			SD		
	Irinotecan	SN-38	SN-38G	Irinotecan	SN-38	SN-38G
Sal/IRI	230.8	357.8	406.6	34.99571402	20.92128103	19.08664455
Novasoy/IRI	133.8	169.2	540.8	33.34966267	60.37963233	57.42995734

Analysis of liver concentrations showed a significant difference of irinotecan and metabolites SN-38, SN-38G between Sal/IRI and NS/IRI groups. Specifically, the concentrations of irinotecan and SN-38 were reduced, whereas SN-38G were increased. As observed in intestinal concentrations, the active metabolite SN-38 concentrations are also elevated in livers of mice treated with Sal/IRI, showing a good correlation with the histological observations of liver damage observed in this group. Whereas, NS/IRI group mice showed a significant reduction in the concentrations of SN-38 in both intestine and liver concentrations, which also correlated with less severe damage observed by histological analysis in this group. Surprisingly, the SN-38G concentrations in the

liver NS/IRI treated mice were increased (Figure 6.6), as opposed to a decrease observed in intestinal concentrations in NS/IRI group (Figure 6.5).

6.3.4 Carboxylesterase and Ugt1a1 Activity

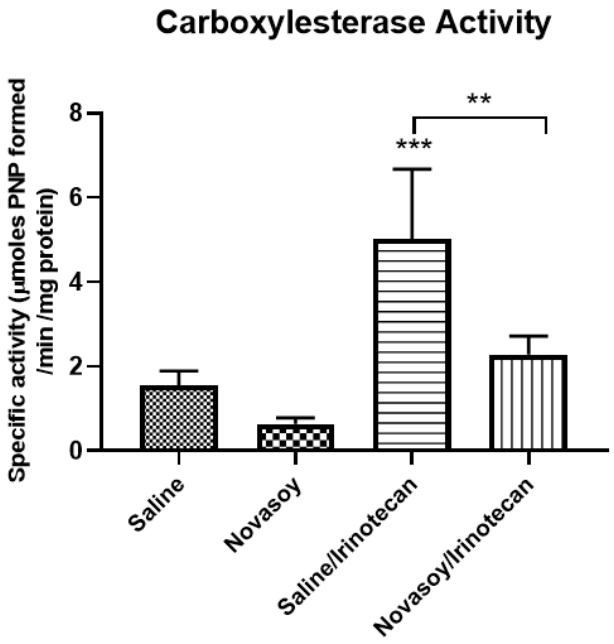

Figure 6.7. Activity of liver carboxylesterase enzyme in mice treated with Saline, NovaSoy, Sal/IRI, or NS/IRI.

The specific activity of liver carboxylesterase (CE) was measured in control and irinotecan treated mice groups and expressed as µmoles of PNP/min/mg of protein (Figure 6.7). The activity was compared among the 4 groups. Although not significant, a noticeable decrease in CE activity was observed with NovaSoy treatment alone as compared to saline treatment, whereas the highest CE activity was observed in Sal/IRI group. The increase in the activity in Sal/IRI group due to irinotecan treatment was inhibited by NovaSoy treatment in NS/IRI group.

Experimental values of Carboxylesterase specific activity

Time (min)	0	2	4	6	8	10	Slope	RSQ	PNP Concentration (moles/L)	PNP Concentration (moles/L/min)
Buffer	0.045	0.045	0.047	0.049	0.049	0.050	0.001	0.925	0.00003	0.000003
Buffer +PNPA	0.054	0.055	0.056	0.058	0.058	0.058	0.000	0.886	0.00002	0.000002
Sal/Sal-Mouse1	0.439	0.450	0.466	0.487	0.501	0.516	0.008	0.994	0.00043	0.000043
Sal/Sal-Mouse2	0.431	0.441	0.454	0.459	0.468	0.480	0.005	0.988	0.00026	0.000026
Sal/Sal-Mouse3	0.414	0.429	0.443	0.462	0.478	0.497	0.008	0.997	0.00045	0.000045
Sal/Sal-Mouse4	0.401	0.429	0.449	0.454	0.467	0.481	0.007	0.952	0.00040	0.000040
Sal/NS-Mouse1	0.382	0.382	0.389	0.394	0.404	0.406	0.003	0.949	0.00015	0.000015
Sal/NS-Mouse2	0.377	0.384	0.383	0.393	0.395	0.405	0.003	0.932	0.00014	0.000014
Sal/NS-Mouse3	0.368	0.373	0.382	0.381	0.385	0.396	0.002	0.915	0.00013	0.000013
Sal/NS-Mouse4	0.385	0.403	0.403	0.421	0.426	0.423	0.004	0.856	0.00021	0.000021
Sal/IRI-Mouse1	0.326	0.388	0.454	0.504	0.536	0.619	0.028	0.990	0.00152	0.000152
Sal/IRI-Mouse2	0.345	0.366	0.383	0.422	0.442	0.464	0.012	0.989	0.00067	0.000067
Sal/IRI-Mouse3	0.325	0.438	0.465	0.551	0.587	0.638	0.030	0.969	0.00163	0.000163
Sal/IRI-Mouse4	0.308	0.460	0.503	0.527	0.569	0.621	0.027	0.895	0.00148	0.000148
Sal/IRI-Mouse5	0.325	0.353	0.386	0.418	0.465	0.503	0.018	0.993	0.00097	0.000097
NS/IRI-Mouse1	0.420	0.436	0.449	0.477	0.483	0.513	0.009	0.979	0.00049	0.000049
NS/IRI-Mouse2	0.405	0.434	0.462	0.487	0.499	0.526	0.012	0.988	0.00064	0.000064
NS/IRI-Mouse3	0.441	0.467	0.488	0.502	0.516	0.520	0.008	0.950	0.00043	0.000043
NS/IRI-Mouse4	0.406	0.448	0.478	0.505	0.522	0.535	0.013	0.962	0.00069	0.000069
NS/IRI-Mouse5	0.400	0.444	0.463	0.486	0.494	0.521	0.011	0.959	0.00060	0.000060

PNP concentration (mMoles/ml/min)	PNP concentration (µmoles/ml/min)	PNP Concentration (umoles/actual reaction volume/min)	Amount of protein in each reaction well (mg)	Specific Activity (uMoles/min/mg)	Average Specific Activity	STDEV	P Value
0.000003	0.003	0.001	0.005	0.121			
0.000002	0.002	0.000	0.005	0.096			
0.000043	0.043	0.009	0.005	1.733	1.540	0.353	
0.000026	0.026	0.005	0.005	1.023			
0.000045	0.045	0.009	0.005	1.795			
0.000040	0.040	0.008	0.005	1.606			
0.000015	0.015	0.003	0.005	0.599	0.639	0.147	0.009
0.000014	0.014	0.003	0.005	0.566			
0.000013	0.013	0.003	0.005	0.537			
0.000021	0.021	0.004	0.005	0.856			
0.000152	0.152	0.030	0.005	6.073	5.017	1.653	0.008
0.000067	0.067	0.013	0.005	2.674			
0.000163	0.163	0.033	0.005	6.507			
0.000148	0.148	0.030	0.005	5.937			
0.000097	0.097	0.019	0.005	3.893			
0.000049	0.049	0.010	0.005	1.962	2.284	0.430	0.025
0.000064	0.064	0.013	0.005	2.560			
0.000043	0.043	0.009	0.005	1.725			
0.000069	0.069	0.014	0.005	2.764			
0.000060	0.060	0.012	0.005	2.409			

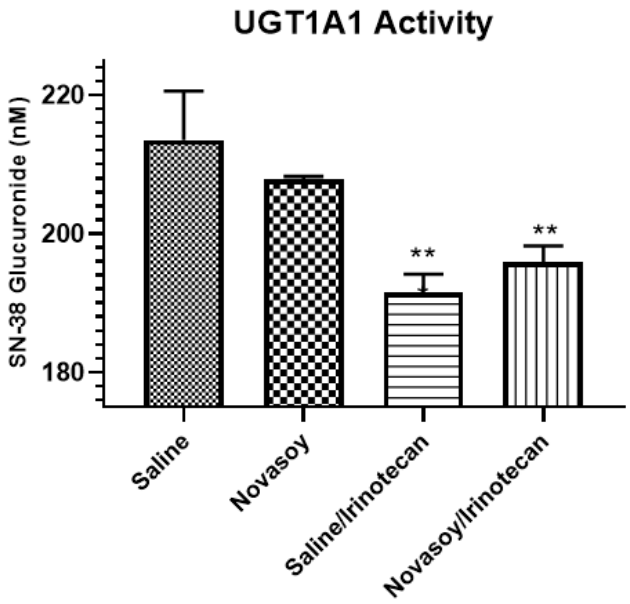

Figure 6.8. Activity of Liver ugta1a1 enzyme in mice treated with Saline, NovaSoy, Sal/IRI, or NS/IRI.

Experimental values of Ugt1a1 specific activity

Group	Concentration (nM)	Average	stdev
g1-m1	216	213.5	7.068448
g1-m2	216.6666667		
g1-m3	218.3333333		
g1-m4	203		
g2-m1	208.3333333	207.8333	0.430331
g2-m2	207.3333333		
g2-m3	207.6666667		
g2-m4	208		
g3-m1	192.6666667	191.6	2.586289
g3-m2	193		
g3-m3	193		
g3-m4	192.3333333		
g3-m5	187		
g4-m1	197.3333333	195.8667	2.375804
g4-m2	197		
g4-m3	197		
g4-m4	196.3333333		
g4-m5	191.6666667		

The liver phase-II enzyme, ugt1a1 activity was determined in control and irinotecan-treated mice livers and expressed by the formation of SN-38 glucuronide in these samples (Figure 6.8). The ugt1a1 activity was compared among the 4 groups to determine the effects of irinotecan and NovaSoy treatments. It was found that the ugt1a1 activity was not altered by the NovaSoy treatment in comparison with saline treatment. However, irinotecan treatment significantly reduced the ugt1a1 activity in both Sal/IRI and NS/IRI mice groups. As opposed to the significant change in CE activity observed with NovaSoy treatment, there was no change in the activity of ugt1a1 observed in NS/IRI group, compared to Sal/IRI mice group.

6.3.5 Toxicokinetic Studies

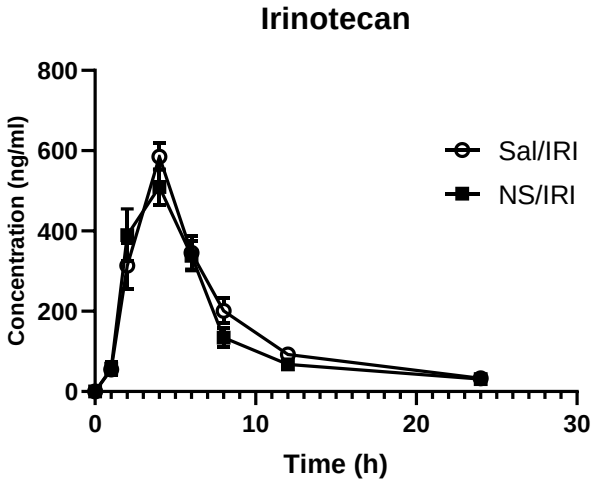

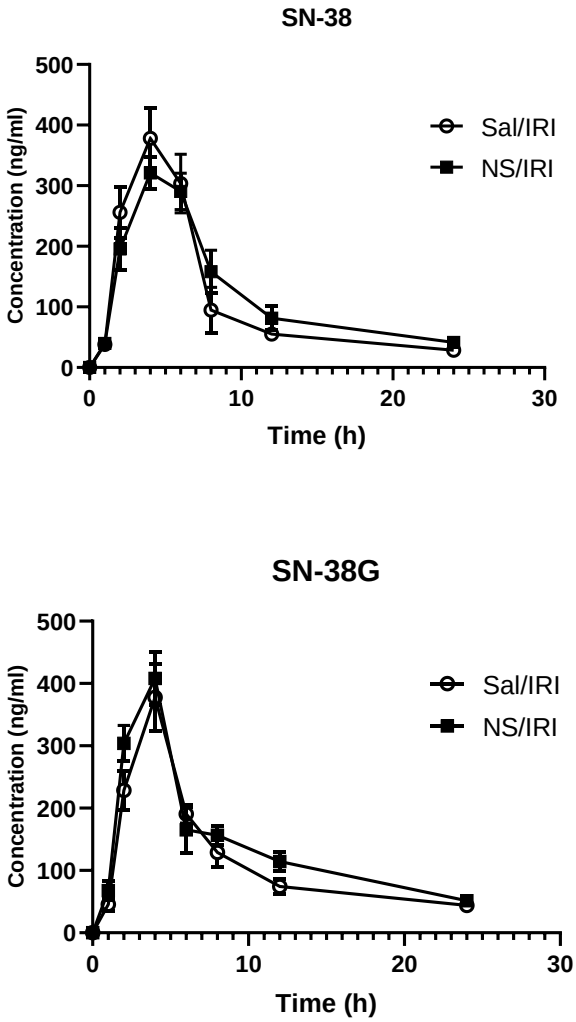

Figure. 6.9. Concentration-time PK profiles of irinotecan, SN-38, SN-38G following the administration of irinotecan on Day 4 in Sal/IRI and NS/IRI treated mice blood samples.

Day 4 Toxicokinetic study Experimental values:

	Irinotecan		SN-38		SN-38G	
Time	Sal/IRI	NS/IRI	Sal/IRI	NS/IRI	Sal/IRI	NS/IRI
0	0.0	0.0	0.0	0.0	0.0	0.0
1	55.3	57.1	38.2	39.6	45.8	67.6
2	313.7	389.8	256.2	195.8	228.7	303.8
4	584.8	509.5	378.2	321.2	377.5	408.3
6	345.7	338.5	303.5	290.8	190.7	165.3
8	201.0	134.2	94.9	158.2	128.9	156.5
12	92.5	67.7	55.4	81.4	74.2	114.3
24	32.9	30.8	28.7	41.5	43.8	51.5

The toxicokinetic (TK) studies were conducted to determine the effects of NovaSoy treatment on irinotecan and metabolites SN-38, SN-38G blood concentrations in mice after multiple oral dosing of irinotecan. Blood samples were collected from the tail vein on days 4 and 7 after irinotecan administration and analyzed for irinotecan and metabolite concentrations using LC-MS/MS. The concentration-time profiles of blood samples collected on day 4 revealed that there was no significant change in the blood concentrations of irinotecan, SN-38, or SN-38G between Sal/IRI and NS/IRI treated mice (Figures 6.9 and 6.10). Similar results were observed for samples collected on day 7, with no statistically significant change in the blood concentrations of irinotecan, SN-38, or SN-38G between Sal/IRI and NS/IRI groups. However, the concentrations of parent and metabolites on day 7 were observed to be higher than the concentrations on day 4 at 0 h timepoint due to multiple dosing of irinotecan.

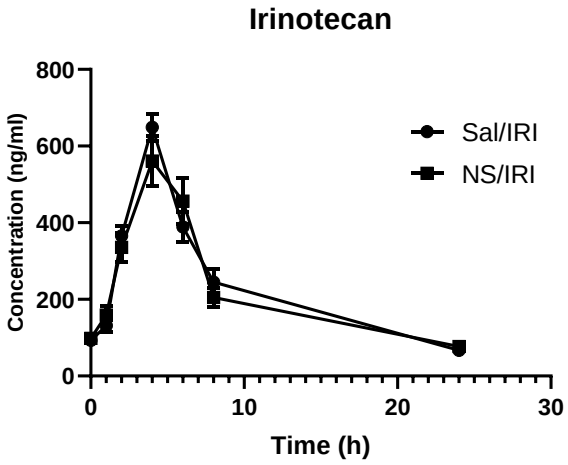

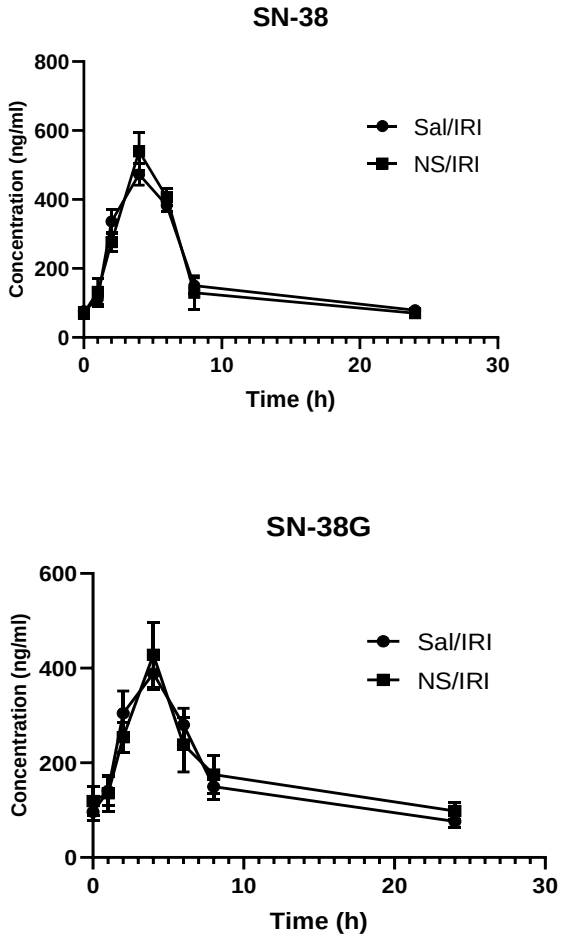

Figure. 6.10. Concentration-time PK profiles of irinotecan, SN-38, SN-38G following the administration of irinotecan on Day 7 in Sal/IRI and NS/IRI treated mice blood samples.

Day 7 Toxicokinetic study Experimental values:

	Irinotecan		SN-38		SN-38G	
	Sal/IRI	NS/IRI	Sal/IRI	NS/IRI	Sal/IRI	NS/IRI
0	92.7	98.1	76.3	71.1	96.4	119.1
1	130.8	159.3	110.8	132.4	140.7	135.6
2	365.5	335.5	336.5	276.2	304.7	254.0
4	649.2	560.8	473.0	539.7	388.8	428.2
6	389.3	456.5	382.8	407.0	280.2	238.5
8	245.3	204.8	150.0	129.5	149.7	175.2
24	66.7	76.9	78.8	70.2	76.3	98.0

	Irinotecan		SN-38		SN-38G	
	Sal/IRI	**NS/IRI**	**Sal/IRI**	**NS/IRI**	**Sal/IRI**	**NS/IRI**
AUC	3927.0	**3466.0***	2685.0	2932.1	2767.9	3363.4
C_{max}	584.8	**509.5***	380.7	**321.2***	377.5	408.3
t_{max}	4.0	4.0	4.7	4.0	4.0	4.0

Table 6.2. Toxicokinetic parameters AUC, C_{max}, t_{max} of irinotecan, SN-38, SN-38G after irinotecan administration on day 4.

Day 4 TK Parameters of Individual Mouse

Saline/Irinotecan								
	Irinotecan							
	M1	M2	M3	M4	M5	M6	Average	STDEV
AUC	3641.6	4196.4	4061	3752.1	3743.4	4167.5	3927	242.53855
Cmax	578	610	567	534	628	592	584.833333	33.1566987
tmax	4	4	4	4	4	4	4	0
	SN-38							
	M1	M2	M3	M4	M5	M6	Average	STDEV
AUC	2727.6	3014.7	2905	2446.6	2538.7	2481.3	2685.65	236.070437
Cmax	389	410	361	296	431	397	380.666667	47.5085957
tmax	4	4	6	6	4	4	4.66666667	1.03279556
	SN-38G							
	M1	M2	M3	M4	M5	M6	Average	STDEV
AUC	2548.7	2964.3	2712.9	2922.3	2688.5	2770.6	2767.88333	154.788635
Cmax	287	439	421	388	352	378	377.5	54.0841936
tmax	4	4	4	4	4	4	4	0

Novasoy/Irinotecan								
	Irinotecan							
	M1	M2	M3	M4	M5	M6	Average	STDEV
AUC	3487.5	3562.1	3650.4	3249.7	3168.2	3678.3	3466.03333	193.322974
Cmax	563	538	478	439	510	529	509.5	40.8605352
tmax	4	4	4	4	4	4	4	0
	SN-38							
	M1	M2	M3	M4	M5	M6	Average	STDEV
AUC	2571.3	2721.9	3244.4	3077	2972.8	3005.4	2932.13333	223.575995
Cmax	289	338	364	306	312	318	321.166667	24.0722293
tmax	4	4	4	4	4	4	4	0
	SN-38G							
	M1	M2	M3	M4	M5	M6	Average	STDEV
AUC	3312.3	3742.4	3162.5	3242	3750	2970.9	3363.35	290.076649
Cmax	448	455	429	361	397	360	408.333333	38.4779879
tmax	4	4	4	4	4	4	4	0

	Irinotecan		**SN-38**		**SN-38G**	
	Sal/IRI	**NS/IRI**	**Sal/IRI**	**NS/IRI**	**Sal/IRI**	**NS/IRI**
AUC	5544.3	5205.0	4346.1	4202.6	3941.6	4282.3
C_{max}	649.2	**560.8***	473.0	539.7	392.0	428.2
t_{max}	4.0	4.0	4.0	4.0	3.7	4.0

Table 6.3. Toxicokinetic parameters AUC, C_{max}, t_{max} of irinotecan, SN-38, SN-38G after irinotecan administration on day 7.

Day 7 TK Parameter values of Individual Mouse

Saline/Irinotecan								
	Irinotecan							
	M1	M2	M3	M4	M5	M6	Average	STDEV
AUC	5540.8	5399.8	5988.1	5724.55	5520.35	5092.3	5544.317	301.73452
Cmax	599	634	673	629	701	659	649.1667	36.0689155
tmax	4	4	4	4	4	4	4	0
	SN-38							
	M1	M2	M3	M4	M5	M6	Average	STDEV
AUC	4010.7	4578.85	4322.65	4428.7	4368.75	4366.8	4346.075	187.072122
Cmax	498	456	482	510	423	469	473	31.2409987
tmax	4	4	4	4	4	4	4	0
	SN-38G							
	M1	M2	M3	M4	M5	M6	Average	STDEV
AUC	3929.9	4115.25	3681.7	4369.45	3973.5	3579.65	3941.575	287.374409
Cmax	428	419	396	387	387	335	392	32.6802693
tmax	4	4	4	2	4	4	3.666667	0.81649658

Novasoy/Irinotecan								
	Irinotecan							
	M1	M2	M3	M4	M5	M6	Average	STDEV
AUC	4574.3	4906.9	5544.7	5709.9	5105.15	5389.15	5205.01667	387.4806
Cmax	489	510	623	585	515	643	560.833333	59.22392
tmax	4	4	4	4	4	4	4	0
	SN-38							
	M1	M2	M3	M4	M5	M6	Average	STDEV
AUC	3411.15	4766.85	4148.55	5105.3	3899.75	3883.75	4202.55833	570.9558
Cmax	458	612	530	591	519	528	539.666667	50.32119
tmax	4	4	4	4	4	4	4	0
	SN-38G							
	M1	M2	M3	M4	M5	M6	Average	STDEV
AUC	4144.1	3673.5	3526.2	4962.4	4985.9	4401.45	4282.25833	567.628
Cmax	358	352	391	504	492	472	428.166667	63.05135
tmax	4	4	4	4	4	4	4	0

PK parameters AUC, C_{max}, and t_{max} values of irinotecan, SN-38, SN-38G in Sal/IRI and NS/IRI groups on day 4 of treatments were determined using NCA analysis by WinNonlin 5.2 software. The AUC and C_{max} values of irinotecan in the NS/IRI group on day 4 were significantly higher in comparison with the Sal/IRI group. However, the active metabolite, SN-38 AUC was not altered in NS/IRI group, although a significant C_{max} of SN-38 was observed in this group. On the other hand, the inactive metabolite SN-38G AUC or C_{max} was not altered between 2 groups.

On day 7, the PK parameter AUC showed no difference between saline and NovaSoy treated groups. However, the C_{max} of irinotecan in NS/IRI treated mice was significantly higher when compared with the Sal/IRI group, similar to the results observed on day 4. Notably, there were no alterations in the AUC and C_{max} values of both SN-38 and SN-38G on day 7.

6.4 Discussion

Diarrhea and steatosis are the significant toxicities associated with irinotecan in patients. In the clinic, a high dose of loperamide or octreotide are typically given for irinotecan-induced late diarrhea. However, these agents are associated with a very high failure rate and the beneficial effects are not promising. As a result, in recent times there is an increasing interest in using medicinal herbs, phytocompounds and dietary supplements as an effective complementary treatmenet to reduce irinotecan induced diarrhea and steatosis. Therefore, in this study, we examined the effects of a natural and safe soy isoflavone extract on irinotecan-induced GI and hepatotoxicity. Specifically, we used a soy isoflavone extract, Novasoy, which contains 40% isoflavones as a treatment to C57BL6 mice prior to and during the irinotecan treatment to examine if isoflavone treatment can exert beneficial effects against irinotecan-induced diarrhea and steatosis.

We divided the mice into 4 groups (Saline, Novasoy, Sal/IRI, and NS/IRI) and a series of experiments were conducted to determine the effects of Novasoy on diarrhea in mice. Body weight loss data is typically used as an indicator of diarrhea during chemotherapy treatment and we measured the loss in body weight of mice treated with saline, Novasoy, Sal/IRI, and NS/IRI. As expected, our data showed that the bodyweight of mice in control group (saline and Novasoy groups) mice showed no loss in their body weight, whereas the mice treated with Sal/IRI showed the maximum body weight loss among the 4 groups, indicating that irinotecan treatment in this group caused significant gastrointestinal damage and diarrhea. The loss in bodyweight was prevented by Novasoy in the NS/IRI group suggesting a protective role of Novasoy in preventing the loss in body weight and occurrence of diarrhea.

We also conducted histological analysis of the intestine and liver section by H&E staining and found no signs of intestinal injury in control groups, whereas Sal/IRI group showed a total disruption of the morphology of the intestine with a shortening of villi and loss of crypts. These histology observations of intestinal damage strongly correlated with diarrhea observed in Sal/IRI group of mice. As expected, the Sal/IRI group showed >90% fat accumulation, which suggests that irinotecan treatment for 7 days caused extensive steatosis in Sal/IRI group. Surprisingly, no accumulation of fat was observed in the NS/IRI group despite the irinotecan treatment for 7 days in this group. Overall, the histological analysis of intestine and liver showed that the soy isoflavone treatment can delay both the intestinal and liver damage caused by irinotecan.

The precise mechanisms of irinotecan-induced diarrhea and steatosis are not clear. However, studies have suggested that higher exposure of intestine and liver to the active metabolite SN-38 concentrations is the primary step in the development of toxicity. Therefore, in this study, we measured the concentrations of irinotecan, SN-38, and SN-38G in mice intestine and liver samples

isolated from the treatment groups (Sal/IRI and NS/IRI). As reported in the results (Figures 6.5 and 6.6), the concentrations of SN-38 were found to be significantly lower in both the intestine and liver tissues of NS/IRI group in comparison with Sal/IRI group, which indicates that mice treated with Novasoy exposed to less SN-38 and therefore may have shown less diarrhea and steatosis. The tissue concentration results were closely correlated with the intestinal and liver damage observed by histological analysis, likely due to the reduced exposure of intestine and liver tissue to SN-38. Yokooji et al. reported that genistein, a soy isoflavone component, interacts with MRPs and reduces the intestinal toxicity by decreasing the MRP-2 mediated biliary excretion of irinotecan and metabolites.[89] Genistein was also reported to interact with P-gp and affect drug transport in P-gp expressing cells.[153] These studies suggest the potential mechanisms by which soy isoflavones can mediate SN-38 concentrations in the intestine and toxicity.

As we observed reduced toxicity in terms of diarrhea and steatosis in mice with NS/IRI treatment, we aimed to identify the possible mechanisms for the lower SN-38 concentrations observed in the intestine and livers of NS/IRI treated mice. Therefore, we measured the activity of carboxylesterase (CE), a phase-I enzyme, which metabolizes irinotecan to SN-38 and Ugt1a1 enzyme, which inactivates SN-38 to SN-38G. As reported in the results (Figures 6.7), the CE activity was significantly increased in mice with Sal/IRI treatment. This finding explains that the increased activity of the carboxylesterase enzyme in the Sal/IRI treated mice may have produced more SN-38 and therefore led to the increase in bloody diarrhea, severe intestinal and liver damage. On the other hand, we observed a significant reduction in the CE activity with Novasoy treatment, which provides a mechanism whereby the mice in this group were protected from both diarrhea and steatosis. Our data also show that the Ugt1a1 enzyme activity was reduced in mice groups treated with irinotecan (Sal/IRI and NS/IRI) compared with control groups (Saline, Novasoy).

Although the Novasoy treatment in NS/IRI group did not alter the Ugt1a1 activity compared to Sal/IRI group, the reduction in carboxylesterase activity with Novasoy treatment could be responsible for reduced diarrhea and steatosis observed in NS/IRI group. The higher concentrations of SN-38G observed in NS/IRI group does not correlate with the unchanged Ugt1a1 activity in this group, which suggests that there can be an involvement of uptake or efflux transporters, which could alter the parent and metabolite concentrations. In addition, soy isoflavones have also been shown to increase the activity of p-gp and irinotecan is a substrate of this transporter. The increased activity of p-gp might result in the efflux of irinotecan, resulting in lower concentrations of irinotecan observed in the NS/IRI group. Apart from the CE and Ugt activities that were measured in this study, the β-glucuronidase enzyme, which is involved in converting SN-38G to SN-38 in the intestine, could play a role in the less SN-38 concentrations observed in NS/IRI group. This could be due to the inhibition of the β-glucuronidase enzyme by Novasoy, which results in reduced formation of SN-38.

We also conducted Toxicokinetic (TK) studies in C57BL6 mice with a 50 mg/kg/day dose of irinotecan and found that the day 4 TK studies (Figure 6.9 and Table 6.2) showed a slight reduction in the AUC and C_{max} values of irinotecan in the NS/IRI group. We observed no significant differences in the AUC values of irinotecan or metabolites SN-38 and SN-38G on day 7 TK studies (Figure 6.10 and Table 6.3). Although the results described earlier showed that Novasoy treatment altered the CE activity and SN-38 concentrations in intestine and liver, the TK studies proved that the blood concentrations or AUC of SN-38 are not altered by the Novasoy, which indicates that the anticancer activity of SN-38 is not affected by Novasoy treatment, whereas the severity of diarrhea and steatosis in mice was reduced.

6.5 Conclusion

We report in this study that treatment with Novasoy, a soy isoflavone concentrate containing genistein, daidzein, and other soy isoflavones, can protect mice from diarrhea and steatosis caused by irinotecan treatment. We further report here that isoflavone treatment reduces the concentrations of SN-38 in mice intestine and liver, thereby reduces the exposure of these tissues to the toxic SN-38 metabolite. Additionally, we demonstrated that the CE activity is reduced with Novasoy treatment, a possible mechanism by which soy isoflavones could prevent intestinal and liver toxicity. In conclusion, our data suggest that soy isoflavone treatment can be used as an intervention to reduce the severity of diarrhea and steatosis associated with irinotecan chemotherapy in metastatic colorectal cancer patients.

CHAPTER 7

DISCUSSION

The research in this dissertation is divided into 3 specific aims and focused to investigate: 1) Effects of inflammation on irinotecan pharmacokinetics and development of a best-fit PK model 2) Role of toll-like receptor 2 (TLR2) in irinotecan-induced diarrhea and steatosis 3) Effects of soy isoflavone extract (Novasoy) on irinotecan induced diarrhea and steatosis. To our knowledge, this is the first study that describes the PK of irinotecan, SN-38, and SN-38G during inflammation.

In specific aim 1, we (1) investigated the effects of inflammation on the PK of irinotecan, SN-38, and SN-38G, and (2) developed a co-model to simultaneously describe the PK of irinotecan and SN-38 during inflammation with parameters characterized. It is well known that during inflammation, the expression and activity of drug-metabolizing enzymes (DMEs) and transporters are reduced, mainly due to transcriptional suppression or as a result of post-translational protein modification, induced by mediators such as pro-inflammatory cytokines (IL-6, TNF-α, IL-1β) [42,44,47,123,127–129]. The reduction in the expression and activity significantly alters drug metabolism, pharmacokinetics, and pharmacodynamics (PK/PD) of drugs, and therefore poses a risk for toxicity and drug-drug interactions[39,41,56,130,131]. As reported in our results, the AUC of irinotecan and SN-38 were significantly elevated in mice after LPS treatment, with an increase of 2.6-folds for irinotecan and 2-folds for SN-38 when compared with the saline group. The significant increase in irinotecan concentrations could be due to the downregulation of carboxylesterase enzyme expression during inflammation, as reported by Mao et al (2011)[51], and confirmed with the decreased conversion rate constant, k12 in our developed PK model. The downregulation of CEs expression and activity could result in reduced phase-I metabolism of irinotecan, which converts the parent compound to SN-38.

As it is known that irinotecan chemotherapy causes severe diarrhea in patients, the 2-fold elevation of SN-38 concentrations during inflammation presents a higher risk of toxicity that may warrant dosage modifications in these patients who receive irinotecan. As ugt1a1 is known to be down-regulated during inflammaton[52,132,133], a possible mechanism for the elevation of SN-38 during inflammation could be the reduction in the expression and activity of ugt1a1.

Furthermore, the reduced expression and activity of UGT1A1 during inflammation may have contributed to the reduction in phase-II metabolism and conversion of SN-38 to inactive SN-38G, which results in a decreased clearance and increased accumulation of SN-38. This observation suggests that patients who receive irinotecan during inflammation may have an increased risk of experiencing severe, life-threatening diarrhea due to the significant elevation of SN-38 concentrations. On the other hand, there is limited evidence present on the regulation of intestinal β-glucuronidase enzyme expression and activity during inflammation *in vivo*. A recent study shows that LPS increases β-glucuronidase activity in liver cells[134]. Based on the elevated concentrations of SN-38 and the observation of a second peak in the PK profile of SN-38, a possible mechanism could also be the increase in the activity of β-glucuronidase enzyme during inflammation, which may have increased the reconversion of inactive SN-38G to active SN-38. This is consistent with our observation that SN-38G blood concentrations were unchanged by LPS treatment. Together, the downregulation of UGT1A1 and upregulation of β-glucuronidase enzymes might have played significant roles in the elevated blood SN-38 concentrations and AUC during inflammation.

As we observed a significant increase in SN-38 concentrations and AUC in mice with LPS treatment, we aimed to develop a PK model that can describe the correlation between irinotecan and SN-38 concentrations during inflammation. To date, a number of pharmacokinetic models

were developed and published in various studies to describe irinotecan and SN-38 PK [110,117,135–138]. However, the co-modeling approach used in this study is novel, as for the first time, the effect of inflammation is incorporated in the PK model building. The proposed and validated PK model in this study can be used to accurately predict the plasma concentration of irinotecan and SN-38. The best fit structural model consisted of compartments for irinotecan, SN-38 and EHR compartment connected with different rate constants. The model fitting exercises revealed a nonlinear PK process of SN-38 transferring between the EHR compartment with V_{max} and K_m. After the inclusion of non-linear PK for SN-38 and EHR compartments, the model was developed and model discrimination was performed on data using Phoenix, by minimizing the Akaike Information Criteria (AIC) and by comparison of the quality of fit plots. With the best fit model of irinotecan and SN-38, good correlations between observed and predicted concentrations were obtained in irinotecan and SN-38 compartments. The PK parameters described in the model were derived from 10 mice (5 mice per group). The standard deviation of PK parameter estimates (Table 4.2) revealed a small variation among 5 mice in each group, which reflected in the stability of the model. The rate constant K12 was significantly decreased, indicating that the conversion of irinotecan to SN-38 is reduced during inflammation. The K_m was significantly increased in the LPS group, indicating that the affinity of SN-38 to transporters involved in the recycling process was decreased during inflammation. Moreover, it is apparent with our model that during inflammation, the EHR increased with a higher Km and resulted in a significant second peak in the SN-38 profile.

The diagnostic plots from the developed model indicate that the best-fit PK model of irinotecan and SN-38 was highly stable to simultaneously describe the PK of irinotecan and SN-38 data with reliability in mice during inflammation. In addition to the effects of inflammation, the model also

allowed us to successfully evaluate the effects of enterohepatic recycling in describing the PK of irinotecan and SN-38. The therapeutic implication of our research is that patients with inflammation should receive lower doses of irinotecan to achieve the same exposure as normal patients without inflammation. Using the developed model, we documented the impact of inflammation on irinotecan PK quantitatively, which is useful to rationally adjust the dose of irinotecan to minimize the toxicity.

A limitation of this study is that only 10 mice were employed. A large sample size would have enhanced the predictive performance of our modeling results. Further studies focusing on irinotecan metabolism should be conducted and the mechanism of EHR elimination should be clearly demonstrated in the future.

In specific aim 2, we investigated the role of toll-like receptor 2 (TLR2) on irinotecan-induced diarrhea and steatosis. As described earlier, gastrointestinal (GI) toxicity is a common complication associated with chemotherapy. GI toxicity presents a severe problem; however, it remains untreatable, resulting in a lower quality of life and in some cases, higher morbidity of patients receiving chemotherapy. Specifically, Irinotecan treatment induces severe GI toxicity, especially late-onset diarrhea. Diarrhea is a common adverse reaction and dose-limiting toxicity of irinotecan therapy and therefore limiting the clinical application of irinotecan.[22] The intestinal toxicity of irinotecan is regulated by its active metabolite, SN-38.[26] Although the SN-38 induced toxicity has been explained by various mechanisms, the explanations are controversial and the underlying pathophysiology is still under investigation.

The pathogenesis of GI toxicity is thought to be mediated by Toll-like receptor family members, leading to epithelial cell apoptosis.[29] Toll-like receptor 2 (TLR2) is a pattern recognition receptor and a member of the TLR family that recognizes the molecular patterns of gram-negative or gram-

positive bacteria.[146] In this study, we investigated the role of TLR2 in irinotecan-induced gut and liver toxicity. According to our hypothesis, we conducted animal studies using TLR2 WT and KO mice and irinotecan treatment to determine if TLR2 plays any role in irinotecan-induced toxicity. TLR2 WT and KO mice were divided into 4 groups and treated with either saline or irinotecan. Our results provide evidence that during the irinotecan treatment period, TLR2 WT mice showed a higher loss in body weight. Although the higher weight loss in the TLR2 WT group is statistically not significant compared with TLR2 KO, the incidence of bloody diarrhea, weakness and less food intake in TLR WT mice were more severe, which suggests that the lack of TLR2 in the KO group is showing less GI toxicity induced by irinotecan. Similarly, the histological images of TLR2-KO mice with irinotecan treatment showed less severe damage of all parts of the small intestine, including duodenum, jejunum, ileum as well as colon, with a total disruption of crypts, obvious shortening of villi (Figure 5.2), whereas TLR2 WT and KO groups with saline treatment did not show any indications of morphological changes in the intestine. Our study also showed that the intestinal damage observed by histological analysis in control and irinotecan treated groups is well-correlated with the trends in body weight loss and incidence of diarrhea observed.

Our data showing that TLR2 KO mice showed less severe damage is well correlated with the previous studies suggesting a role of TLR2 in chemotherapy-induced GI toxicity or intestinal mucositis. TLR2 has been shown to play a key role in the initiation and maintenance of innate immune responses and previous research has shown that TLRs expression may be altered after chemotherapy treatment and correlate well with gastrointestinal mucositis.[61] Several studies have found an increased mRNA expression and protein levels of TLR2 along with TLR4 in samples of patients with gastrointestinal inflammatory diseases such as coeliac disease, inflammatory bowel disease and ulcerative colitis .[62–64] These studies suggest a potential mechanism that TLRs mediate

gastrointestinal dysfunction and pain. TLR4 has been identified as a mediator of irinotecan-induced gut toxicity and pain, suggesting that TLR4 can be a target for improved toxicity outcomes.[65] The expression of TLR2 and TLR4 in Biopsy samples of patients with inflammatory bowel diseases revealed that TLR2 expression in the terminal ileum of the collected patients' samples was significantly upregulated compared to controls.[64] Similarly, Amitriptyline, an inhibitor of TLR2 and TLR4 activity in in vitro models, also inhibited diarrhea and colonic apoptosis caused by chemotherapy treatment in rats.[66] TLR mediated inflammatory pathways have also been linked with chemotherapy-induced gut toxicity and pain.[67] The alimentary mucositis caused by chemotherapy is also heavily linked with the human gut microbiome and bacteria and these bacteria are tightly regulated by the TLR family, because TLRs play a vital role in the gut homeostasis and bacterial regulation.[68] A review reports that TLR2 is a potential therapeutic target to modulate or minimize the toxicity associated with chemotherapy, and also to optimize cancer treatment dosing and clinical outcomes. Stringer et al. report that TLR2 along with TLR4, TLR5, and TLR9 are involved in intestinal mucositis.[69] It is also shown that TLR2 regulates the severity of intestinal toxicity caused by another chemotherapy drug, doxorubicin.[70] More importantly, TLRs and MyD88 were found to be involved in the pathogenesis of intestinal mucositis caused by anticancer regimens using MyD88- and TLR2-knock out mice. It is also found that genetic deletion of TLR2 and MyD88 effectively controlled the signs of intestinal injury when compared with wild-type control mice.[71]

In patients who have borderline resectable liver disease are typically given irinotecan as neoadjuvant chemotherapy for tumor regression. Irinotecan chemotherapy in this case also presents with a high risk of mortality post resection of colorectal liver metastasis due to the hepatotoxicity induced by irinotecan in the forms of steatosis or steatohepatitis. Toll-like receptors

have also been suggested to play a role in the development of steatosis. Therefore, we also studied the role of TLR2 in the development of steatosis and steatohepatitis after irinotecan treatment in mice. The H&E and Oil-Red-O stained liver sections showed extensive fat accumulation in the TLR2 WT group with up to 80% fat accumulation with a steatosis score of 4. This finding is in good agreement with past studies suggesting TLR2 is involved in the development of steatosis. For example, metabolic syndrome is well known to induce fat accumulation in hepatocytes and a study by Himes et al. reported that mice lacking TLR2 are protected from hepatic steatosis and these mice also showed diminished inflammatory cytokine expression.[59] As the literature suggests, with irinotecan induced steatohepatitis, there is typically hepatic inflammation present in the liver. Moreover, the conversion from SN-38 to SN-38G by the Ugt1a1 enzyme determines the concentration levels of SN-38 and the associated gut and liver toxicity. Therefore, we aimed to measure the gene expression of TNF-α cytokine and Ugt1a1 in livers of TLR2 WT and KO mice treated with saline or irinotecan. Interestingly, we found that with the irinotecan treatment, the TNF-α expression was significantly induced in the TLR2 WT mice when compared to TLR2 WT mice with saline treatment (control). Most importantly, we found that the TNF-α expression in TLR2WT mice was significantly higher compared to TLR2 KO mice with irinotecan treatment, which suggests that irinotecan upregulates pro-inflammatory cytokine (TNF-α) expression in the liver and therefore may contribute to steatohepatitis. On the contrary to the TNF-α gene expression results, we observed that the Ugt1a1 expression was significantly downregulated with irinotecan treatment in the TLR2 WT mice when compared with TLR2 WT mice with saline treatment. Overall, the gene expression results of TNF-a and Ugt1a1 indicate that TLR2 may be involved in inducing the inflammation in mice liver due to the increased TNF-a expression levels observed in the TLR2 WT mice treated with irinotecan.

We measured the specific activity of liver carboxylesterase (CE) in TLR2 WT and KO groups with saline or irinotecan treatments and compared the activity among 4 groups. We observed a significantly higher carboxylesterase activity in both TLR2 WT and KO mice with irinotecan treatment compared to saline, which indicates that irrespective of TLR2, irinotecan treatment alone significantly increases the activity of carboxylesterase and may lead to increased conversion of irinotecan to SN-38. However, we did not find any significant change between the TLR2 WT and KO mice with either saline or irinotecan treatment, which signifies the finding that TLR2 is not involved in altering the carboxylesterase activity with or without irinotecan treatment. On the other hand, the activity of Ugt1a1 is significantly downregulated in both TLR2 WT and KO mice with irinotecan treatment, which suggests a less conversion of SN-38 to inactive SN-38G. Although irinotecan downregulated the Ugt1a1 activity in both TLR2 WT and KO mice, similar to the carboxylesterase activity, we did not find any significant difference in the Ugt1a1 activity between TLR2 WT and KO mice with either saline or irinotecan treatment, which further suggests that TLR2 may not be involved in regulating Ugt1a1 activity. Altogether, our results strongly suggest that the TLR2 is involved in both gastrointestinal and hepatotoxicity induced by irinotecan, as evidenced by the incidence of diarrhea, histological analysis, and the gene expression of pro-inflammatory cytokine in the liver.

In specific aim 3, we investigated the effects of soy isoflavones on irinotecan induced steatosis and diarrhea. Diarrhea and steatosis are the significant toxicities associated with irinotecan in patients. In the clinic, a high dose of loperamide or octreotide are typically given for irinotecan-induced late diarrhea. However, these agents are associated with a very high failure rate and the beneficial effects are not promising. As a result, in recent times there is an increasing interest in using medicinal herbs, phytocompounds and dietary supplements as an effective complementary

treatmenet to reduce irinotecan induced diarrhea and steatosis. Therefore, in this study, we examined the effects of a natural and safe soy isoflavone extract on irinotecan-induced GI and hepatotoxicity. Specifically, we used a soy isoflavone extract, Novasoy, which contains 40% isoflavones as a treatment to C57BL6 mice prior to and during the irinotecan treatment to examine if isoflavone treatment can exert beneficial effects against irinotecan-induced diarrhea and steatosis.

We divided the mice into 4 groups (Saline, Novasoy, Sal/IRI, and NS/IRI) and a series of experiments were conducted to determine the effects of Novasoy on diarrhea in mice. Body weight loss data is typically used as an indicator of diarrhea during chemotherapy treatment and we measured the loss in body weight of mice treated with saline, Novasoy, Sal/IRI, and NS/IRI. As expected, our data showed that the bodyweight of mice in control group (saline and Novasoy groups) mice showed no loss in their body weight, whereas the mice treated with Sal/IRI showed the maximum body weight loss among the 4 groups, indicating that irinotecan treatment in this group caused significant gastrointestinal damage and diarrhea. The loss in bodyweight was prevented by Novasoy in the NS/IRI group suggesting a protective role of Novasoy in preventing the loss in body weight and occurrence of diarrhea.

We also conducted histological analysis of the intestine and liver section by H&E staining and found no signs of intestinal injury in control groups, whereas Sal/IRI group showed a total disruption of the morphology of the intestine with a shortening of villi and loss of crypts. These histology observations of intestinal damage strongly correlated with diarrhea observed in Sal/IRI group of mice. As expected, the Sal/IRI group showed >90% fat accumulation, which suggests that irinotecan treatment for 7 days caused extensive steatosis in Sal/IRI group. Surprisingly, no accumulation of fat was observed in the NS/IRI group despite the irinotecan treatment for 7 days

in this group. Overall, the histological analysis of intestine and liver showed that the soy isoflavone treatment can delay both the intestinal and liver damage caused by irinotecan.

The precise mechanisms of irinotecan-induced diarrhea and steatosis are not clear. However, studies have suggested that higher exposure of intestine and liver to the active metabolite SN-38 concentrations is the primary step in the development of toxicity. Therefore, in this study, we measured the concentrations of irinotecan, SN-38, and SN-38G in mice intestine and liver samples isolated from the treatment groups (Sal/IRI and NS/IRI). As reported in the results (Figures 6.5 and 6.6), the concentrations of SN-38 were found to be significantly lower in both the intestine and liver tissues of NS/IRI group in comparison with Sal/IRI group, which indicates that mice treated with Novasoy exposed to less SN-38 and therefore may have shown less diarrhea and steatosis. The tissue concentration results were closely correlated with the intestinal and liver damage observed by histological analysis, likely due to the reduced exposure of intestine and liver tissue to SN-38. Yokooji et al. reported that genistein, a soy isoflavone component, interacts with MRPs and reduces the intestinal toxicity by decreasing the MRP-2 mediated biliary excretion of irinotecan and metabolites.[89] Genistein was also reported to interact with P-gp and affect drug transport in P-gp expressing cells.[153] These studies suggest the potential mechanisms by which soy isoflavones can mediate SN-38 concentrations in the intestine and toxicity.

As we observed reduced toxicity in terms of diarrhea and steatosis in mice with NS/IRI treatment, we aimed to identify the possible mechanisms for the lower SN-38 concentrations observed in the intestine and livers of NS/IRI treated mice. Therefore, we measured the activity of carboxylesterase (CE), a phase-I enzyme, which metabolizes irinotecan to SN-38 and Ugt1a1 enzyme, which inactivates SN-38 to SN-38G. As reported in the results (Figures 6.7), the CE activity was significantly increased in mice with Sal/IRI treatment. This finding explains that the

increased activity of the carboxylesterase enzyme in the Sal/IRI treated mice may have produced more SN-38 and therefore led to the increase in bloody diarrhea, severe intestinal and liver damage. On the other hand, we observed a significant reduction in the CE activity with Novasoy treatment, which provides a mechanism whereby the mice in this group were protected from both diarrhea and steatosis. Our data also show that the Ugt1a1 enzyme activity was reduced in mice groups treated with irinotecan (Sal/IRI and NS/IRI) compared with control groups (Saline, Novasoy). Although the Novasoy treatment in NS/IRI group did not alter the Ugt1a1 activity compared to Sal/IRI group, the reduction in carboxylesterase activity with Novasoy treatment could be responsible for reduced diarrhea and steatosis observed in NS/IRI group. The higher concentrations of SN-38G observed in NS/IRI group does not correlate with the unchanged Ugt1a1 activity in this group, which suggests that there can be an involvement of uptake or efflux transporters, which could alter the parent and metabolite concentrations. In addition, soy isoflavones have also been shown to increase the activity of p-gp and irinotecan is a substrate of this transporter. The increased activity of p-gp might result in the efflux of irinotecan, resulting in lower concentrations of irinotecan observed in the NS/IRI group. Apart from the CE and Ugt activities that were measured in this study, the β-glucuronidase enzyme, which is involved in converting SN-38G to SN-38 in the intestine, could play a role in the less SN-38 concentrations observed in NS/IRI group. This could be due to the inhibition of the β-glucuronidase enzyme by Novasoy, which results in reduced formation of SN-38.

We also conducted Toxicokinetic (TK) studies in C57BL6 mice with a 50 mg/kg/day dose of irinotecan and found that the day 4 TK studies (Figure 6.9 and Table 6.2) showed a slight reduction in the AUC and C_{max} values of irinotecan in the NS/IRI group. We observed no significant differences in the AUC values of irinotecan or metabolites SN-38 and SN-38G on day 7 TK studies

(Figure 6.10 and Table 6.3). Although the results described earlier showed that Novasoy treatment altered the CE activity and SN-38 concentrations in intestine and liver, the TK studies proved that the blood concentrations or AUC of SN-38 are not altered by the Novasoy, which indicates that the anticancer activity of SN-38 is not affected by Novasoy treatment, whereas the severity of diarrhea and steatosis in mice was reduced.

This research has helped us in identifying a novel finding that during inflammation, SN-38 concentrations were elevated, which may lead to increased toxicity in patients who receive irinotecan. Additionally, the developed PK model showed a good correlation between observed and predicted concentrations of irinotecan, SN-38, and SN-38G and will be helpful in predicting both irinotecan and SN-38 concentrations during inflammation. This study also has helped understand the role of TLR2 in irinotecan-induced diarrhea and steatosis. In the future, TLR2 may be pharmacologically inhibited or knocked out, which may prevent or help in the healing of irinotecan-induced GI and hepatotoxicity. Finally, this research also investigated the effects of soy isoflavones on irinotecan-induced toxicity and found that Novasoy, an extract from soybeans containing 40% of isoflavones prevents mice from diarrhea and steatosis induced by irinotecan treatment.

In the future, studies should be conducted in humans to evaluate the effects of inflammation on irinotecan pharmacokinetics and PK models can be built with human concentration-time data in order to develop a new dosing regimen for irinotecan during inflammation. In addition, a colorectal cancer tumor model with inflammation can be used to determine if the tumor environment still exhibits the same effects on irinotecan PK. Moreover, the TLR2 inhibitors can be used to determine if pharmacological inhibtionof TLR2 produces less diarrhea and steatosis associated with irinotecan therapy.

APPENDIX

Appendix:

Chapter A: Effects of PXR activation on Drug Metabolizing Enzymes and Proinflammatory Cytokines During Inflammation

Abstract:

Pregnane X Receptor (PXR) is a nuclear receptor and a key regulator of the CYP3A in different species[154–156]. Activation of PXR by its ligands such as Pregnenolone 16α-carbonitrile (PCN), induces the expression of many drug-metabolizing Enzymes. Conversely, activation of toll-like receptors by ligands such as LPS is known to downregulate the expression and activity of drug-metabolizing enzymes.[41,131,157,158] Several studies have attempted previously to understand the role of inflammation during PXR activation.[156,159–163] However, the regulation of enzymes and transporters is not clearly understood when PXR and TLRs are activated by their respective ligands. Therefore, in this study, we aimed to investigate the expression of key enzymes and pro-inflammatory cytokines to better understand their regulation when PXR and TLRs are activated simultaneously. Animal experiments were conducted using C57BL6 mice and PCN and LPS were used to activate PXR and TLRs, respectively. Gene expression of enzymes and cytokines were studied using RT-PCR. Results indicate that combined activation of PXR and LPS showed an anti-inflammatory effect by PXR and downregulated cytokine expression. Surprisingly, PXR activation by PCN alone upregulated cytokine expression.

Study Design and Drug Treatments:

C57BL6 mice (age 5 weeks, male) were divided into 4 groups (n=4 per group): 1) Corn oil/Saline 2) Corn oil/LPS 3) PCN/Saline 4) PCN/LPS. Mice were i.p. injected with either corn oil or PCN (50 mg/kg/day) once a day for 3 days. On day 4, mice were i.p. injected either saline or LPS. After

LPS injection, mice were sacrificed at prescheduled time points (1h, 2h, 4h, and 16h) and mouse livers were isolated immediately after sacrificing. Collected liver samples were used for the measurement of gene expression of cytokines and enzymes using the RT-PCR procedure described earlier.

Results and Discussion:

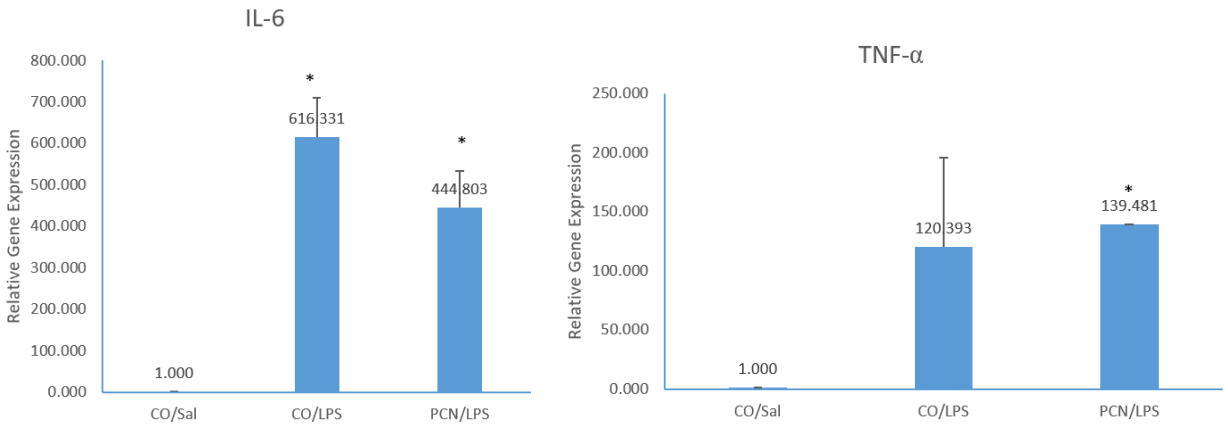

Fig. A

Fig. B

Figure A.1. Relative gene expression of IL-6 and TNF-α with 3-day PCN and 1h LPS treatments.

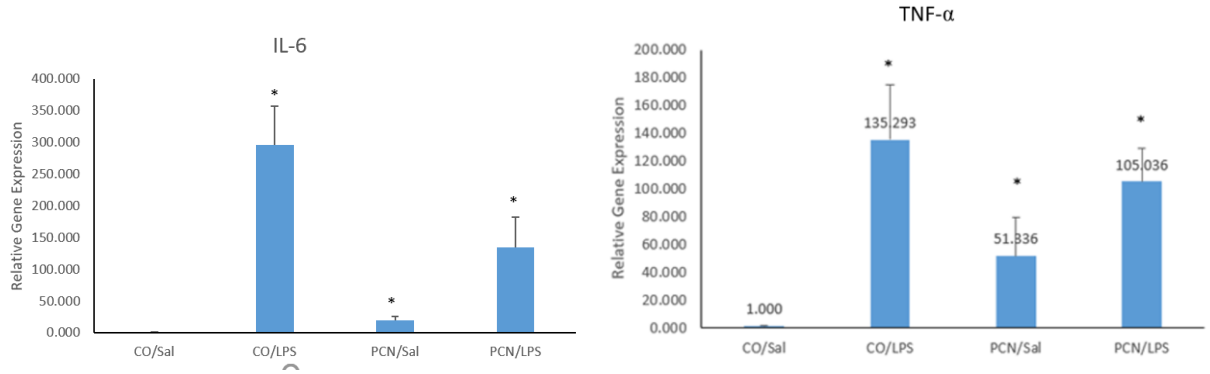

Fig. C

Fig. D

Figure A.2. Relative gene expression of IL-6 and TNF-α with 3-day PCN and 2h LPS treatments.

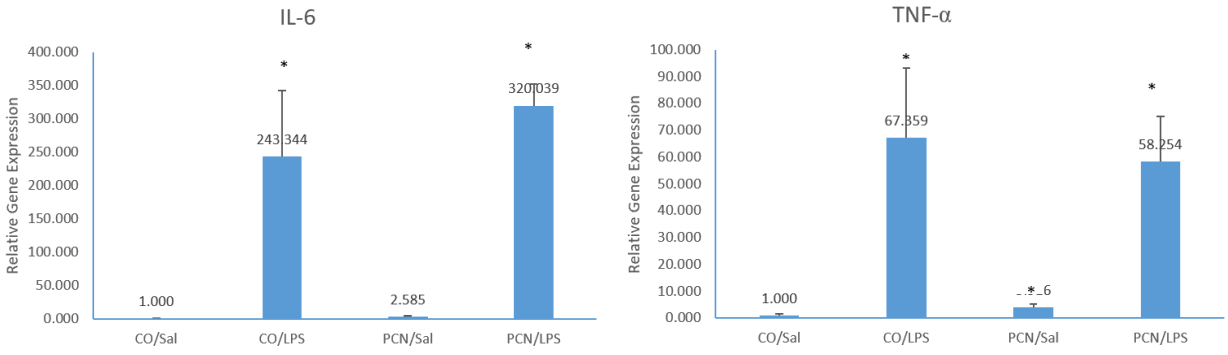

Fig. E

Fig. F

Figure A.3. Relative gene expression of IL-6 and TNF-α with 3-day PCN and 4h LPS treatments.

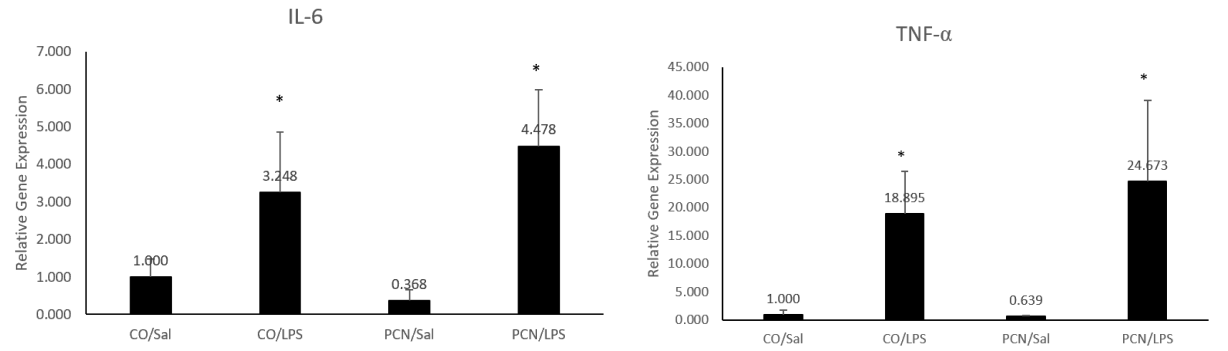

Fig. G

Fig. H

Figure A.4. Relative gene expression of IL-6 and TNF-α with 3-day PCN and 16h LPS treatments.

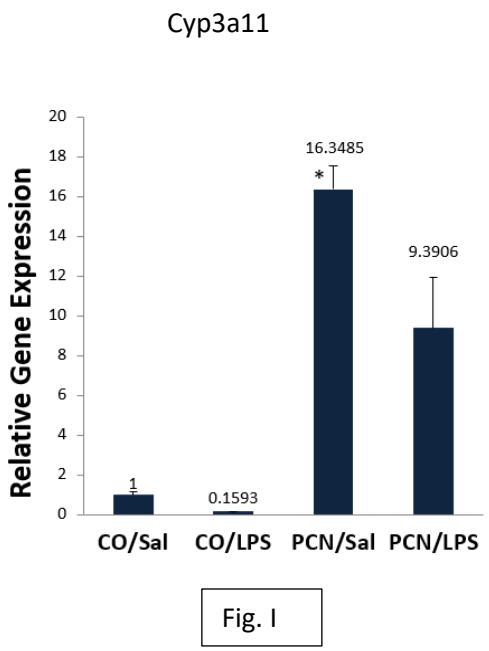

Figure A.5. Relative gene expression of Cyp3a11 with 3-day PCN and 16h LPS treatments.

The gene expression results indicate that with PCN 3 day and LPS 1 h treatment (Fig A.1), the LPS treatment significantly upregulated the IL-6 by 600-fold induction whereas TNF-α was induced by 120-fold. However, PCN/LPS combined treatment only reduced the expression of IL-6, but not TNF-α. With 2-hour LPS treatment (Fig. A2), as expected there was 430-fold induction of IL-6 and 135-fold induction of TNF-α. Surprisingly, the PCN/Sal treatment alone upregulated IL-6 and TNF-α by 65- and 51-folds, respectively. With the combined PCN/LPS treatment, although there was a reduction in the IL-6 and TNF-α expression compared with CO/LPS, a statistical significance was not observed. A similar trend in the relative gene expression of IL-6 and TNF-α with 4 h LPS treatment (Fig. A.4), except that there was no induction of cytokines with PCN/Sal treatment. The activation of PXR and TLRs together with PCN/LPS treatmenet did not show any anti-inflammatory effect when compared with LPS treatment alone with 16h LPS treatment (Fig A.4), while Cyp3a11 showed a 16 fold induction with PCN treatment (Fig. A.5). Together, these results indicate that an anti-inflammatory effect was not observed with PXR

activation in the presence of LPS treatment for 16 h. Moreover, surprisingly PCN/Sal treatment markedly upregulated IL-6 and TNF-α expression by 65 and 51-folds with 2h LPS treatment. In summary, the findings indicate that PXR and TLR simultaneous activation does not show a significant anti-inflammatory effect and at the same PCN treatment alone upregulated cytokine expression, which limits using PXR as a target to reduce inflammation and therefore does not alter the drug-metabolizing enzyme expression.

Chapter B: Effects of Inflammation on Irinotecan Pharmacokinetics with IV dosing

Abstract:

Irinotecan is a chemotherapeutic drug used in the treatment of advanced colorectal cancer and elevated blood concentrations of its active metabolite, SN-38 leads to increased gastrointestinal (GI) toxicity and diarrhea in patients. In this study, we investigated the effects of inflammation on the pharmacokinetics (PK) of irinotecan (CPT-11) and its active metabolite, SN-38. Mice were i.p.-injected with either saline or lipopolysaccharide (LPS) to induce inflammation. After 16 h, irinotecan was intravenously (I.V) administered via tail vein. Blood was collected from the tail vein of mice from 0-24 h after dosing. Concentrations of irinotecan, SN-38 and SN-38G were analyzed using LC-MS/MS. The AUC, C_{max}, and t_{max} were derived using WinNonlin® 5.2. Results indicated a significant increase in the blood concentrations of irinotecan and SN-38 in mice during inflammation. The AUC of irinotecan and SN-38 in the LPS group were 1.5 and 1.6-folds, respectively, of those in control saline-treated mice. The C_{max} of irinotecan and SN-38 in LPS treated mice were 1.7 and 1.5-folds of those in saline-treated mice. Together, this study reveals that SN-38 concentrations are elevated during inflammation, which may increase the GI toxicity and diarrhea in patients who receive irinotecan.

Results and Discussion:

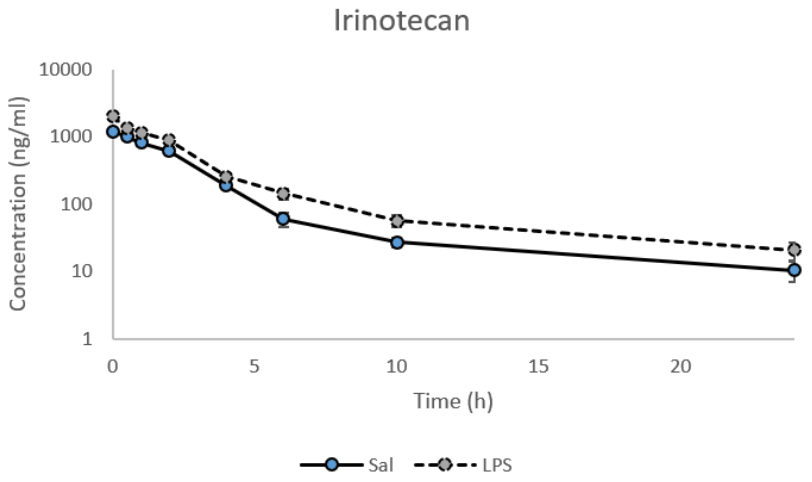

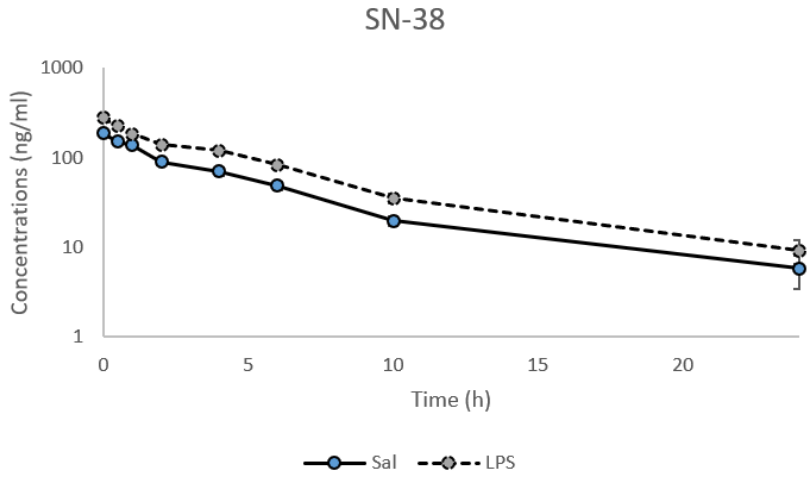

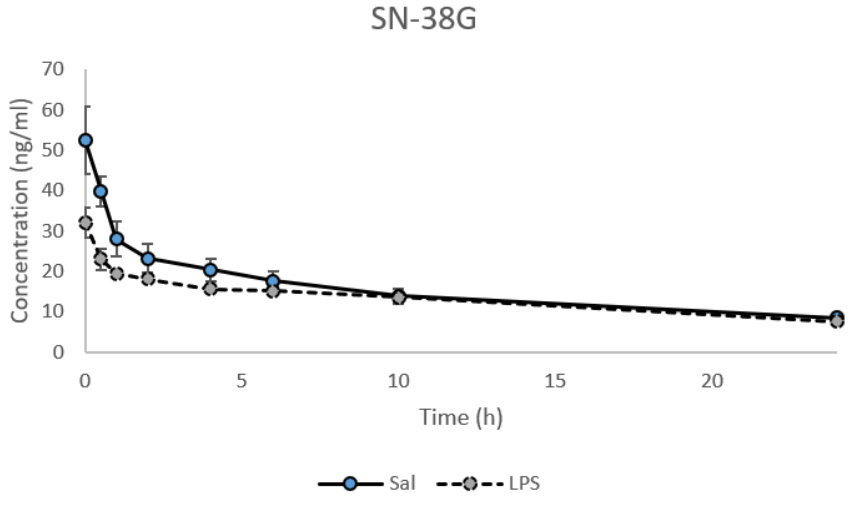

Figure B.1. Concentration-time profiles of irinotecan, SN-38, and SN-38G after an IV dose of 10 mg/kg irinotecan.

IV PK Parameters						
	Irinotecan		SN-38		SN-38G	
	Saline	LPS	Saline	LPS	Saline	LPS
AUC	3204.3	**4940.0**	861.0	**1392.5**	365.6	313.5
Cmax	1198.3	**2003.0**	185.8	**275.5**	52.5	32.1
tmax	0.0	0.0	0.0	0.0	0.0	0.0

Table B.1. PK parameters AUC, C_{max}, T_{max} after an IV dose of 10 mg/kg irinotecan.

The concentration-time profiles plotted indicate that the irinotecan and SN-38 concentrations were significantly elevated in LPS treated mice compared with Saline treated mice (Fig. B.1). The AUC of irinotecan and SN-38 in the LPS group were were also significantly higher in LPS treated mie, of those in control saline-treated mice. The C_{max} of irinotecan and SN-38 in LPS treated mice were also significantly higher, indicating that the active metabolite, SN-38 concentrations were significantly elevated during inflammation and may lead to increased toxicity in patients with irinotecan administration.

Chapter C: Role of TLR4 in Irinotecan-Induced Diarrhea and Steatosis

Abstract:

Irinotecan (CPT-11) is a chemotherapy drug used in first- and second-line treatment of metastatic colorectal cancer. Irinotecan undergoes phase-I metabolism by hepatic and peripheral carboxylesterase to produce active metabolite, SN-38, which is 100-1000-fold more active than irinotecan and shows its cytotoxic activity by inhibiting the topoisomerase-I enzyme and causing irreversible DNA damage and cell death. The major toxicities associated with irinotecan chemotherapy in patients are gastrointestinal (GI) toxicity (diarrhea) and hepatotoxicity (steatosis or steatohepatitis). These toxicities result in life-threatening complications in patients and reduce the use of irinotecan as a chemotherapeutic agent. Evidence from the literature strongly suggests that toll-like receptors (TLRs), including TLR4, are involved in the pathogenesis of gastrointestinal and hepatotoxicity. Several studies have found an increased mRNA expression and protein levels of TLR4 in samples of patients with gastrointestinal inflammatory diseases such as coeliac disease, inflammatory bowel disease and ulcerative colitis .[62–64] Specifically, a study by Wardill et al. identified that TLR4 mediates the irinotecan-induced gut toxicity and pain and suggest that TLR4 can be a target for improved toxicity outcomes.[65] Moreover, the intestinal permeability and LPS translocation were higher in wild-type mice than mice with TLR4 deletion.[65] Therefore, in this study, we investigated the role of TLR4 in irinotecan-induced toxicity. Specifically, we used TLR4 WT and Mutant mice and treated with either saline (control) or irinotecan (treatment group) for 8 days and sacrificed the mice on day 9. To measure the extent of GI toxicity in TLR4 WT and Mutant mice, we conducted body weight measurements, the incidence of diarrhea, and histological analysis of intestinal damage. Similarly, to determine the role of TLR4 in irinotecan-induced hepatotoxicity, H&E histological analysis of liver sections,

gene expression of enzymes and pro-inflammatory cytokines were conducted. The results indicate that there was no significant difference between the TLR4 WT and Mutant in terms of diarrhea and steatosis with irinotecan treatment.

Results and Discussion:

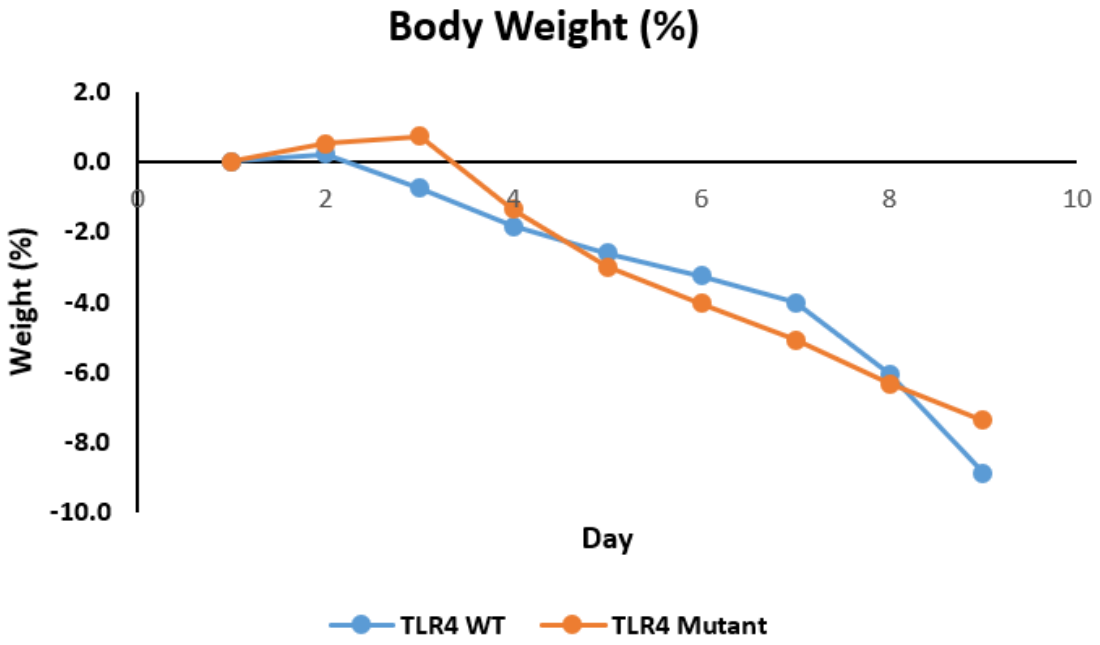

Figure C.1. Body Weight loss in TLR4 WT and Mutant mice groups from day 1-9.

Treatment Group	Mice Number per Group	Diarrhea Score (Grade Given Based on the Toxicity Criterion Defined by the National Cancer Institute (NCI)								
		Day 1	Day 2	Day 3	Day 4	Day 5	Day 6	Day 7	Day 8	Day 9
Group 1 (TLR4 WildType)	n=5	No Diarrhea	No Diarrhea	No Diarrhea	No Diarrhea	No Diarrhea	Signs of Diarrhea (Sluggishness, slight weakness)	Grade 2 (liquidy stools, weakness, less mobility)	Grade 3 (weakness, liquidy stools, Bloody Diarrhea in mice 1, 3, and 4)	Grade 4 (Severe bloody diarrhea in all mice, severe weakness, less movement, mice sacrificed)
Group 2 (TLR4 Mutant)	n=5	No Diarrhea	No Diarrhea	No Diarrhea	No Diarrhea	No Diarrhea	Signs of Diarrhea (Sluggishness, slight weakness and diarrhea symptoms in mouse 3)	Grade 1 diarrhea (signs of liquidy stools, appearance of weakness)	Grade 2 diarrhea, (grade 3 bloody diarrhea in mouse 3), weakness and liquidy stools	Grade 3-4 (Severe bloody diarrhea in all mice, severe weakness, less movement, mice sacrificed)

Table C.1. Incidence of diarrhea and diarrhea Score

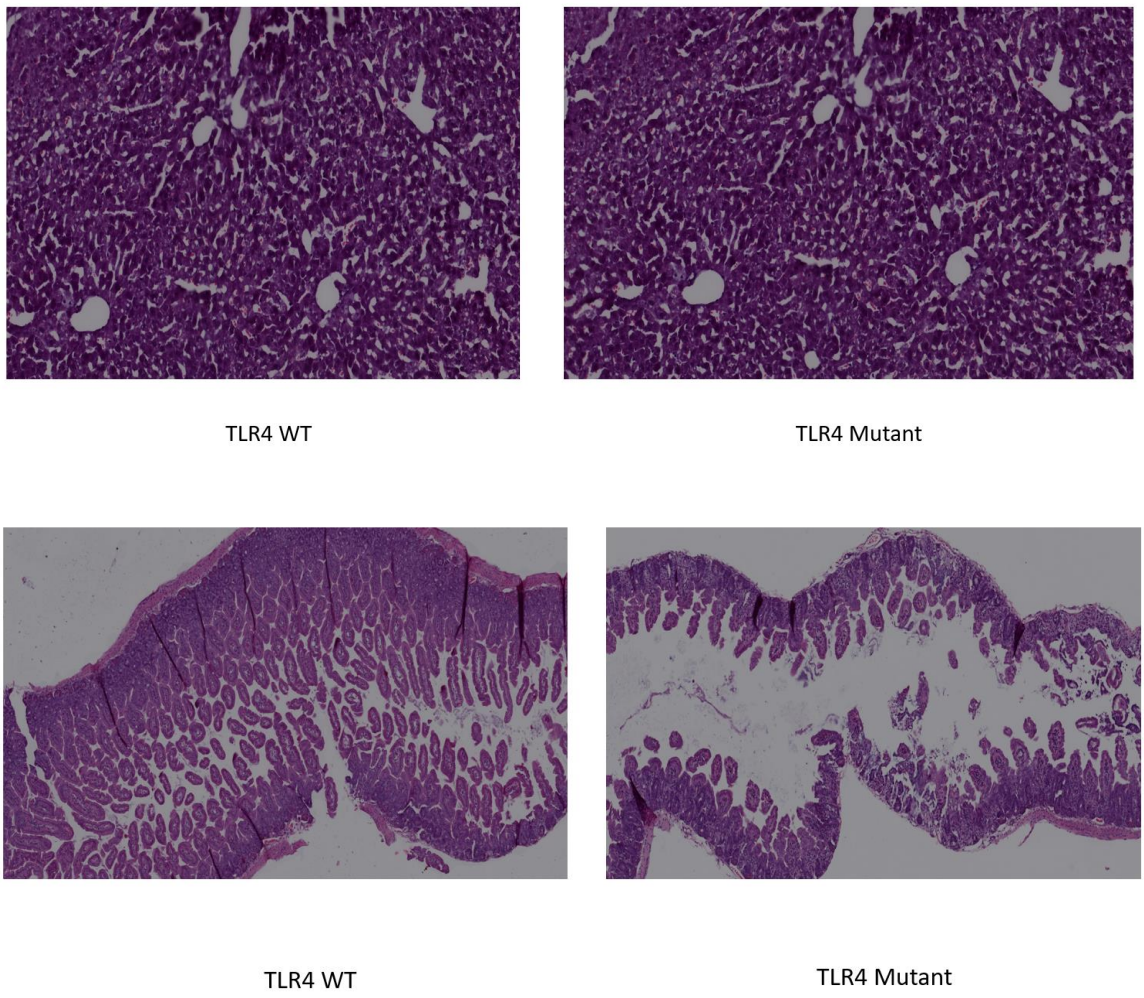

Figure C.2. Histological images of liver and intestine of TLR4 WT and TLR4 mutant mice.

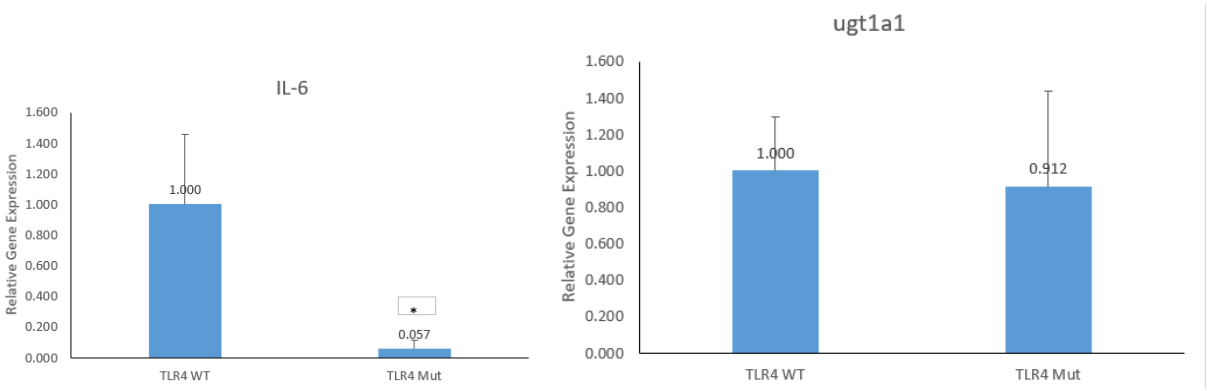

Figure C.3. Relative gene expression of IL-6 and Ugt1a1 in TLR4 WT and Mutant mice.

Results and Discussion:

The TLR4 WT and mutant mice were treated with irinotecan for 8 days and mice were sacrificed on day 9. The body weight loss and incidence of diarrhea observations revealed that there was no significant difference between TLR4 WT and Mutant mice (Fig C.1. and Table C.1.). Similarly, the histology images of the liver and intestine did not show a significant difference between TLR4 WT and Mutant mice (Fig. C.2.). However, the gene expression experiments showed significant downregulation of IL-6 cytokine in TLR4 Mutant mice, whereas Ugt1a1 expression was not altered (Fig. C.3). Overall, the results did not indicate that TLR4 plays a role in irinotecan-induced diarrhea or steatosis.

REFERENCES

1. Bray, F. *et al.* Global cancer statistics 2018: GLOBOCAN estimates of incidence and mortality worldwide for 36 cancers in 185 countries. *CA. Cancer J. Clin.* **68**, 394–424 (2018).

2. Gustavsson, B. *et al.* A review of the evolution of systemic chemotherapy in the management of colorectal cancer. *Clin. Colorectal Cancer* **14**, 1–10 (2015).

3. Key Statistics for Colorectal Cancer. https://www.cancer.org/cancer/colon-rectal-cancer/about/key-statistics.html.

4. Araghi, M. *et al.* Global trends in colorectal cancer mortality: projections to the year 2035. *Int. J. Cancer* **144**, 2992–3000 (2019).

5. Globocan. Colorectal cancer Source: Globocan 2018 Number of new cases in 2018, both sexes, all ages. **876**, 1–2 (2018).

6. Al-Sohaily, S., Biankin, A., Leong, R., Kohonen-Corish, M. & Warusavitarne, J. Molecular pathways in colorectal cancer. *J. Gastroenterol. Hepatol.* **27**, 1423–1431 (2012).

7. Treatment options for metastatic colorectal cancer. https://www.cancercenter.com/cancer-types/colorectal-cancer/types/metastatic-colorectal-cancer.

8. Young, A. & Rea, D. ABC of Colorectal cancer: Treatment of advanced disease. *Clin. Rev.* **321**, 1278–1281 (2000).

9. Chemotherapy for Colorectal Cancer. https://www.cancer.org/cancer/colon-rectal-cancer/treating/chemotherapy.html.

10. Mullangi, R., Ahlawat, P. & Srinivas, N. R. Irinotecan and its active metabolite, SN-38: Review of bioanalytical methods and recent update from clinical pharmacology perspectives. *Biomed. Chromatogr.* **24**, 104–123 (2010).

11. Irinotecan Label accessed from Drugs@FDA. 1–39 (2019).

12. Mathijssen, R. H. J. *et al.* Clinical pharmacokinetics and metabolism of irinotecan (CPT-11). *Clin. Cancer Res.* **7**, 2182–2194 (2001).

13. Arbuck, S. & Takimoto, C. An overview of Topoisomerase-I targeting agents. *Semin. Hematol.* **35**, 3–12 (1998).

14. Frese, S. & Diamond, B. Structural modification of DNA-a therapeutic option in SLE? *Nat. Rev. Rheumatol.* **7**, 733–738 (2011).

15. Fujita, K. I., Kubota, Y., Ishida, H. & Sasaki, Y. Irinotecan, a key chemotherapeutic drug for metastatic colorectal cancer. *World J. Gastroenterol.* **21**, 12234–12248 (2015).

16. Lokiec, F. *et al.* Pharmacokinetics of irinotecan and its metabolites in human blood, bile, and urine. *Cancer Chemother. Pharmacol.* **36**, 79–82 (1995).

17. Slatter, J. G. *et al.* Pharmacokinetics, metabolism, and excretion of irinotecan (CPT-11) following i.v. infusion of [14C]CPT-11 in cancer patients. *Drug Metab. Dispos.* **28**, 423–433 (2000).

18. Treatment for Metastatic Colon Cancer. https://www.mskcc.org/cancer-care/types/colon/treatment/metastases.

19. Saltz, L. B. *et al.* IRINOTECAN PLUS FLUOROURACIL AND LEUCOVORIN FOR METASTATIC COLORECTAL CANCER. *N. Engl. J. Med.* **343**, 905–914 (2000).

20. Masi, G. *et al.* First-line treatment of metastatic colorectal cancer with irinotecan, oxaliplatin and 5-fluorouracil/leucovorin (FOLFOXIRI): Results of a phase II study with a simplified biweekly schedule. *Ann. Oncol.* **15**, 1766–1772 (2004).

21. Hu, Z. *et al.* St. John's wort modulates the toxicities and pharmacokinetics of CPT-11 (Irinotecan) in rats. *Pharm. Res.* **22**, 902–914 (2005).

22. Tang, L. *et al.* Herbal Medicines for Irinotecan-Induced Diarrhea. *Front. Pharmacol.* **10**, 1–8 (2019).

23. Hoff, P. M. *et al.* Randomized phase III trial exploring the use of long-acting release octreotide in the prevention of chemotherapy-induced diarrhea in patients with colorectal cancer: The LARCID trial. *J. Clin. Oncol.* **32**, 1006–1011 (2014).

24. Barbounis, V., Koumakis, G., Vassilomanolakis, M., Demiri, M. & Efremidis, A. P. Control of irinotecan-induced diarrhea by octreotide after loperamide failure. *Support.*

Care Cancer **9**, 258–260 (2001).

25. Stein, A., Voigt, W. & Jordan, K. Review: Chemotherapy-induced diarrhea: Pathophysiology, frequency and guideline-based management. *Ther. Adv. Med. Oncol.* **2**, 51–63 (2010).

26. Zhang, X. *et al.* Darunavir alleviates irinotecan-induced intestinal toxicity in Vivo. *Eur. J. Pharmacol.* **834**, 288–294 (2018).

27. Liu, X., Cheng, D., Kuang, Q., Liu, G. & Xu, W. Association of UGT1A1*28 polymorphisms with irinotecan-induced toxicities in colorectal cancer: A meta-analysis in Caucasians. *Pharmacogenomics J.* **14**, 120–129 (2014).

28. Logan, R. M. *et al.* Characterisation of mucosal changes in the alimentary tract following administration of irinotecan: Implications for the pathobiology of mucositis. *Cancer Chemother. Pharmacol.* **62**, 33–41 (2008).

29. Ribeiro, R. A. *et al.* Irinotecan- and 5-fluorouracil-induced intestinal mucositis: insights into pathogenesis and therapeutic perspectives. *Cancer Chemother. Pharmacol.* **78**, 881–893 (2016).

30. Stringer, A. M. *et al.* Irinotecan-induced mucositis is associated with changes in intestinal mucins. *Cancer Chemother. Pharmacol.* **64**, 123–132 (2009).

31. Mahvi, D. A. & Mahvi, D. M. *Liver Metastases*. *Abeloff's Clinical Oncology* (Elsevier Inc.). doi:10.1016/B978-0-323-47674-4.00058-X.

32. Vauthey, J. N. *et al.* Chemotherapy regimen predicts steatohepatitis and an increase in 90-day mortality after surgery for hepatic colorectal metastases. *J. Clin. Oncol.* **24**, 2065–

2072 (2006).

33. Parikh, A. *et al.* Perioperative Complications in Patients Undergoing Major Liver Resection With or Without Neoadjuvant Chemotherapy. *Artif. Intell. Med.* **7**, 1082–1088 (2003).

34. Zorzi, D. *et al.* Chemotherapy-associated hepatotoxicity and surgery for colorectal liver metastases. 274–286 (2007) doi:10.1002/bjs.5719.

35. McWhirter, D. *et al.* Chemotherapy induced hepatotoxicity in metastatic colorectal cancer: A review of mechanisms and outcomes. *Crit. Rev. Oncol. Hematol.* **88**, 404–415 (2013).

36. Zhang, H. *et al.* Human mitochondrial topoisomerase I. *Proc. Natl. Acad. Sci. U. S. A.* **98**, 10608–10613 (2001).

37. Kosovsky, M. J. & Soslau, G. Mitochondrial DNA topoisomerase I from human platelets. *Biochim. Biophys. Acta (BBA)/Protein Struct. Mol.* **1078**, 56–62 (1991).

38. Kosovsky, M. J. & Soslau, G. Immunological idenTIFication of human platelet mitochondrial DNA topoisomerase I. *Biochim. Biophys. Acta (BBA)/Protein Struct. Mol.* **1164**, 101–107 (1993).

39. Renton, K. W. Alteration of drug biotransformation and elimination during infection and inflammation. *Pharmacol. Ther.* **92**, 147–163 (2001).

40. Yang, K. H. & Lee, M. G. Effects of endotoxin derived from Escherichia coli lipopolysaccharide on the pharmacokinetics of drugs. *Arch. Pharm. Res.* **31**, 1073–1086 (2008).

41. Morgan, E. T. Impact of Infectious and Inflammatory Disease on Cytochrome P450 – Mediated Drug Metabolism and Pharmacokinetics. *Nature* **85**, 434–438 (2009).

42. Donald Harvey, R. & Morgan, E. T. Cancer, inflammation, and therapy: Effects on cytochrome P450-mediated drug metabolism and implications for novel immunotherapeutic agents. *Clin. Pharmacol. Ther.* **96**, 449–457 (2014).

43. Rivory, L. P., Slaviero, K. A. & Clarke, S. J. Hepatic cytochrome P450 3A drug metabolism is reduced in cancer patients who have an acute-phase response. *Br. J. Cancer* **87**, 277–280 (2002).

44. Robertson, G. R., Liddle, C. & Clarke, S. J. Inflammation and altered drug clearance in cancer: Transcriptional repression of a human CYP3A4 transgene in tumor-bearing mice. *Clin. Pharmacol. Ther.* **83**, 894–897 (2008).

45. Monshouwer, M. *et al.* A lipopolysaccharide-induced acute phase response in the pig is associated with a decrease in hepatic cytochrome P450-mediated drug metabolism. *J Vet Pharmacol Ther* **19**, 382–388 (1996).

46. Watson, A. M., Warren, G., Howard, G., Shedlofsky, S. I. & Blouin, R. A. Activities of conjugating and antioxidant enzymes following endotoxin exposure. *J. Biochem. Mol. Toxicol.* **13**, 63–69 (1999).

47. Jover, R., Bort, R., Gómez-Lechón, M. J. & Castell, J. V. Down-regulation of human CYP3A4 by the inflammatory signal interleukin-6: molecular mechanism and transcription factors involved. *FASEB J.* **16**, 1799–1801 (2002).

48. Aitken, A. E. & Morgan, E. T. Gene-Specific Effects of Inflammatory Cytokines on

Cytochrome P4502C, 2B6 and 3A4 mRNA Levels in Human Hepatocytes. *Ratio* **35**, 1687–1693 (2007).

49. Ghose, R., Guo, T. & Haque, N. Regulation of gene expression of hepatic drug metabolizing enzymes and transporters by the Toll-like receptor 2 ligand, lipoteichoic acid. *Arch. Biochem. Biophys.* **481**, 123–130 (2009).

50. Ghose, R., White, D., Guo, T., Vallejo, J. & Karpen, S. J. Regulation of hepatic drug-metabolizing enzyme genes by Toll-like receptor 4 signaling is independent of Toll-interleukin 1 receptor domain-containing adaptor protein. *Drug Metab. Dispos.* **36**, 95–101 (2008).

51. Mao, Z. *et al.* Lipopolysaccharide down-regulates carbolesterases 1 and 2 and reduces hydrolysis activity in vitro and in vivo via p38MAPK-NF-κB pathway. *Toxicol. Lett.* **201**, 213–220 (2011).

52. Richardson, T. A., Sherman, M., Kalman, D. & Morgan, E. T. Expression of UDP-glucuronosyltransferase isoform mRNAs during inflammation and infection in mouse liver and kidney. *Drug Metab. Dispos.* **34**, 351–353 (2006).

53. Gibson, C. J., Hossain, M. M., Richardson, J. R. & Aleksunes, L. M. Inflammatory regulation of ATP binding cassette efflux transporter expression and function in microglia. *J. Pharmacol. Exp. Ther.* **343**, 650–660 (2012).

54. Kalitsky-Szirtes, J., Shayeganpour, A., Brocks, D. R. & Piquette-Miller, M. Suppression of drug-metabolizing enzymes and efflux transporters in the intestine of endotoxin-treated rats. *Drug Metab. Dispos.* **32**, 20–27 (2004).

55. Le Vee, M., Gripon, P., Stieger, B. & Fardel, O. Down-regulation of organic anion transporter expression in human hepatocytes exposed to the proinflammatory cytokine interleukin 1β. *Drug Metab. Dispos.* **36**, 217–222 (2008).

56. Renton, K. W. Cytochrome p450 regulation and drug biotransformation during inflammation and infection. *Curr.Drug Metab* **5**, 235–243 (2004).

57. Akira, S. & Takeda, K. Toll-like receptor signalling. *Nat. Rev. Immunol.* **4**, 499–511 (2004).

58. Takeda, K. & Akira, S. TLR signaling pathways. *Semin. Immunol.* **16**, 3–9 (2004).

59. Himes, R. W. & Smith, C. W. Tlr2 is critical for diet-induced metabolic syndrome in a murine model. *FASEB J.* **24**, 731–739 (2010).

60. Wagnerberger, S. *et al.* Toll-like receptors 1-9 are elevated in livers with fructose-induced hepatic steatosis. *Br. J. Nutr.* **107**, 1727–1738 (2012).

61. Bowen, J., Coller, J., Hutchinson, M. & Gibson, R. 96. Expression of TLRs in the rat intestine following chemotherapy for cancer. *Brain. Behav. Immun.* **26**, S27 (2012).

62. Fan, Y. & Liu, B. Expression of Toll-like receptors in the mucosa of patients with ulcerative colitis. *Exp. Ther. Med.* **9**, 1455–1459 (2015).

63. Szebeni, B. *et al.* Increased mucosal expression of toll-like receptor (TLR)2 and TLR4 in coeliac disease. *J. Pediatr. Gastroenterol. Nutr.* **45**, 187–193 (2007).

64. Frolova, L., Drastich, P., Rossmann, P., Klimesova, K. & Tlaskalova-Hogenova, H. Expression of Toll-like receptor 2 (TLR2), TLR4, and CD14 in biopsy samples of patients with inflammatory bowel diseases: Upregulated expression of TLR2 in terminal ileum of

patients with ulcerative colitis. *J. Histochem. Cytochem.* **56**, 267–274 (2008).

65. Wardill, H. R. *et al.* Irinotecan-Induced Gastrointestinal Dysfunction and Pain Are Mediated by Common TLR4-Dependent Mechanisms. *Mol. Cancer Ther.* **15**, 1376–1386 (2016).

66. Fakiha, K., Coller, J. K., Logan, R. M., Gibson, R. J. & Bowen, J. M. Amitriptyline prevents CPT-11-induced early-onset diarrhea and colonic apoptosis without reducing overall gastrointestinal damage in a rat model of mucositis. *Support. Care Cancer* **27**, 2313–2320 (2019).

67. Gibson, R. J. *et al.* Chemotherapy-induced gut toxicity and pain: involvement of TLRs. *Support. Care Cancer* **24**, 2251–2258 (2016).

68. Thorpe, D. W., Stringer, A. M. & Gibson, R. J. Chemotherapy-induced mucositis: The role of the gastrointestinal microbiome and toll-like receptors. *Exp. Biol. Med.* **238**, 1–6 (2013).

69. Stringer, A. M. Interaction between host cells and microbes in chemotherapy-induced mucositis. *Nutrients* **5**, 1488–1499 (2013).

70. Kaczmarek, A., Brinkman, B. M., Heyndrickx, L., Vandenabeele, P. & Krysko, D. V. Severity of doxorubicin-induced small intestinal mucositis is regulated by the TLR-2 and TLR-9 pathways. *J. Pathol.* **226**, 598–608 (2012).

71. Wong, D. V. T. *et al.* The adaptor protein Myd88 is a key signaling molecule in the pathogenesis of irinotecan-induced intestinal mucositis. *PLoS One* **10**, (2015).

72. de Piano, A., Masquio, D. C. L. & Dâmaso, A. R. The Effects of Soy Products and

Isoflavones in Metabolic Syndrome and Nonalcoholic Fatty Liver Disease. *Bioact. Food as Diet. Interv. Diabetes* 121–136 (2019) doi:10.1016/b978-0-12-813822-9.00008-4.

73. Characteristics, T. Novasoy 400. (2001).

74. Qiu, L.-X. & Chen, T. Novel insights into the mechanisms whereby isoflavones protect against fatty liver disease. *World J. Gastroenterol.* **21**, 1099–1107 (2015).

75. Paradkar, P. N., Blum, P. S., Berhow, M. A., Baumann, H. & Kuo, S. M. Dietary isoflavones suppress endotoxin-induced inflammatory reaction in liver and intestine. *Cancer Lett.* **215**, 21–28 (2004).

76. Ali, A. A., Velasquez, M. T., Hansen, C. T., Mohamed, A. I. & Bhathena, S. J. Effects of soybean isoflavones, probiotics, and their interactions on lipid metabolism and endocrine system in an animal model of obesity and diabetes. *J. Nutr. Biochem.* **15**, 583–590 (2004).

77. Akhlaghi, M. Non-alcoholic Fatty Liver Disease: Beneficial Effects of Flavonoids. *Phyther. Res.* **1571**, 1559–1571 (2016).

78. Xiao, C. W. *et al.* Dietary supplementation with soy isoflavones or replacement with soy proteins prevents hepatic lipid droplet accumulation and alters expression of genes involved in lipid metabolism in rats. *Genes Nutr.* **9**, (2014).

79. Kim, M. H. & Kang, K. S. Isoflavones as a smart curer for non-alcoholic fatty liver disease and pathological adiposity via ChREBP and Wnt signaling. *Prev. Med. (Baltim).* **54**, S57–S63 (2012).

80. Crespillo, A. *et al.* Reduction of body weight, liver steatosis and expression of stearoyl-CoA desaturase 1 by the isoflavone daidzein in diet-induced obesity. *Br. J. Pharmacol.*

164, 1899–1915 (2011).

81. Kim, M. H., Kang, K. S. & Lee, Y. S. The inhibitory effect of genistein on hepatic steatosis is linked to visceral adipocyte metabolism in mice with diet-induced non-alcoholic fatty liver disease. *Br. J. Nutr.* **104**, 1333–1342 (2010).

82. Yoo, N. Y. *et al.* Dietary supplementation of genistein alleviates liver inflammation and fibrosis mediated by a methionine-choline-deficient diet in db / db mice. *J. Agric. Food Chem.* **63**, 4305–4311 (2015).

83. Guan, H. yu *et al.* Shengjiang Xiexin decoction alters pharmacokinetics of irinotecan by regulating metabolic enzymes and transporters: A multi-target therapy for Alleviating the gastrointestinal toxicity. *Front. Pharmacol.* **8**, 1–13 (2017).

84. Lam, W. *et al.* Chemotherapy: The four-herb Chinese medicine PHY906 reduces chemotherapy-induced gastrointestinal toxicity. *Sci. Transl. Med.* **2**, 1–10 (2010).

85. Meng, H. *et al.* Ameliorative Effect of Daidzein on Cisplatin-Induced Nephrotoxicity in Mice via Modulation of Inflammation, Oxidative Stress, and Cell Death. *Food Chem. Toxicol.* 1–10 (2017) doi:10.1016/j.fct.2019.04.031.

86. Sergent, T., Piront, N., Meurice, J., Toussaint, O. & Schneider, Y. J. Anti-inflammatory effects of dietary phenolic compounds in an in vitro model of inflamed human intestinal epithelium. *Chem. Biol. Interact.* **188**, 659–667 (2010).

87. Kao, T. H., Wu, W. M., Hung, C. F., Wu, W. B. & Chen, B. H. Anti-inflammatory effects of isoflavone powder produced from soybean cake. *J. Agric. Food Chem.* **55**, 11068–11079 (2007).

88. Chinta, S. J., Ganesan, A., Reis-rodrigues, P., Lithgow, G. J. & Andersen, K. Anti-Inflammatory Role of the Isoflavone Diadzein in Lipopolysaccharide-Stimulated Microglia: Implications for Parkinson's Disease. **23**, 145–153 (2013).

89. Yokooji, T., Kawabe, Y., Mori, N. & Murakami, T. Effect of genistein, a natural soy isoflavone, on the pharmacokinetics and intestinal toxicity of irinotecan hydrochloride in rats. *J. Pharm. Pharmacol.* **65**, 280–291 (2013).

90. Sahin, I., Bilir, B., Ali, S., Sahin, K. & Kucuk, O. Soy Isoflavones in Integrative Oncology: Increased Efficacy and Decreased Toxicity of Cancer Therapy. *Integr. Cancer Ther.* **18**, (2019).

91. Weng, Z. M. *et al.* Characterization and structure-activity relationship studies of flavonoids as inhibitors against human carboxylesterase 2. *Bioorg. Chem.* **77**, 320–329 (2018).

92. Ronis, M. J. J. Effects of soy containing diet and isoflavones on cytochrome P450 enzyme expression and activity. *Drug Metab. Rev.* **48**, 331–341 (2016).

93. Froyen, E. B., Reeves, J. L. R., Mitchell, A. E. & Steinberg, F. M. Regulation of phase II enzymes by Genistein and daidzein in male and female Swiss Webster mice. *J. Med. Food* **12**, 1227–1237 (2009).

94. Yuan-Jing, F., Wei, W., Jian-Ping, L., Yu-Xia, J. & Zi-Ling, D. Genistein promotes the metabolic transformation of acetaminophen to glucuronic acid in human L-O2, HepG2 and Hep3b cells: Via the Nrf2/Keap1 pathway. *Food Funct.* **7**, 4683–4692 (2016).

95. Cermak, R. Effect of dietary flavonoids on pathways involved in drug metabolism. *Expert*

Opin. Drug Metab. Toxicol. **4**, 17–35 (2008).

96. Sun, X. Y., Plouzek, C. A., Henry, J. P., Wang, T. T. Y. & Phang, J. M. Increased UDP-glucuronosyltransferase activity and decreased prostate specific antigen production by biochanin A in prostate cancer cells. *Cancer Res.* **58**, 2379–2384 (1998).

97. Clavel, T. *et al.* Isoflavones and Functional Foods Alter the Dominant Intestinal Microbiota in Postmenopausal Women. *J. Nutr.* **135**, 2786–2792 (2005).

98. Lesinski, G. B. *et al.* Consumption of soy isoflavone enriched bread in men with prostate cancer is associated with reduced proinflammatory cytokines and immunosuppressive cells. *Cancer Prev. Res.* **8**, 1036–1044 (2015).

99. Mace, T. A. *et al.* Soy isoflavones and their metabolites modulate cytokine-induced natural killer cell function. *Sci. Rep.* **9**, 1–12 (2019).

100. Mallick, P., Shah, P., Gandhi, A. & Ghose, R. Impact of obesity on accumulation of the toxic irinotecan metabolite, SN-38, in mice. *Life Sci.* **139**, 132–138 (2015).

101. Mallick, P. *et al.* Impact of diet on irinotecan toxicity in mice. *Chem. Biol. Interact.* **291**, 87–94 (2018).

102. Atasilp, C. *et al.* Determination of irinotecan, SN-38 and SN-38 glucuronide using HPLC/MS/MS: Application in a clinical pharmacokinetic and personalized medicine in colorectal cancer patients. *J. Clin. Lab. Anal.* **32**, 3–6 (2018).

103. Tian, C. *et al.* Value of plasma SN-38 levels and DPD activity I irinotecan-based individualized chemotherapy for advanced colorectal cancer with heterozygous type UGT1A1*6 or UGT1A1*. *Cancer Manag. Res.* **10**, 6217–6226 (2018).

104. Manzanares, A. *et al.* Tissue Compatibility of SN-38-Loaded Anticancer Nanofiber Matrices. *Adv. Healthc. Mater.* **7**, 1–11 (2018).

105. Heske, C. M. *et al.* STA-8666, a novel HSP90 inhibitor/SN-38 drug conjugate, causes complete tumor regression in preclinical mouse models of pediatric sarcoma. *Oncotarget* **7**, (2016).

106. Zhuang, Q., Liu, X., Sun, Z., Wang, H. & Jiang, J. A validated UPLC-MS/MS method to determine free and total irinotecan and its two metabolites in human plasma after intravenous administration of irinotecan hydrochloride liposome injection. *J. Pharm. Biomed. Anal.* **170**, 112–123 (2019).

107. Coriat, R. *et al.* Pharmacokinetics and safety of DTS-108, a human oligopeptide bound to SN-38 with an esterase-sensitive cross-linker in patients with advanced malignancies: A phase I study. *Int. J. Nanomedicine* **11**, 6207–6216 (2016).

108. Kawato, Y., Aonuma, M., Hirota, Y., Kuga, H. & Sato, K. Intracellular Roles of SN-38, a Metabolite of the Camptothecin Derivative CPT-11, in the Antitumor Effect of CPT-11. *Cancer Res.* **51**, 4187–4191 (1991).

109. Basili, S. & Moro, S. Novel camptothecin derivatives as topoisomerase I inhibitors. *Expert Opin. Ther. Pat.* **19**, 555–574 (2009).

110. Xie, R., Mathijssen, R. H. J., Sparreboom, A., Verweij, J. & Karlsson, M. O. Clinical pharmacokinetics of irinotecan and its metabolites: A population analysis. *J. Clin. Oncol.* **20**, 3293–3301 (2002).

111. Roberts, M., Magnusson, B., Burczynski, F. & Weiss, M. Enterohepatic circulation:

Physiological, pharmacokinetic and clinical implications. *Clin. Pharmacokinet.* **41**, 751–790 (2002).

112. Riera, P. *et al.* Relevance of CYP3A4*20, UGT1A1*37 and UGT1A1*28 variants in irinotecan-induced severe toxicity. *Br. J. Clin. Pharmacol.* **84**, 1389–1392 (2018).

113. Haaz, M.-C., Rivory, L., Christian, R., Vernillet, L. & Robert, J. Metabolism of Irinotecan (CPT-11) by Human Hepatic Microsomes: Participation of Cytochrome P-450 3A and Drug Interactions. *Cancer Res* **58**, 468–472 (1998).

114. Haaz, M.-C., Christian, R., Rivory, L. & Robert, J. BIOSYNTHESIS OF AN AMINOPIPERIDINO METABOLITE OF IRINOTECAN [7-ETHYL-10-[4-(1-PIPERIDINO)-1-PIPERIDINO]CARBONYLOXYCAMPTOTHECINE] BY HUMAN HEPATIC MICROSOMES. *Drug Metab Dispos.* **26**, 769–775 (1998).

115. Ma, M. K. *et al.* Pharmacokinetics of Irinotecan and Its Metabolites SN-38 and APC in Children with Recurrent Solid Tumors after Protracted Pharmacokinetics of Irinotecan and Its Metabolites SN-38 and APC in Children with Recurrent Solid Tumors after Protracted Low-Dose Ir. *Clin. Cancer Res.* **6**, 813–819 (2000).

116. Xie, R., Mathijssen, R. H. J., Sparreboom, A., Verweij, J. & Karlsson, M. O. Clinical pharmacokinetics of irinotecan and its metabolites in relation with diarrhea. *Clin. Pharmacol. Ther.* **72**, 265–275 (2002).

117. Sasaki Yasutsuna *et al.* A pharmacokinetic and pharmacodynamic analysis of CPT-11 and its active Metabolite SN-38. 101–110 (1995).

118. Forni, M. de *et al.* Phase I and pharmacokinetic Study of the Camptothecin Derivative

Irinotecan, Adminstered on a Weekly Schedule in Cancer Patients. *Cancer Res* **54**, 4347–4354 (1994).

119. Eiji, A. *et al.* Relationship between development of diarrhea and the concentration of SN-38, an active metabolite of CPT-11. 697–702 (1993).

120. De Jong, F. A. *et al.* Irinotecan-induced diarrhea: Functional significance of the polymorphic ABCC2 transporter protein. *Clin. Pharmacol. Ther*. **81**, 42–49 (2007).

121. Cheng, K. W. *et al.* Pharmacological inhibition of bacterial β-glucuronidase prevents irinotecan-induced diarrhea without impairing its antitumor efficacy in vivo. *Pharmacol. Res.* **139**, 41–49 (2019).

122. Chamseddine, A. N. *et al.* Intestinal bacterial β-glucuronidase as a possible predictive biomarker of irinotecan-induced diarrhea severity. *Pharmacol. Ther.* (2019) doi:10.1016/j.pharmthera.2019.03.002.

123. Aitken, A. E., Richardson, T. A. & Morgan, E. T. REGULATION OF DRUG-METABOLIZING ENZYMES AND TRANSPORTERS IN INFLAMMATION. *Annu. Rev. Pharmacol. Toxicol.* **46**, 123–149 (2006).

124. Cressman, A. M., Petrovic, V. & Piquette-Miller, M. Inflammation-mediated changes in drug transporter expression/activity: Implications for therapeutic drug response. *Expert Rev. Clin. Pharmacol.* **5**, 69–89 (2012).

125. Petrovic, V., Teng, S. & Piquette-Miller, M. Regulation of Drug Transporters: During Infection and Inflammation. *Mol. Interv.* **7**, 99–111 (2007).

126. Gandhi, A. & Ghose, R. Altered Drug Metabolism and Transport in Pathophysiological

Conditions. **2**, (2010).

127. Li-Masters, T. & Morgan, E. T. Down-regulation of phenobarbital-induced cytochrome P4502B mRNAs and proteins by endotoxin in mice: Independence from nitric oxide production by inducible nitric oxide synthase. *Biochem. Pharmacol.* **64**, 1703–1711 (2002).

128. Fang, C. *et al.* Hepatic expression of multiple acute phase proteins and down-regulation of nuclear receptors after acute endotoxin exposure. *Biochem. Pharmacol.* **67**, 1389–1397 (2004).

129. Cherrington, N. J., Slitt, A. L., Li, N. & Klaassen, C. D. Lipopolysaccharide-mediated regulation of hepatic transporter mRNA levels in rats. *Drug Metab. Dispos.* **32**, 734–741 (2004).

130. Morgan, E. T. Regulation of Cytochrome P450 by Inflammatory Mediators: Why and How? *Drug Metab. Dispos.* **29**, 207–212 (2001).

131. Morgan, E. T. *et al.* Symposium Report Regulation of Drug-Metabolizing Enzymes and Transporters in Infection, Inflammation, and Cancer. *Pharmacology* **36**, 205–216 (2008).

132. Panaro, M. A. *et al.* Expression of UDP-glucuronosyltransferase 1A6 isoform in Caco-2 cells stimulated with lipopolysaccharide. *Innate Immun.* **16**, 302–309 (2009).

133. Zhou, X. *et al.* Disturbance of Hepatic and Intestinal UDP-Glucuronosyltransferase in Rats with Trinitrobenzene Sulfonic Acid-Induced Colitis. *Drug Metab. Pharmacokinet. (DMPK)2* **450**, 1–31 (2012).

134. Yao, D., Dong, Q., Tian, Y., Dai, C. & Wu, S. Lipopolysaccharide stimulates endogenous

β-glucuronidase via PKC/NF-κB/c-myc signaling cascade: a possible factor in hepatolithiasis formation. *Mol. Cell. Biochem.* **444**, 93–102 (2018).

135. Van Groeningen, C. J. *et al.* Altered pharmacokinetics and metabolism of CPT-11 in liver dysfunction: A need for guidelines. *Clin. Cancer Res.* **6**, 1342–1346 (2000).

136. Rouits, E., Guichard, S., Canal, P. & Chatelut, E. Non-linear pharmacokinetics of irinotecan in mice. *Anticancer. Drugs* **13**, 631–635 (2002).

137. Xie, R., Mathijssen, R. H. J., Sparreboom, A., Verweij, J. & Karlsson, M. O. Clinical pharmacokinetics of irinotecan and its metabolites in relation with diarrhea. *Clin. Pharmacol. Ther.* **72**, 265–275 (2002).

138. Klein, C. E. *et al.* Population pharmacokinetic model for irinotecan and two of its metabolites, SN-38 and SN-38 glucuronide. *Clin. Pharmacol. Ther.* (2002) doi:10.1067/mcp.2002.129502.

139. Gibson, R. J., Bowen, J. M., Alvarez, E., Finnie, J. & Keefe, D. M. K. Establishment of a single-dose irinotecan model of gastrointestinal mucositis. *Chemotherapy* **53**, 360–369 (2007).

140. Stein, A., Voigt, W. & Jordan, K. Review: Chemotherapy-induced diarrhea: Pathophysiology, frequency and guideline-based management. *Ther. Adv. Med. Oncol.* **2**, 51–63 (2010).

141. McWhirter, D. *et al.* Chemotherapy induced hepatotoxicity in metastatic colorectal cancer: A review of mechanisms and outcomes. *Crit. Rev. Oncol. Hematol.* **88**, 404–415 (2013).

142. Campbell, J. M. *et al.* Irinotecan-induced toxicity pharmacogenetics: an umbrella review of systematic reviews and meta-analyses. *Cancer Chemother. Pharmacol.* **17**, 27–39 (2017).

143. Fang, Z. Z. *et al.* Irinotecan (CPT-11)-induced elevation of bile acids potentiates suppression of IL-10 expression. *Toxicol. Appl. Pharmacol.* **291**, 21–27 (2016).

144. Lee, C. S., Ryan, E. J. & Doherty, G. A. Gastro-intestinal toxicity of chemotherapeutics in colorectal cancer: The role of inflammation. *World J. Gastroenterol.* **20**, 3751–3761 (2014).

145. Gibson, R. J., Bowen, J. M., Inglis, M. R. B., Cummins, A. G. & Keefe, D. M. K. Irinotecan causes severe small intestinal damage, as well as colonic damage, in the rat with implanted breast cancer. *J. Gastroenterol. Hepatol.* **18**, 1095–1100 (2003).

146. Cario, E. Toll-like receptors in the pathogenesis of chemotherapy-induced gastrointestinal toxicity. *Curr. Opin. Support. Palliat. Care* **10**, 157–164 (2016).

147. Yahagi, M., Tsuruta, M., Hasegawa, H., Okabayashi, K. & Kitagawa, Y. Non-alcoholic fatty liver disease fibrosis score predicts hematological toxicity of chemotherapy including irinotecan for colorectal cancer. *Mol. Clin. Oncol.* **6**, 529–533 (2017).

148. Costa, M. L. V. *et al.* Chemotherapy-associated steatohepatitis induced by irinotecan: A novel animal model. *Cancer Chemother. Pharmacol.* (2014) doi:10.1007/s00280-014-2434-8.

149. Vauthey, J. N. *et al.* Chemotherapy regimen predicts steatohepatitis and an increase in 90-day mortality after surgery for hepatic colorectal metastases. *J. Clin. Oncol.* (2006)

doi:10.1200/JCO.2005.05.3074.

150. Paradkar, P. N., Blum, P. S., Berhow, M. A., Baumann, H. & Kuo, S. M. Dietary isoflavones suppress endotoxin-induced inflammatory reaction in liver and intestine. *Cancer Lett.* **215**, 21–28 (2004).

151. Yokooji, T., Kawabe, Y., Mori, N. & Murakami, T. Effect of genistein, a natural soy isoflavone, on the pharmacokinetics and intestinal toxicity of irinotecan hydrochloride in rats. *J. Pharm. Pharmacol.* **65**, 280–291 (2013).

152. Weng, Z. M. *et al.* Structure-activity relationships of flavonoids as natural inhibitors against E. coli β-glucuronidase. *Food Chem. Toxicol.* **109**, 975–983 (2017).

153. Castro, A. F. & Altenberg, G. A. Inhibition of drug transport by genistein in multidrug-resistant cells expressing P-glycoprotein. *Biochem. Pharmacol.* **53**, 89–93 (1997).

154. Nallani, S. C. *et al.* Induction of Cytochrome P450 3a By Paclitaxel in Mice : Pivotal Role of the Nuclear Xenobiotic Receptor , Pregnane X Receptor Abstract : *Drug Metab. Dispos.* **31**, 681–684 (2003).

155. Shah, Y. M., Ma, X., Morimura, K., Kim, I. & Gonzalez, F. J. Pregnane X receptor activation ameliorates DSS-induced inflammatory bowel disease via inhibition of NF- □ B target gene expression. **20892**, 1114–1122 (2007).

156. Gu, X. *et al.* Role of NF-κB in regulation of PXR-mediated gene expression: A mechanism for the suppression of cytochrome P-450 3A4 by proinflammatory agents. *J. Biol. Chem.* **281**, 17882–17889 (2006).

157. Aitken, A. E., Richardson, T. A. & Morgan, E. T. Regulation of Drug-Metabolizing

Enzymes and Transporters in Inflammation. *Annu. Rev. Pharmacol. Toxicol* **46**, 123–49 (2006).

158. Aitken, A. E. & Morgan, E. T. Gene-specific effects of inflammatory cytokines on cytochrome P450 2C, 2B6 and 3A4 mRNA levels in human hepatocytes. *Drug Metab. Dispos.* **35**, 1687–1693 (2007).

159. Martínez, A. *et al.* Role of the PXR gene locus in inflammatory bowel diseases. *Inflamm. Bowel Dis.* **13**, 1484–1487 (2007).

160. Teng, S. & Piquette-miller, M. The Involvement of the Pregnane X Receptor in Hepatic Gene Regulation during Inflammation in Mice. **312**, 841–848 (2005).

161. Cheng, J. *et al.* Therapeutic role of rifaximin in inflammatory bowel disease: Clinical implication of human pregnane X receptor activation. *J. Pharmacol. Exp. Ther.* **335**, 32–41 (2010).

162. Richardson, T. a & Morgan, E. T. Hepatic Cytochrome P450 Gene Regulation during Endotoxin- Induced Inflammation in Nuclear Receptor Knockout Mice. *J. Pharmacol. Exp. Ther.* **314**, 703–709 (2005).

163. Beigneux, A. P., Moser, A. H., Shigenaga, J. K., Grunfeld, C. & Feingold, K. R. Reduction in cytochrome P-450 enzyme expression is associated with repression of CAR (constitutive androstane receptor) and PXR (pregnane X receptor) in mouse liver during the acute phase response q. **293**, 145–149 (2002).